Analysis of Fire Performance, Smoke Development and Combustion Gases from Flame Retarded Rigid Polyurethane Foams

by

David Olabode Adeosun

A thesis

presented to the University of Waterloo

in fulfillment of the

thesis requirement for the degree of

Doctor of Philosophy

in

Mechanical Engineering

Waterloo, Ontario, Canada, 2014

Author's Declaration

I hereby declare that I am the sole author of this thesis. This is a true copy of the thesis, including any required final revisions, as accepted by my examiners.

I understand that my thesis may be made electronically available to the public.

Abstract

Rigid polyurethane foam is a polymeric material which is widely used for thermal insulation in building construction and other applications. Given recent emphasis on energy conservation and efficiency, there has been continuous growth in its use over the years. This raises significant fire safety concerns since polyurethanes are inherently very flammable and prone to release toxic gases as the foam thermally decomposes and burns. To improve fire safety characteristics by reducing ignitability and flammability of the foams, various flame retardants (FR) have been introduced into base foam formulations. But with the introduction of FR agents, there has been rising concern within the fire safety community and general public regarding the overall benefits versus detrimental impacts of even commonly used FR agents. In the case of rigid polyurethane foam, however, such an assessment is difficult as there are few cross comparisons in the literature that detail the impacts of different concentrations of common fire retardants, such as brominated, phosphorus-based and expandable graphite agents, on the fire behavior, smoke development and toxic gas production for even single base foam formulations.

The present experimental work focuses on a systematic evaluation of these factors using three common, commercial fire retardants added in concentrations of 0%wt, 10%wt and 20%wt to a single formulation of rigid polyurethane foam. Cone calorimeter and smoke density tests are used to simulate well ventilated and poorly ventilated fire conditions during material fire performance assessment, while FTIR, Novatech P 695 gas analyzers and TD-GC/MS methods are used to investigate the gases evolved during oxidative pyrolysis and combustion of the samples. Concentration measurements of principal fire gases such as CO, CO_2, reduced O_2, and NO_x

are combined with more detailed investigation of the volatile organic compounds generated during the fire testing. Use of gas absorption sampling followed by off-line Thermal Desorption/Gas Chromatography/Mass Spectrometry (TD-GC-MS) analysis for identification of toxic gases has proven of significant benefit in this application. The full set of data obtained provides a more comprehensive identification of the evolved products during three characteristic periods in the combustion process. As such, it expands current knowledge and provides valuable new insight and understanding of thermal degradation, combustion and smoke development, as well as overall fire performance, of fire retarded rigid polyurethane foams in well-ventilated and poorly ventilated environments.

Acknowledgements

Finally, I acknowledge the help and faithfulness of God in the pursuit of this study. I owe it all to Him. And to my wife and family who have always spurred and encouraged me into excellence in life and ministry. Thank you all for being there.

Table of Contents

List of Figures

List of Tables

Nomenclature

$\dot{Q}$ = Heat release rate [kW]

$X_{O_2}^i$ = mole fraction of incoming oxygen

X_{O_2} = mole fraction of oxygen in exhaust duct

$X_{CO_2}^i$ = mole fraction of incoming carbon dioxide

X_{CO_2} = mole fraction of carbon dioxide in exhaust duct

X_{CO} = Mole fraction of carbon monoxide in exhaust

$\dot{V}$ = volume flow rate of gas in the exhaust duct referred to 25^0C [m^3/s]

E = Heat produced per unit mass of oxygen consumed for complete combustion [E =13.1MJ/Kg]

φ = Oxygen depletion factor

$\dot{m}_e$ = exhaust duct mass flow rate [kg/s]

C = orifice plate calibration constant in the exhaust duct [$\sqrt{m.kg.K}$]

ΔP = pressure drop across orifice plate in the exhaust duct [P_a]

T_e = exhaust gas temperature at orifice plate [k]

k = smoke extinction coefficient by smoke meter [m^{-1}]

L = extinction beam path length defined as the diameter of the exhaust duct [m]

I = actual light beam intensity reaching the detector

I_o = light beam intensity reaching the detector without smoke

σ_m = the specific extinction area [m^2/kg]

D_s = specific optical density

T = percent transmittance

m_i = initial specimen mass [kg]

m_f = specimen mass at time t [kg]

t = time in [s]

Acronyms

HRR = Heat Release Rate

THR = Total Heat Release

SEA = Specific Extinction Area

MLR = Mass Loss Rate

EHC = Effective Heat of Combustion

t_{ig} = Time to Ignition

UTH = Unburned Total Hydrocarbons

NOx = Nitrogen Oxides

EGFR = Expandable Graphite Flame Retardant

PFR = Phosphorous-based Flame Retardant

BFR = Brominated Flame Retardant

FR = Flame Retardant

FTIR = Fourier Transform Infrared

TD-GC/MS = Thermal Desorption Gas Chromatography/Mass Spectrometry

TGA = Thermo Gravimetric Analysis

LOI = Limiting Oxygen Index

VOCs = Volatile Organic Compounds

TSP = total smoke production [m^2]

SPR = Smoke Production Rate [m^2/s]

TML = Total Mass Loss [kg]

G   = Geometric constant in the smoke density chamber

ASTM = American Society for Testing and Materials

ISO = International Standards Organization

UL = Underwriters Laboratory

Chapter One: Introduction

1.1 Polyurethane Foams and Fires

Polyurethane is one of the most versatile materials today, with a wide range of commercially established applications. Polyurethane foams are all around us in different forms in living rooms and offices, inside vehicles, trains, ships and aircraft. Flexible foams are used in upholstered furniture, bedding, automotive interiors, carpet underlay and packaging. Rigid foams are used as structural insulation panels in building walls and roofs. Thermoplastic polyurethanes are used in medical devices and footwear and as coatings, adhesives, sealants and elastomers, which are used on floors and in automotive interiors [1]. The origin of polyurethane dates back to the beginning of World War II where it was first developed as a replacement for rubber [2]. The uniqueness of this class of polymeric material lies in its versatility, light volume-to-weight ratio, resilience and ease of handling. All of these have spurred its use in a wide variety of applications.

In the building and construction industry, rigid polyurethane (PUR) is one of the most efficient thermal insulation materials available and is gaining wide acceptance in this regard. Since insulation is one of the most critical components of building walls and roofs, recent emphasis on energy conservation and efficiency has been a major driver in increasing the demand for rigid foam insulation panels, which provide much needed thermal performance in today's energy conscious world. To put this demand in context, in Canada between 2008 and 2012, there were an average of 177,000 new homes built annually [3]; leading to an increasing demand for high performance materials that are not only structurally strong and reliable but can help reduce energy consumption. The rigid PUR foams are not only appropriate for construction applications; they are also used in many other

thermal insulation applications such as water heaters, refrigerated transport, and commercial and residential refrigeration.

Unfortunately, polyurethanes, being organic materials, will readily combust when exposed to sufficient heat or other ignition sources in the presence of oxygen. They can result in rapidly developing fires which quickly reach the flashover stage [4]. At this point, all combustible materials, including thermal insulation panels, can become involved in the fire. Even though rigid polyurethane foams provide effective thermal insulation from an energy conservation perspective, in fire scenarios, they can also contribute to rapid fire development and flame spread [5].

In the event of building fires, toxic, visually obscuring and corrosive combustion products are actually responsible for a large number of fire deaths [6]. More victims are claimed by exposure to, and inhalation of, combustion products in fires than by exposure to any other fire hazard [7]. Studies have shown that in North America, $3/4$ of all fire deaths are due to smoke inhalation and $2/3$ of these occur outside the room of fire origin [8]. In fact, there are many fires in which most victims have not had any severe burns, but have been killed by the toxic fire gases. For example, 63 people died as a result of inhalation of toxic gases in the discotheque fire in Gothenburg in 1998 [9]. A similar event was the Scandinavian Star fire in 1990, in which 156 passengers and crewmembers were killed [10]. In both cases, a large number of people were gathered in an unfamiliar and confined space with restricted access to escape, and many of the victims were overcome by toxic smoke [11].

Not all fires occur in public places however, and home fires in Canada still remain an area of utmost concern despite our current regulations and test procedures. In 2002 for instance, Canada had a total of 53,589 fires, of

which 22,186 fires were in the '*residential property'* category. These incidents resulted in a monetary loss of $712 million and more critically, 250 deaths, which was approximately 82% of the nation's fire fatalities that year [12]. Trends are similar across North America [13, 14], illustrating the serious problem of residential building fires and highlighting the importance of proper selection of building and construction materials and fire prevention in our homes.

Preventing occupant exposure to smoke during a building fire is extremely difficult. While the number of fatal burn cases has decreased by 34% within the last decade in the USA as compared to the period from 1975-1985, there has been little change in the number of fatalities due to smoke inhalation [15]. Although, the total number of fire deaths is actually declining, the percentage attributed to smoke inhalation has risen 1% every year since 1979, exacerbated by the increasing use of synthetic polymers in a wide variety of applications in our buildings and as construction materials in furniture and transportation systems [16]. The introduction of these polymers has heightened the concern of fire authorities and regulatory bodies over the nature and toxicity of combustion products generated as these materials thermally decompose under different fire conditions; however, detailed research into these phenomena is still quite scarce [15, 17]. In part, this is because of the effort required to systematically investigate combustion products from even a single class of material with multiple FR additives under the widely varying ventilation conditions that can be encountered during a fire. At the onset of a fire, the oxygen level is high and thermo-oxidative pyrolysis occurs in a well-ventilated environment. As the fire continues to develop to steady burning and flaming combustion, there are periods of time when oxygen levels in the environment may decrease and burning may proceed under oxygen deficient (poorly

ventilated) conditions leading to formation of a different range of combustion products even from the same material. The products and their concentrations will again vary both as the fuel burns out in the later stages of the fire and in the post fire environment.

Various fire ventilation scenarios can be simulated in small scale tests in the laboratory by using the cone calorimeter and the smoke density chamber fire performance test methods. Cone calorimetery (ASTM E 1354) is recognized as a standard small scale test by which to determine the fire performance of a material under well ventilated conditions, while the smoke density chamber (ISO 5659) test method more closely simulates fire performance of materials under non-steady state, partially-ventilated conditions. By using the cone calorimeter and smoke density chamber to test the same material, then, different fire ventilation conditions and thereby different fire effluents can be produced. Since a material may be exposed to both conditions in a real fire situation, use of these complementary tests form the core of the present experimental approach. Details of their application will therefore be further discussed in Section 3.2.

Over the past three decades, considerable research has been conducted to characterize the fire behaviour of rigid foams and design new formulations with reduced flammability [5, 18, 19]. Work on the flammability of flexible and rigid polyurethane foams has led to the introduction of unique combustion modifiers, otherwise known as flame retardants (FR), which improve the fire properties of the foams by adapting characteristics such as ignition time and flame spread or lowering heat release rates from the materials as they burn. The incorporation of flame retardants into polyurethane materials has again changed the combustion products generated during modern fires; yet the mechanisms for, and details of, these changes are not well understood. Therefore, there is a critical need to study heat release rate, smoke development and the identity and

concentrations of fire gases produced from both fire retarded and non-fire retarded foam materials during thermal decomposition and combustion under various fire conditions. Since chemical composition dictates which toxic products will be produced from the combustion of a given material, this knowledge may be used over the longer term to develop tools by which to predict the evolution of the main toxic products arising from a fire.

1.2 Motivation

The potential fire hazard resulting from the increased use of synthetic polymers, and rigid polyurethane foams in particular, as insulation in buildings has heightened concern over fire safety. References to such hazards have frequently appeared in technical literature and at scientific gatherings [19]. This has led to a variety of mitigation strategies, from use of more standard fire protection coverings through to addition of one or more fire retardant additives to the base foam formulations. Nonetheless, fires will occur and information on the composition and toxicity of smoke and fire gases produced from various materials are necessary inputs for fire risk analysis models in terms of assessing the potential severity of exposure, likelihood of occupant egress from an area and probability of occupant survival in the event of a fire. According to the National Research Council, USA, "our poor understanding of smoke and toxicity is a critical barrier to further incorporation of polymers and their composites in building contents and structural applications" [20].

Building and fire codes are becoming more stringent in terms of the fire performance of materials used in the construction of residential and commercial buildings. Foam and flame retardant manufacturers have found themselves in a dilemma as to whether their attempts to suppress the flammability and ignitability of PUR foams by adding flame retardant agents into the base foams give rise to extremely toxic products or pose other

environmental concerns [21-22]. There are also concerns within the fire safety community and general public regarding the use of flame retardant additives to reduce the burning rate of materials and furnishings [23-25]. As such, it is still not clear if the use of flame retardants has actually paid off to provide an overall net safety benefit considering the attendant smoke and toxic gases that are generated during the combustion of flame retarded rigid polyurethane foams. No doubt, there is a general consensus amongst many fire researchers that addition of sufficient FR chemicals reduces flammability of PUR foams. But to date, there are still disagreements and strings of contradictions on the effects of FR additives on smoke levels, toxic gas generation and the overall fire performance of flame retarded products [24, 26].

In Babrauskas's study on the effects of FR agents on polymer performance, he concluded that the use of FR significantly improved the overall fire performance of flame retarded products in terms of ignitability and flame spread, but that there was no significant reduction in smoke production between FR and NFR products [24]. In another study conducted by Mouritz et al., he claimed that the use of some FR reduces the yield of smoke and toxic gases, while other flame retardants can increase the yield of toxic gases [27]. Due to the dearth of systematic, detailed, scientific information with respect to FR additives and rigid polyurethane foams, there is little or no consensus within the fire science community in terms of amounts of smoke and nature of gaseous products generated across different foam formulations [24, 26, 28]. This is exacerbated in practice by the fact that multiple FR additives are generally used in combination to improve fire performance [23-24, 26, 28].

Therefore, in spite of the extensive work which has been documented in the literature on ignition, combustion, toxicity and flame retardancy of polyurethane foams [29], the detailed physics and attendant impacts of

flame retardants on smoke generation, combustion gas toxicity and any related overall safety concerns is not clearly understood [17]. These are the issues that propel the present work with the specific objectives outlined in the next section.

1.3 Research Objectives

The main objective of the present research is to provide broad-based information on fire performance, smoke development and combustion products generated during non-flaming and flaming combustion of newly developed rigid polyurethane foams designed for use as thermal insulation in residential and commercial buildings.

In the present study, small-scale experiments were conducted at the University of Waterloo Live Fire Research Facility to systematically examine overall fire performance, as well as composition of effluents (smoke and volatile organic compounds) released, during thermal decomposition and controlled burning of a matrix of flame retarded polyurethane rigid foams under varied ventilation conditions. For this, each of three commercially available fire retardant additives were individually added to a single base (reference) foam composition at two predetermined concentrations. The fire performance of the resulting materials was assessed using cone calorimetry and smoke density tests. Effluents were collected at three characteristic stages during each of the tests and analyzed to determine the identity of the major fire gases present at those times, as well as to screen the wide range of organic vapours that were contained in the hot product gases.

Specific objectives of the research are as follows:

(i)   To characterize fire gases evolved from thermo-oxidative pyrolysis and combustion of a single formulation of rigid

7

polyurethane foam to which various quantities of three main fire retardants were added. Over the long term, this will lead to development of a quality database of fire performance characteristics, smoke and fire gas compositions from these materials which, over time may be extended for use in fire hazard analysis tools

(ii)   To systematically study and better understand the influence of different types of commercially available fire retardants on smoke generation and gases released under well-ventilated and vitiated conditions at different stages of fire growth for the rigid polyurethane insulation foam under study

(iii)   To utilize and assess different gas analysis methods available at the UW Live Fire Research laboratory with a view to determining appropriate instrumentation and developing a consistent method for detailed characterization of pyrolysis and combustion gases evolved during cone calorimeter and smoke density fire performance tests

Most of the studies that have been conducted on flame retardancy of rigid polyurethane foams have focused on the performance of specific flame retardant additives in different resins and polymers at levels ranging from 5-30%wt [23, 30]; however, since the additives are added to different base foam formulations, the results do not allow for cross comparison of the individual or incremental effects of each fire retardant additive on smoke development and toxic gas release. The present study takes these existing results a step further by conducting a systematic investigation of the impact of three commercially available flame retardants on fire performance when they are added at different levels to the same base foam formulation. This should allow comparative analysis of smoke development, fire gases and other fire hazard indices related to the addition of these three additives to

common base foam. The experimental study will further advance the development of a gas analysis method suitable to examine volatile organic compounds which evolve from combustion of flame retarded rigid polyurethane foams. Results would be used to develop the gas sampling methods and data analysis techniques that are necessary to obtain consistent data across tests. The work should result in significant improvement in current understanding of the chemistry of interactions between fires, fire retardants and pyrolysis/combustion gases evolved from rigid polyurethane foams. Over the longer term, greater understanding of small-scale fire behavior across samples will allow various fire retardants to be ranked relative to their expected performance in larger scale standardized fire tests such as those currently used to rank building materials.

The next chapter provides the background information on polyurethane foams and fire retardants related to this work; and various studies that have been conducted on fire retarded rigid polyurethane foams to date. It also provides information on the gaseous products expected from different stages of fire development in a typical fire scenario; followed by a review of fire performance characteristics and combustion products evolved from fire retarded polyurethane foams under different fire conditions.

CHAPTER TWO: Literature Review

2.1 Polyurethane Foam Production

The name 'polyurethane foam' refers to a number of different types of foam consisting of polymers made of molecular chains bound together by urethane links. Polyurethane foam can be flexible or rigid, but generally has a low density making it lightweight for many applications. Flexible foams are comprised mainly of open cells, formed by gas bubbles included in the foam during the manufacturing process. Air can pass through the foam easily, resulting in a soft, resilient, flexible material. On the other hand, the cells in rigid foams are for the most part closed, making the material harder and less resilient. By controlling the proportion of open cells to closed cells during the production process, the properties of foam can be manipulated, thus increasing the material's versatility.

Polyurethanes are chemically complex polymeric materials, usually formed by the reaction of a poly-isocyanate with a poly-hydroxyl combination to produce the covalent bonds of polyurethane [31]. The poly-addition reaction is presented in the equation below [32]:

$$nOCN\text{-}R\text{-}NCO + \quad nHO\text{-}R'\text{-}OH = (R\text{-}NHCOO\text{-}R'\text{-}NHCOO)n \qquad (1)$$

poly-isocyanate   Polyol   Polyurethane
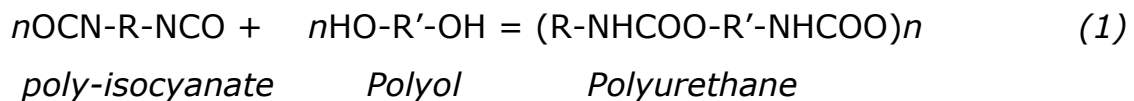
where R' is typically the polyester or a polyether chain. Water or amines may also be added as chain extenders.

During the production of rigid polyurethane foams, chemical additives such as catalysts, surfactants, antioxidants and colorants are added to the base compounds to produce the desired grade of foam. These additives are incorporated to impart specific, desirable properties into the foam. In addition, flame retardant (FR) agents are incorporated to improve fire

10

performance and safety of the products. Independent of any FR agent combinations used; however, details of the base chemical compositions of polyurethane foams are also directly linked to their flammability properties and their propensity to generate toxic smoke when involved in a fire. Therefore, in reality, the combustion (burning) characteristics of the foam can be altered by one of several means: by varying the base chemical formulation, through the addition of fire retardants or via the modification of other additives during the production. Due to their importance in the present context, fire retardant additives are specifically addressed in the next section.

2.2 Flame retardants mechanisms in rigid polyurethane foams

The terms fire retardants or flame retardants are often used loosely and therefore can be easily misinterpreted. The term is used in this study in a way consistent with ASTM E 176 [83]. Fire retardant is a "chemical, which when added to a combustible material, delays ignition and combustion of the resulting material when exposed to fire". Flame retardant additives are incorporated into rigid polyurethane foams during production to modify the combustion properties of the foam and reduce the flammability of the final products. As a result of advancements in fire retardant chemistry over time, there are more than 175 different flame retardants on the market, which can be characterized into four major chemical groups: inorganic, organo-phosphorous, halogenated organic and nitrogen-based compounds [33-34].

These flame retardants are additionally grouped into two categories designated additive fire retardants and reactive fire retardants, respectively, depending upon whether they molecularly mix into, or bind with, the base foam. Additive flame retardant substances are dispersed in the final polymer product, but they do not bind chemically to the

polyurethane polymer chain(s). As a result, they may leach out of the polymer during the service life of the treated products, thereby reducing the flame retardant properties over time. Reactive flame retardants, on the other hand, are monomers that can be co-polymerized with other monomers and chemically bond within the polymer structure. For these, the loss of fire retardancy during the service life of the treated products is usually limited.

Individual fire retardants can work by several mechanisms to slow down or prevent fires in a material. For example, while it is difficult to generalize across chemical categories, most inorganic flame retardants decompose endothermically, releasing water vapour and/or carbon dioxide, both of which inhibit burning. Some heat from the flame is absorbed in such reactions and the residue also conducts heat away from the reaction zone, contributing further to the extinction of the fire. Some flame retardants act chemically to quench the formation of key combustion radical species and thereby quench the chemical reactions driving the flames. Still, other flame retardants act as smoke suppressants and promote char formation.

Various combinations of additives and flame retardant approaches have been used for different applications depending on factors such as cost, the base foam material and its application, and the required safety levels of the final materials. Each approach can lead to different results. For example, inducing surface char formation by modification of the polymer base and the use of char forming additives are both common practices and often beneficial in rigid polyurethane foam production [37]. It has been established that char yields have a linear relationship with the FR concentrations in the parent foams [35]. The flame retarded PUR foams which produce chars tend to protect the virgin material from the direct feedback of energy to the bulk fuel. The flow of heat to the virgin material is reduced as the char layer

12

thickens, and the rate of decomposition is reduced depending on the properties of the char. Under the char layer, a progressive chemical pyrolysis may continue. This will be influenced by thermal and mass transport occasioned by energy feedback to the char and will result in continued evolution of pyrolyzed gaseous products. As the char layer becomes thicker, its shape and resistance to flow may cause it to crack, leading to further pyrolysis of the virgin material and release of additional pyrolysis products or even gaseous fuel vapour into the hot combusting zones products [36]. In terms of toxicity, combustion of high char-forming rigid PUR foams tends to produce less carbon monoxide under most conditions, though it has also been shown that under laboratory pyrolysis conditions, the toxicity of gases evolved during combustion of some high char forming foams may be increased [37]. There is therefore a significant trade-off between material composition, level of fire retardancy and hazard potential.

In a different vein, there are also growing concerns about the environmental and health effects of many of the common flame retardants. In principle, all flame retardants are environmentally relevant since they release their decomposition products into the environment during manufacturing, incorporation into polymers and any subsequent combustion process. The potential extent of environmental damage and health impacts of these products depend largely on the chemistry of the flame retardants and that of the substrates to which they are applied [38]. There are cases where the FR-compounds themselves are significantly toxic and may be released from the product during use or following disposal [39]. For instance, experimental research conducted on rigid PUR foam containing a bicyclo-phosphate ester based flame retardant indicated that bicyclic phosphate compounds were produced during burning [6, 40-41]. As a result, rigid PUR foam containing this fire retardant never became commercially available. Such work and more recent insights into possible environmental or

13

toxicological impacts of certain FR additives have indeed spurred significant interest for more in-depth study of the combustion toxicology of PUR foam. Since there are no prescriptive requirements relating to FR additives for PUR foams, the choice of flame retardants is left entirely to the product manufacturer. Overall though, there is virtually no group of flame retardants appropriate for polyurethane foams that has not raised some environmental and health concerns [42]. Therefore, testing of new foam formulations containing various combinations of fire retardant compounds has become imperative in order to understand the link between fire retardant additives and generation of smoke and combustion gases from rigid PU foam during fires [40].

To help further outline the present understanding of available options for foam fire retardant additives, and some possible issues with each, the modes of action of the three main categories of flame retardant systems that were examined as part of this work are discussed in the next three sections. Additives in the fourth category of flame retardants (nitrogen-based compounds), especially melamine, are more applicable to flexible PUR foams and are therefore outside the scope of this work.

2.2.1 Brominated Flame Retardants

Halogenated organic compounds are among the most widely used additives that have been reported in the literature as fire retardants for polyurethane foams [43-44]. This is largely due to their efficiency in terminating the free radical reactions required to sustain chemical reaction during hydrocarbon combustion. Among all halogens, fluorine- and iodine are not used as fire retardants in practice because fluorine forms strong bonds to carbon and large quantities of energy are required to break these bonds and release the fluorine radicals into the combusting zones. In direct contrast, iodine is attached to carbon quite loosely, such that little energy is required to release

iodine radicals into combustion zones. In the case of fluorine then, the combustion process will be completed before the fluorine radicals are released. On the other hand, iodine radicals are released too early, before the combustion process begins. As a result, neither of these halogens is effective as a fire retardant.

Out of the remaining halogens, bromine is more effective as a fire retardant than chlorine. This is because of the weaker bond formed between bromine and carbon, which enables bromine radicals to interfere at a more favourable point in the combustion process than does chlorine [6, 29]. Brominated fire retardants can therefore be used effectively in low concentrations, and they can also be readily incorporated as both reactive and additive fire retardant agents. Because of their low cost, high performance, efficiency and wide application, bromine based chemicals (as applied in brominated flame retardants or BFRs) currently comprise the largest market sector for fire retarding of synthetic materials. Bromine represents 25–30%wt of the total flame retardant consumption in the United States [45]. In fact, Deca-BDE which is a general purpose flame retardant is used in virtually all types of polymers. As such, a bromine-based FR additive was chosen as a representative halogen-based FR additive for the purpose of this research. The action of bromine as an FR agent is discussed in more detail below.

Flame retardancy by brominated chemicals is achieved through chemical interaction in the gas phase between dissociated bromine radicals (Br*) and high energy free radical intermediates (H*, OH*) released during combustion of the burning polymer. The chain decomposition reaction taking place during polymer combustion in the presence of a brominated flame retardant is as follows [46]:

$$RBr \rightarrow R* + Br*$$

$$Br* + R'H \rightarrow R'* + HBr$$

$$HBr + H* \rightarrow H_2 + Br*$$

$$HBr + OH* \rightarrow H_2O + Br*$$
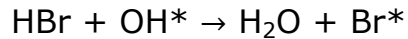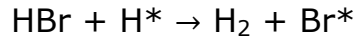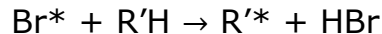
The brominated flame retardant releases hydrogen bromide gas (HBr), which then acts as a free radical scavenger to interfere with the chain reactions that drive combustion, thereby interrupting the oxidation process [46-47] and decreasing the intensity of the normal exothermic combustion reactions resulting in an overall cooling of the system. Essentially therefore, halogenated fire retardants slow down the combustion process via a series of chemical/thermal mechanisms. Although, brominated flame-retarded products have great potential to save lives and minimize property damage in the event of a fire, there are increasing concerns about their environmental and health effects in general. On the environmental side, it should be noted that use of poly brominated diphenyl ethers (PBDE) is thought to be related to the increased levels of PBDEs found in human milk in North America [48]. Although, this is by no means the only bromine based FR on the market, available data does raise more general concerns over the use of any brominated flame retardants from an environmental perspective and their use has come under severe criticism. Presently, however, it should also be noted that there is little environmental toxicity information for nearly half of the existing BFRs [49]. Due to the efficiency and effectiveness of bromine as an FR agent therefore, new more environmentally compatible formulations are under development and their use will continue into the foreseeable future.

The possibility that brominated, and indeed all forms of halogenated, FR additives might be linked to environmental concerns leads to another

important issue that must be considered with respect to their use. This issue is centered around the identification of possible risks to fire fighters and building occupants from potentially toxic chemicals that are created when products containing BFRs burn. This subject is one that has received relatively little attention to date, yet there is clearly a need for systematic scientific study to understand and relate how the chemical action of brominated flame retardants will affect smoke and toxic gas release during fires. Where BFRs have been used, either individually or in synergy with other FR agents, studies have shown a significant increase in measured Limiting Oxygen Index (LOI), attesting to their positive impacts in terms of overall flammability of the material under test. However, the LOI test method does not allow evaluation of the smoke and toxic gases evolved during pyrolysis and combustion of the samples [50].

Indeed, most issues raised about the use of BFR agents have been focused on the issue of potential environmental contamination and less towards toxicology of their decomposition products in the fire environment. The question of whether halogenated flame retardants need replacement is still an open question that will not be entirely resolved on scientific grounds until much additional research has been completed [51]. Our understanding of the interactions between specific BFRs and gaseous species generation during pyrolysis or combustion of complex materials such as rigid polyurethane foams is still limited, and where studies have been conducted, the brominated FR additives were mostly used in synergy with other FR agents.

Other studies relating to the impact of BFR on fire performance of polymers involved the use of cone calorimeter tests. One such investigation is Babrauskas' work which represents one of the most comprehensive studies

on the subject to date [24, 52]. He used cone calorimeter tests and an NBS cup furnace combustion toxicity apparatus to examine the effects of adding FR agents to material samples from five different plastic products namely, *polystyrene* TV cabinets, *polyphenylene oxide* business machines housing, *polyurethane* foam-padded upholstered chair, electrical cable with *polyethylene* wire insulation and *rubber* jacketing and a *polyester/glass* electric circuit board. Entire articles were also tested in a furniture calorimeter to determine the rate of heat release, ignitability, smoke production rate and the rates of production of various toxic combustion gases. Using a concentration of 12%wt decabromodiphenyl oxide in synergy with 4%wt antimony oxide on TV cabinet housing materials, it was concluded that the use of BFR agent significantly decreased peak heat release rate and total heat release and increased ignition time, while the CO yield was about 7-fold greater in the FR product compared to NFR specimen [52].

Another study conducted by Checchin et al. [53] involved post ignition behaviour of rigid PUR foams modified with different fire retardants. The modifications were applied to the polyol and isocyanurate foam components or as additives to the overall foam formulation itself. They included brominated polyester polyol, different isocyanurates, a phosphorous-based agent (dimethyl methyl phosponated), and char forming expandable graphite. These were compared with a non-fire retarded polymeric MDI-based foam as reference sample, using cone calorimeter standard test method under the action of 40kW/m^2 heat flux. Results indicated that although there was a reduction in the heat release rate (HRR), the presence of bromine and volatile phosphorous compounds caused considerable increase in smoke production and CO yields. The best achieved result was found to be with the intumescent flame retardant. Unfortunately, the FR

agents were incorporated into different resins and single concentrations of each different FR agent was not stated making it difficult to generalize the results to other agents or base foam formulations and to interpret them in the context of the interactions of BFR agents and rigid polyurethanes such as those under study here.

In the present study, therefore, the fire performance, smoke development and gas production from rigid polyurethane foam samples of the same base formulation but containing concentrations of 10% and 20% of a single BFR agent with no other additives will be compared in attempts to isolate the action of the BFR agent on pyrolysis and combustion of rigid polyurethane foam. Furthermore, in contrast to the cup furnace apparatus used in [52], which does not simulate real fire conditions and involves much smaller samples that are not necessarily representative of the end product, cone and smoke density chamber tests, with their respective sample sizes of 100cm x 100cm and 75cm x 75cm, will be used to better simulate well-ventilated and poorly ventilated fire conditions.

Despite the continuing importance of halogenated fire retardants, environmental concerns and recent public scrutiny engendered by the use of halogen-containing flame retardants, especially those based on bromine, has prompted renewed effort in finding halogen-free flame retardants. Therefore, flame retardants based on other chemicals, like phosphorus and nitrogen, have been developed and many flame retardant manufacturers and end users are now focusing on these categories of agent. Therefore, phosphorous-based and other non-halogenated flame retardants [51] are discussed in the context of the present work in the next two sections.

2.2.2 Phosphorus Flame Retardants

There has been tremendous development in flame retarded rigid PUR foams that incorporate phosphorous-based polyethers and polyesters, although such FR agents are often considered to be significantly more effective in oxygen- or nitrogen-containing polymers such as polyesters, polyamides and cellulose than in polyurethanes [54]. Independent of polymer base, phosphorous can act in several ways to promote fire retardant action; first, in the condensed phase by enhancing char formation, intumescence or inorganic glass formation. The dehydration of the polymeric structure induces cyclization, cross-linking, aromatization or graphitization; and phosphoric acid which may be produced by phosphorous compounds and their decomposition products can also act as cross-linkers and formation of inorganic glasses such as poly phosphates. Second, phosphorous can also act in the gas phase through flame inhibition where hydrogen and hydroxyl radicals are replaced by PO-radicals thereby slowing down the oxidation of hydrocarbon reactions in the gas phase [120].

Once thermal decomposition of phosphorous containing compounds leads to the production of phosphoric acid, it readily condenses to produce poly-phosphoric acid thereby liberating water vapour that dilutes the oxidizing gas phase [46] according to the following reaction:

$$2\ \text{HO-}\underset{\overset{|}{O}}{\overset{|}{P}}\text{-OH} \rightarrow \text{HO-}\underset{\overset{|}{O}}{\overset{|}{P}}\text{-O-}\underset{\overset{|}{O}}{\overset{|}{P}}\text{-OH} + H_2O \qquad\qquad (2)$$

Phosphoric acid   Poly-phosphoric acid
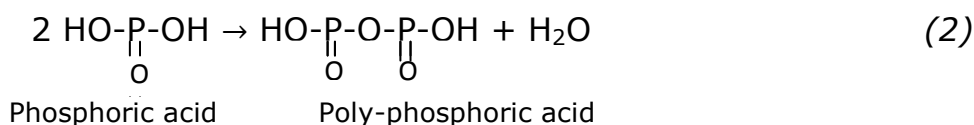
Dehydration reactions of polymer end chains are also catalyzed through interactions of some phosphorous containing FRs, resulting in formation of a protective layer of highly cross-linked carbonaceous char. As it builds on the surface, the carbonized layer (char) isolates and protects the polymer from the flames, insulating the surface of the burning material and restricting the

flow of heat into the polymer matrix. This reduces volatilization of the fuel and also obstructs the outward flow of combustible gases originating from thermal degradation of the polymer, while at the same time limiting oxygen diffusion towards the fuel surface. The net effect is not only chemical, via a reduction in reaction intensity through decreased availability and mixing of fuel and oxygen, but also thermal, since the char-forming reactions are endothermic and the protective, insulating layer of char protects the bulk material from direct heating and leads to cooling of the fuel surface with time.

In general, the higher the phosphorous content, the more phosphorous-rich residue is formed during thermal decomposition, resulting in increased char yield on the surface of the polymer. At the same time, formation of char on the surface means that less hydrocarbon material is actually consumed, with a resulting reduction in quantity of fire effluent gases produced. Even further, char formation is often accompanied by the release of water vapour which can dilute any combustion products. All these effects are factored into the flame retardant action of condensed phase (char) forming FR additives such as phosphorous.

To enhance the FR action further, some phosphorous-based flame retardant compounds may also volatilize and form active radical species such as PO_2*, $PO*$, and $HPO*$. Much as in the case of halogen FR additives discussed above, these can act as scavengers of the highly reactive $H*$ and $OH*$ radicals, further decreasing the efficiency of, or even inhibiting those reactions that drive hydrocarbon combustion. The trade off, however, is that the resulting vapour phase may contain a variety of potentially toxic phosphorous-containing products [39]. This again speaks to one of the major, but as yet little studied, controversies surrounding the use of phosphorous-based fire retardants i.e their effects on smoke and toxic gas generation during fires. Studies involving phosphorous-based fire retardants

show reductions in the thermal decomposition temperatures of foams resulting in an increase in smoke density, while the formation of char in rigid foams has been shown to promote generation of more CO in the product gases [6, 29].

Most studies conducted on the flame retardant action of phosphorous-containing compounds have been conducted with very small samples, focusing primarily on use of such techniques as thermo-gravimetric analysis (TGA), LOI and UL 94 ratings to determine thermal stability, ignitability and flame spread for different types and concentrations of phosphorous FR additives in various materials. In some cases, other fire performance parameters such as HRR and THR were also measured using the cone calorimeter test method, usually without recourse to investigation of any details related to smoke and toxic gas evolution during decomposition and burning of the samples [47, 54-55].

Most of the studies on phosphorous-based compounds are again in relation to synergy of phosphorous based additives with other FR agents. In his review of recent progress of phosphorous-based flame retardants, Levchik [51] suggested that PFR has two mechanisms of action: as char formers or char enhancers in the condensed phase but also that there is an increasing recognition of vapour-phase action. The existence of these two different modes of action suggests many synergistic combinations of phosphorous-based compounds. The review also revealed that different phosphorous flame retardants improve thermal stability of PUR products [51].

To investigate the effects of PFR agents in rigid polyurethane foams, the present work is focused on comparative studies for the same base foam formulations at different concentrations of PFR with aim to determine how a phosphorous FR additive affects the formation of char and attendant overall fire performance characteristics, as well as the nature and degree of smoke

and gas production during decomposition and combustion. There is the need for systematic study across a range of concentrations of a single PFR added to the same base foam in order to understand more detail of the interactions between that PFR and the fire performance of rigid polyurethane foam. Because of emerging fire safety standards and regulations, coupled with ever-increasing environmental awareness, smoke density and gas toxicity are also important parameters to be considered in the evaluation particularly since phosphorous flame retardants have their own peculiar attribute. For example, to obtain the desired performance, they may require a high level of loading into the polymer, which may also deteriorate the original properties of the material. In a quest to find flame retardants as effective as the phosphorous and halogen compounds used to date, then, it is more imperative than ever to conduct systematic studies to characterize fire performance parameters for a range of concentrations of other FR additives in a variety of fire test situations as well [39]. Expandable graphite is one candidate that has been found to fill that gap, as is discussed further in the following section.

2.2.3 Intumescent Flame Retardants

Expandable Graphite Flame Retardant (EGFR) is an example of an intumescent FR system. The graphite will expand to more than 100 times its original volume when heated, forming a foamed multi-cellular charred layer with a worm-like structure that covers the entire burning surface of a polyurethane foam sample. Sulphuric acid, which is intercalated between the graphite layers boils under exposure to heat and generates blowing gases which are responsible for the exfoliation of graphite according to the following reaction:

$$C + 2H_2SO_4 = CO_2\uparrow + 2H_2O\uparrow + 2SO_2\uparrow \qquad (3)$$
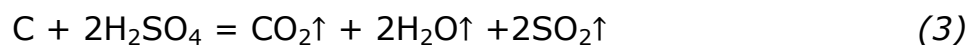
The expanded graphite material forms an insulating char layer over the burning material. This layer serves as a physical barrier that prevents heat transfer from the flames into the foam matrix, inhibiting vaporization of the fuel, as well as slowing the diffusion of oxygen into the underlying fuel. This is shown schematically in Figure 2.1. Addition of expandable graphite impacts both the physical-mechanical properties and fire behaviour of rigid polyurethane foams [56].

Zone A — Flame heat source and oxygen rich zone

Zone B — Insulating char layer (which creates the physical barrier between zone A & C)

Zone C — Burning fuel (where combustible gases, heat and mass transfer are located)
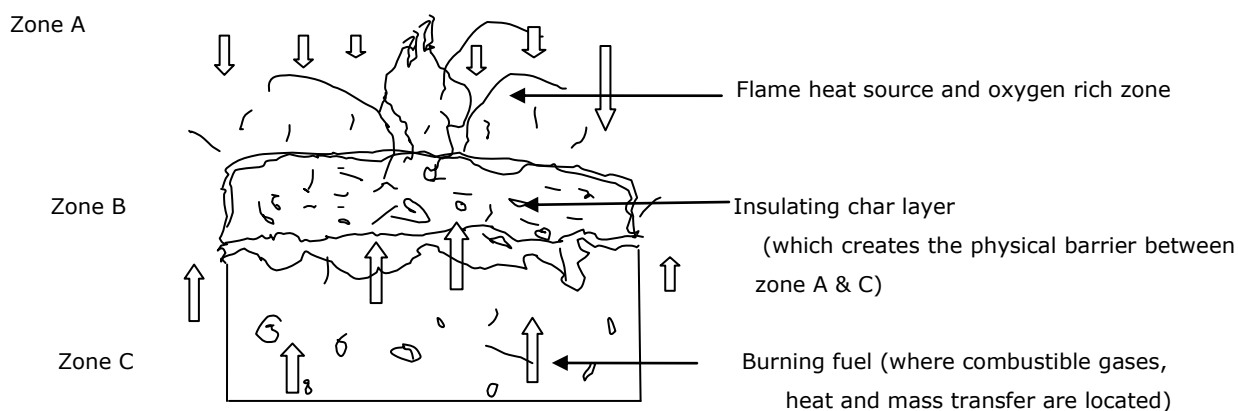
Figure 2.1: Flame retarded expandable graphite forming a physical char layer over polymer matrix

The majority of work into this area was done by Modesti and his co-workers who investigated the influence of expandable graphite loading and particle size on both the physical-mechanical properties and the fire behaviour of rigid polyurethane foams using cone calorimeter and oxygen index tests [56-59]. They also studied synergistic effects of adding both expandable graphite and some phosphorous based compounds in terms of the fire performance of the foams [56-57, 60]. Other researchers have studied the flame retardant characteristics of expandable graphite when added to foams of different density [61]. Most of the evaluations of the fire performance of the foams have involved measurement of LOI, burning rate, HRR, CO/CO_2 weight ratio and thermal stability using the TGA technique. It has been shown that the

use of EGFR significantly improves the fire behaviour of rigid foams by increasing the oxygen index and reducing the value of peak HRR; however, studies also show that increases in EG content lead to the generation of more carbon monoxide during burning.

Similarly, combinations of complementary FR additives such as expandable graphite and triethyl phosphate (TEP) were not found to improve the smoke and toxic gas generation during burning of foam samples [57]. As such, it is again of interest to determine how different concentrations of expandable graphite FR additive, used in isolation from other synergistic agents, affects the formation of char and attendant overall fire performance characteristics, as well as the nature and degree of smoke and gas production, during decomposition and combustion of a rigid polyurethane foam.

2.3 Summary of work to date on flame retarded rigid polyurethane foams

The above discussion indicates that most studies into the impacts of brominated, phosophorous-based and expanded graphite fire retardant additives on fire performance of rigid PUR foams involve the use of TGA, LOI, UL-94 and cone calorimeter test methods for different concentrations of a single class of FR additive [47, 50-52, 55-56, 61]. It has also been shown that using the LOI test to characterize ignitability and flammability of polymers can be misleading since LOI measurements are carried out at ambient temperature. In general, LOI values decrease when temperature increases and hence, the apparent self-extinguishing property inferred from room temperature LOI indices cannot be relied upon in a real fire, since materials with high LOI values at room temperature may burn without self-extinguishing under intense fire conditions. Depending on the type of polymer, there can also be a melting and dripping effect during LOI tests, leading to incorrectly high LOI values. The UL-94 test method is also less appropriate as a fire performance indicator for specimens that flow more

easily than for more cohesive materials. The dripping of burning polymer can take flames and heat away from the surface of the specimen, causing it to extinguish prematurely. The use of TGA, LOI and UL-94 test methods involve relatively small amounts of sample which may not be representative of the material of interest. Further, none of these tests include evaluation of smoke and toxic gas generation except perhaps TGA when interfaced to appropriate gas analysis instrumentation. Therefore, using TGA, LOI and/or UL-94 to assess flame retardant systems are not sufficient in themselves. A wealth of research has been done with respect to each class of fire retardants in PUR foam using TGA, LOI and UL-94 test methods. Later researchers have used the cone calorimeter test method to extend understanding of the interactions between FR additives and thermal decomposition/combustion of PUR foams under different conditions with aim in the longer term to attempt to correlate the results with performance of the same materials in full scale fire tests.

Despite the quantity of research that has been undertaken, there have been few studies conducted which compare the physical and chemical impacts of additives from the different FR agent classes to one another when they are used in the same base foam formulation. In a limited number of cases, parameters such as HRR, THR, SEA, MLR and EHC were measured [56-57], but even fewer studies investigated any details related to smoke and toxic gas evolution during thermal decomposition and combustion of comparable samples [25,62]. Rather than looking into details of the nature and concentrations of effluent gases evolved from different stages of testing of the same base foam formulations with various concentrations of different FR agents, researchers have generally looked into either thermal decomposition products in different atmospheres or combustion products as averaged across the entire fire performance test period [25, 62].

There are even fewer studies which focus on identification of gaseous products in post fire environments [63]. Instead, most researchers have used a measure of the CO/CO_2 weight ratio to assess smoke toxicity, largely because CO is the most abundant toxic gas responsible for fire death [6]. During incomplete combustion in either flaming or non-flaming modes, however, many other compounds such as hydrogen cyanide (HCN), oxides of nitrogen (NO), hydrocarbons, oxygenated organic compounds and nitrogen-containing organic compounds are produced [62] and can also be linked to the overall toxicity of the fire and post-fire environments. Since relatively small amounts of HCN and NO can be lethal, more in depth study into the evolution of effluent fire gases during burning of rigid polyurethane foams should go beyond measurement of only the CO/CO_2 weight ratio.

Based on the toxicity and speed of human incapacitation by substances such as HCN, coupled with the generation of a wide range of other toxic products, it is of interest to better identify and measure concentrations of product gases that are evolved at various stages during the thermal decomposition and combustion processes. Such a study can be justified based on toxicity of the environment but should also be extremely enlightening with respect to better defining the nature of the physical and chemical interactions that might take place between the various flame retardant additives and a base material in different ventilation conditions. This, in turn, may provide new insight in the design and optimization of candidates for next generation FR additives for rigid polyurethane foams.

The present experimental work will focus on the systematic evaluation of three commercially available fire retardants applied within a range of 0-20%wt into a single formulation of rigid polyurethane foam and examined under varying ventilation conditions. Analysis of the gases generated during cone calorimeter and smoke density chamber testing and assessment of CO, smoke and organic vapour yields will further elucidate the completeness of

combustion and nature of the gas mixtures produced at various stages during the testing. Finally, results will be compared with other thermal pyrolysis and fire performance studies available in literature.

Studies show that as phosphorous-based FR and expandable graphite flame retardant content increases, the combustion process is slowed down in many materials due to the formation of the carbonaceous char layer over the burning polymer matrix [29]. These physical effects and interactions should lead to the improvement of fire behaviour (i.e reduced HRR, THR, MLR, t_{ig},) of flame retarded rigid PUR foam. Similarly, the chemical impacts of increasing levels of bromine-based FR additives should improve fire behaviour of the foam. However, due to the complexity of interactions and physical processes occurring during heating and combustion of flame retarded rigid polyurethane foams, the phenomena related to smoke development and toxic gas generation are still not well understood. Through cone calorimeter and smoke density testing of rigid polyurethane foam thermal insulation containing differing concentrations of brominated, phosphorous and expandable graphite FR additives, the present study should further enhance our knowledge of fundamental mechanisms and correlations between polymer decomposition and combustion, fire performance characteristics and smoke and toxic gas generation. To interpret the results, the stages of fire development must be understood and linked to various phases in the fire performance testing undertaken. This forms the basis for discussion in the next section.

2.4 Stages of Fire Development

Rigid polyurethane foam may be decomposed under conditions of either non-flaming or flaming combustion during different stages of fire development. The temperature, to which the material is exposed, as well as the ambient oxygen concentration, varies significantly during different

stages of a fire, so that gases produced at various times during a fire may vary significantly in both their nature and concentrations. Gases evolved during the various stages of a real fire may be due to pyrolysis, thermo-oxidative and/or flaming combustion of the foam, but in all cases will consist of a complex mixture of many different compounds. In order to assess how the material might respond to a real fire situation, then it is important to relate the conditions encountered during a real fire to conditions to which a sample is subjected during fire performance tests.

Figure 2.2 shows a general schematic of the main stages of fire development, including pyrolysis, fully developed and decay stages. From the onset, a fire can begin with a slow induction period, during which thermal decomposition occurs in an oxygen rich environment.
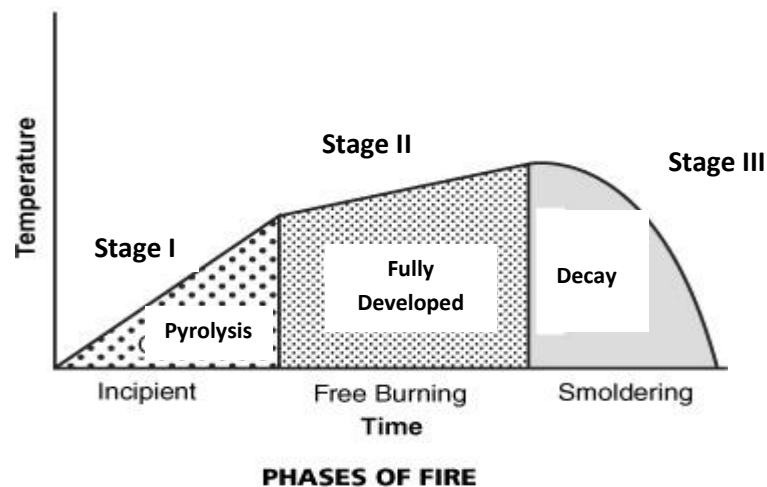
Figure 2.2: Idealized temperature-time phases of well-ventilated compartment fire

After ignition, the fire grows very rapidly until its size is limited either by the accessibility of oxygen or the availability of fuel. The shape of a fire curve depends on parameters such as the fuel type, amount and surface area, the compartment geometry and ventilation conditions. Further, since each phase of fire development has its own unique characteristics, the impact of fire

retardant additives on material decomposition and combustion during each stage should be understood thoroughly to determine the mechanisms of gas evolution and possible implications on the safety of occupants of fire response personnel.

In the work of Alajberg [64], a rigid PUR foam produced from diphenylmethane diisocyanate(MDI) and poly(oxy-tetramethylene) glycol copolymer was decomposed during non-flaming combustion under the temperatures and atmospheric conditions that were intended to simulate the main stages in fire development. The non-flaming conditions consist of temperatures: 550°C to simulate the (beginning of fire), 750°C (developing fire), 950°C (mature fire); and the atmospheres consist of mixtures of oxygen and nitrogen adjusted to represent air (fire beginning or the presence of good ventilation when the oxygen in the surrounding atmosphere corresponds to the content in normal air), air-nitrogen (1:1) (the state when half the oxygen is already consumed by thermo-oxidation), and nitrogen (the state when the oxygen is completely consumed).

Light gases, organic and condensable volatile organic compounds were produced and identified using GC-MS analysis. Yield of each specie varied depending on the decomposition temperature and the oxygen content in the surrounding atmosphere. Table 2.1 shows the general decomposition products under all the conditions studied. In the present research, conditions similar to those encountered in each stage of fire development will be established in either the cone calorimeter or the smoke density chamber (or both) based on the characteristics of each stage as discussed in the following sections.

Table 2.1: Gaseous Products from Non Flaming Combustion of Rigid Polyurethane Foam

Category	Combustion Products
Inorganic Light Gases	CO_2, CO, HCN, Hcl
Organic Gases	Alkanes
	Alkenes
	Alkadiene [range up to C5]
Volatile Organic Compounds	Isocyanates
	Amines [aniline, toluidine, methyldianiline]
	Nitriles [cyanobenzene, cyanotoluene]
	Nitrogen-containing heterocyles
	Aromatics [toluene, ethylbenzene, xylene, styrene, methyl styrene]
	Fused aromatic compounds [indene, naphthalene, acenaphthalene, fluorene, phenanthrene, anthracene, pyrene]

2.4.1 Stage I: Thermo-oxidative pyrolysis

The first stage in exposure of polymeric materials to fire conditions may involve thermal decomposition of the material, usually in well ventilated conditions, closely followed by additional oxidation, ignition and combustion. Generally speaking, thermo-oxidative decomposition of polyurethane foam is an irreversible chemical scission of the long polymer chains due to exposure to sufficient heat in the presence of oxygen in the air. It has been established amongst earlier researchers that the general decomposition pathways of rigid PUR foams in both oxidizing and inert atmospheres occur by a combination of three independent mechanisms [62, 65-67]. It begins with a primary scission reaction of the material to an isocyanate and

polyol(s) followed by a complex series of secondary reactions. Subsequent intermediate mechanisms of decomposition depend upon the specific structure of the polyurethane foam, while detailed combustion behaviour and products also depend on other conditions such as ventilation and temperature. The proposed mechanisms for each step are as follows:

i). Dissociation of urethane to isocyanate and alcohol

$$R-\underset{\underset{H}{|}}{N}-\overset{\overset{O}{||}}{C}-O-R' \longrightarrow R-N=C=O + OH-R' \qquad (4)$$

Urethane   isocyanate   Alcohol
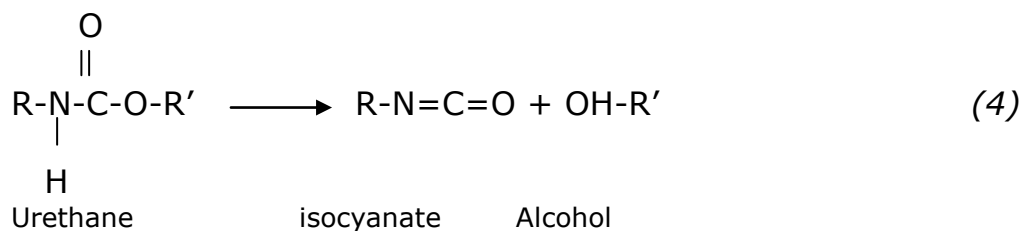
ii). Dissociation to primary amine, olefin and carbon dioxide

$$R-\underset{\underset{H}{|}}{N}-\overset{\overset{O}{||}}{C}-O-CH_2-CH_2-R' \longrightarrow [R-\underset{\underset{H}{|}}{N}-\overset{\overset{O}{||}}{C}-OH] + CH_2=CH-R'$$

Urethane   Olefins

$$R-NH_2 + CO_2 \qquad (5)$$
Primary amine
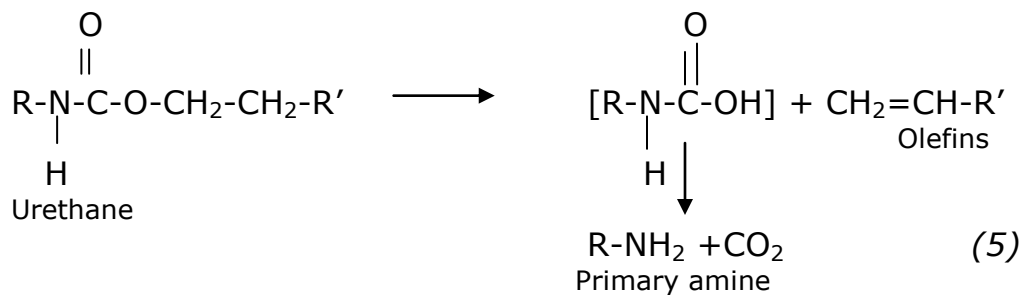
iii). Elimination of carbon dioxide, leading to the formation of a secondary amine

$$R-\underset{\underset{H}{|}}{N}-\overset{\overset{O}{||}}{C}-O-R' \longrightarrow R-\underset{\underset{H}{|}}{N}-R' + CO_2 \qquad (6)$$

urethane   secondary amine
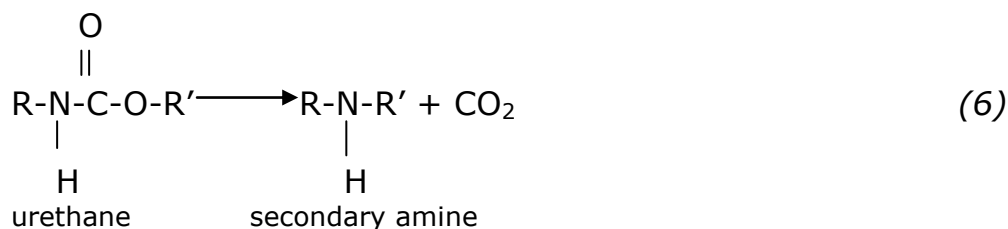
Simultaneous occurrence of the three reactions during thermal degradation of a urethane of phenyl-isocyanate and 1-phenylethanol in a nitrogen atmosphere at 300°C was reported by Dyer et al. [65]. Secondary reactions,

which are likely to occur under all conditions, may lead to formation of products such as urea, allophonate, biuret, trimers of isocyanate and carbodiimide [68]. The isocyanate functional group (-NCO) is one potential source of nitrogen-containing decomposition products. Therefore, pyrolysis or flaming combustion under conditions of high O_2 concentration and temperature will lead to the generation of nitrogen oxides [62].

In his work, Backus et al. [66], observed that, with sufficient oxygen, the urethanes do not dissociate to isocyanate but oxidize to less toxic amines, olefins, and CO_2. He studied the degradation of rigid polyether and polyester based PUR foams in air using thermo-gravimetric analysis (TGA), differential thermal analysis (DTA) and infrared spectroscopy of both char and volatile products. Results agreed in general with the processes noted above and indicated that the formation of chars on urethane foam in air involved oxidation to a more stable structure. The array of products found was considerably increased in the presence of oxygen since bonds other than the urethane linkage are broken and reactions of the resulting degradation products occur, particularly under conditions of high temperature. In terms of fire retardants, Backus et al. noted that the introduction of phosphorous based FR agent to the base foam lowered the reaction temperature, which enhanced solid char formation and decreased formation of flammable products during thermal decomposition; suggesting that the composition under study formed an effective fire retardant.

In another study conducted by Woolley and his co-workers [69], thermal decomposition of rigid polyurethane foams containing organo-phosphorous compounds was studied in both air and nitrogen over the temperature range 200 to $1000^{\circ}C$ in a reaction furnace and using elemental analysis and gas chromatography. The general decomposition mechanisms were determined

to involve a preferential release of some of the polyol content followed by an apparently uniform fragmentation of the polymer matrix to release particulate material. This particulate material (smoke) appears to volatilize from the furnace zone at temperatures up to 600°C but decomposes above 700°C to generate the typical family of nitrogen containing products of low molecular weight (hydrogen cyanide, acetonitrile, acrylonitrile, pyridine and benzonitrile) that have also been observed during decomposition of flexible polyurethane foams [69].

In general, the primary volatile organic compounds (VOCs) which have been previously observed during thermo-oxidative degradation and combustion of fire retarded and non-fire retarded rigid polyurethane products include propene, acetaldehyde, acetone, acetonitrile, benzonitrile, 2-ethylhexanol, benzene, toluene, xylene, styrene and benzofuran [62,64,66]. The generation of these products is supported by the general decomposition mechanisms of PUR foam which involves steps such as dissociation of the long PUR chains into carbon dioxide, olefins and amines as highlighted above. The presence of diaminodiphenyl-methane during thermal decomposition or combustion of rigid PUR foams is an indication of an MDI base foam, since diaminodiphenyl methane is used in the preparation of isocyanates and polyisocyanates and therefore, is a key component in the production of MDI-based rigid polyurethane foam formulations [70].

Under well ventilated conditions in which the oxygen level is relatively high, while the reaction temperature is fairly low (between 250–300°C) [66], many components of the polyurethane base foam can be identified from the composition of evolved gases, and evolution profiles of selected components can be related to structure of the polymer [71]. In her review of gaseous products generated from pyrolysis and combustion of rigid polyurethane foams, Paabo et al. [62] noted small scale tests which were performed on

rigid foams under conditions akin to non-flaming oxidative pyrolysis which represented early stages of a fire in which oxygen levels were relatively high (>16%) and heat flux low (25kW/m^2). Under such conditions, she observed volatile product profiles were very complex, containing chemical species such as hydrocarbons, aldehydes, ketones and nitrogen-containing compounds [62]. This suggests that the decomposition process leads to the continuous generation of smoke and potentially flammable volatiles from the material until the flammability limit and auto ignition temperature of the fuel vapours is reached. The amount and type of volatile compounds depend on the specific local ambient and chemical conditions, but the components are generally rich in partially decomposed organic molecules, many of which may be irritants, as well as carbon monoxide and smoke particulates.

Table 2.2, taken from [62] shows a compilation of the thermal degradation products identified from thermal decomposition studies of rigid polyurethane in air. This review paper [62] compiles the results of various studies conducted over a wide temperature range, 220-750°C, in a tube furnace and glass reaction vessel with volatile gases identified by various analytical techniques such as infrared spectroscopy (IR), nuclear magnetic resonance (NMR) and GC/MS. The composition of these products depends largely upon the initial formulations of the foam and the thermal degradation conditions such as temperature, oxygen availability, ventilation and nature of FR additives. In all cases, pyrolyzed gaseous products are very complex due to inefficient oxidation of the material and high production of CO such as might be seen at an early stage of a fire. Through these studies, thermal decomposition of polymers, particularly polyurethane foams, has been found to be dependent on the following factors: type of polymer, atmosphere, heating rate, oxygen concentration, and catalysts used in the production, fire retardants, and other parameters [72].

Table 2.2: Thermal degradation products produced from rigid PUR foam under oxidative atmosphere [62]

1	Acetaldehyde	40	Ethylene oxide
2	Acetamide	41	4-Ethyl-1 -phospha-2,6,7-trioxabicyclo [2.2.2] octane-1 – oxide [bicyclic phosphate ester]
3	Acetic acid	42	4-Ethylquinoline
4	Acetone	43	Formaldehyde
5	Aacetylene	44	Formamide
6	Acrolein	45	Hydrocarbons (C4)
7	Alkene	46	Hydrocarbons(CxHy)
8	Ammonia	47	Hydrogen bromide
9	Aniline	48	Hydrogen chloride
10	Aniline hydrochloride	49	Hydrogen cyanide
11	Benzene	50	Hydrogen fluoride
12	Benzoquinoline	51	Indazole
13	Butyraldehyde	52	Indole
14	Carbazole	53	Methanol
15	Carbon dioxide	54	3-Methyl benzoquinoline
16	Carbon monoxide	55	Methyl ethyl ketone
17	Carbon tetrachloride	56	Methyl quinoline
18	Chlorine	57	Nitric oxide
19	Chlorobenzene	58	Nitrogen dioxide
20	Chloroethanol	59	Nitrogen oxides
21	Chloroethylene	60	3,8-Phenathroline
22	Chloroisopropanol	61	p-Phenylenediamine
23	Chloromethane	62	N-phenyl P-toluidine
24	Chloropropylene	63	Polycyclic aromatics

25	4,4'- Diamino dimethyl diphenylmethane	64	Propane
26	4,4'- Diamino diphenylmethane	65	n-Propanol
27	4,4'- Diamino methyl diphenylmethane	66	Propylene
28	4,4'- Diamino trimethyl diphenylmethane	67	Propylene oxide
29	Dichlorobenzene	68	Quinoline
30	Dichloroethane	69	Toluene
31	Dichlorofluoromethane	70	2,4-Toluenediarnine
32	Dimethyl benzoquinoline	71	Toluene monoisocyanate
33	2,6-DimethyI quinoline	72	Toluidine
34	Dimethyl toluidine,	73	Toluidine hydrochloride
35	1,4-Dioxane	74	N-tolyl butylurethane
36	Diphenylamine	75	Trichlorofluorornethane
37	Dipropylene glycol methyl ether	76	Trichloroethyl phosphate
38	Ethane	77	Trimethyl benzoquinone
39	Ethanol	78	Tripropylene glycol methyl ether
		79	Ethylene

However, information on specific toxic gases produced from rigid polyurethane foam at this stage in fire development is scanty, and in some cases not very well documented. Better understanding of the complex interactions requires a systematic study of the decomposition behaviour of a single base foam formulation with different levels of commonly used fire retardant additives under various fire conditions as is proposed in the current study.

More detailed investigation of the gases evolved during thermal degradation is particularly important in the case of fire retarded foams since fire growth in these foams may be delayed, leading to increased concentrations of the

decomposition products in the smoke produced during the early stages of a fire. Such data could also assist in the design and optimization of new FR foam formulations through enhanced understanding of the thermal decomposition pathways undergone by foams containing different amounts of each of the key fire retardant additives. These will form a large focus of the present research.

2.4.2 Stage II: Fully Developed Fires

Upon ignition, the fire begins to grow and, if it is not suppressed, can grow in size until all combustible materials within the compartment are involved. Once flaming combustion begins, radiative heat transfer and energy released in the reaction zones will continue to drive the combustion reactions by increasing the temperature and hence the key reaction rates. In well ventilated conditions (those in which there is more oxygen required than is needed to sustain efficient combustion), this will drive the oxidation reactions towards completion, generally favouring the production of carbon dioxide over that of carbon monoxide so that under these conditions, the profile of combustion products may be relatively less complex, consisting of more thermally stable organic compounds such as aromatics [62].

This concept was supported by an experiment conducted by Ball et al. [74] in which a flame-retarded rigid polyurethane foam was burned under flaming conditions in a 23 m^3 room. The combustion products were analyzed by GC/MS and Infrared spectroscopy. Table 2.3 shows a list of organic compounds that were detected. Therefore, contrary to chemical species produced during thermo-oxidative decomposition which are generally characterized by partially oxidized, higher molecular compounds as indicated in Table 2.2, flaming combustion tends to produce compounds that are relatively less complex and more stable compared with those produced under thermal decomposition conditions.

Table 2.3: Combustion products produced from flame retarded rigid PUR foam under flaming conditions

1	Acetone
2	Acetamide
3	Ammonia
4	Ethanol
5	Carbon tetrachloride
6	Trichlorofluoromethane
7	Methane
8	Aniline
9	Toluidine
10	Toluene
11	Benzene
12	Dichlorobenzene

At the same time, as the fire grows, the higher heat flux to the surface of the fuel will result in increased vapourization and pyrolysis of fuel. This may then lead to conditions of fuel controlled burning in which there is no longer sufficient oxygen to sustain efficient combustion, in turn resulting in decreasing temperatures and increased concentrations of carbon monoxide and other organic gases in the hot combustion products. A point may also be reached in fire development when there is a sudden transition between a growing and a fully developed fire, often marked by the point where flaming combustion rapidly extends throughout an entire compartment. This very dangerous phenomenon is marked by very rapid growth of the fire and is often referred to as 'flashover'. Due to the difficulty in generating characteristic and repeatable conditions of flashover using controlled laboratory fire test equipment, gas evolution during the flashover phase was considered outside the scope of the present research [73]. Instead, investigation focused on the behaviour of rigid polyurethane with the various FR additives in the well and partially ventilated conditions that could be generated in cone calorimeter and smoke density test units.

2.4.3 Stage III: Post Flashover Fires

The final or decay stage of a fire is that stage during which the available fuel is largely consumed or the fire self-extinguishes due to very low concentrations of oxygen in the fire environment. This is usually the longest stage of a fire; however, information on the amount and nature of combustion products that continue to be generated during this stage has been the subject of very limited investigation to date. On the other hand, the nature of the gases produced during this stage of the fire is very important, particularly to fire fighters, fire investigators and others engaged in post fire overhaul operations, as they are invariably exposed to gases produced in the post flashover stages and during suppression of the fire. This stage of a fire is also important since the number of toxic substances is likely to be greater at the lower combustion temperatures characteristic of the latter stages of a fire.

Available information on post-fire environments is mainly focused on wild land and municipal fires. These have been shown to produce toxic gases including carbon monoxide, irritant gases, carcinogens, polycyclic aromatic hydrocarbons and respirable particles to which fire fighters are exposed [63]. In her work, Austin [75] conducted a study on the exposure of municipal firefighters to toxic gases and vapours and identified three potential carcinogens (benzene, 1,3 butadiene and styrene) which accounted for 25% of the 123 VOCs found in the post-fire environments in the study. Therefore, more detailed investigation of the gases evolved during this stage in fires involving rigid polyurethane foams is important since these foams may become involved in the later stages of a fire and it is presently not clear which gases will be produced or in what combination under these conditions.

2.5 Fire Performance Characteristics

From the discussion above, it is clear that different combinations of compounds are generated from rigid polyurethane foams depending on the local conditions under which they are burned and therefore, the conditions in which testing is carried out. The potential variability in results is exacerbated because the relative fire performance of materials is assessed using a wide variety of test methods depending on the performance indicator under test, as well as the intended application of the material and the geographic area for which the testing is required. These different test conditions will mimic more or less closely the environmental conditions that might be encountered during the early growth stages of a fire, during ventilated or poorly ventilated burning of a fuel or during the fire decay.

For example, the cone calorimeter test has recently been recognized as one of the most important tools for measuring parameters that relate to potential fire hazard of a material or product that is subjected to a constant incident radiant heat flux under well ventilated conditions [76]. It is mainly used to measure the heat release rate (HRR) of a material exposed to a constant incident heat flux under well ventilated conditions and, as such, can be used to mimic the environment that might be encountered during any of the three stages of a fire when those conditions remain well ventilated. HRR of the burning material is determined using measured concentrations of oxygen, carbon dioxide and carbon monoxide and the principle of oxygen depletion calorimetry, which is based on Huggett's principle that the gross heat of combustion of any organic material is directly related to the amount of oxygen that is consumed during combustion of that material. For most hydrocarbon materials, the average value of heat released is 13.1 MJ/kg of oxygen consumed; a value which is accurate to within $\pm 5\%$ for a wide range of materials and that has long been used for practical applications [77].

During operation, the cone calorimeter is quite versatile because a sample is exposed to a constant heat flux before ignition and essentially undergoes oxidative pyrolysis while heating to the point of ignition. After ignition, the sample will burn in a well-ventilated environment until the fuel begins to deplete, after which the flaming combustion processes will decay and only the burning/burned residue remains in a fashion somewhat akin to a well-ventilated post-fire environment. Since its beginning, therefore, the oxygen consumption method has been widely used in testing fire performance, whether in small-scale testing of materials samples, room fire tests, laboratory scale heat release rate calorimeters, large scale furniture calorimeters or heat release rate measurements of assemblies in fire endurance furnaces.

Closely related to the cone calorimeter test is the smoke density chamber test, in which a material or product is subjected to a constant incident radiant heat flux in a sealed chamber such that pyrolysis gases and smoke gradually build up in the chamber with time. In contrast to the cone calorimeter, the test environment in the smoke density chamber more closely mimics conditions that might be encountered in a poorly ventilated fire situation. Since these are the test systems to be used in the present study, the concepts behind, and key parameters measured by, each are discussed below. Details of the experimental systems used in this research, and their particular theory of operation, are covered in Sections 3.2.1 and 3.2.2 respectively.

Key parameters measured in one or both of the cone calorimeter and smoke density tests include heat release rate (HRR), total heat release (THR), mass loss rate (MLR), time to ignition (t_{ig}), carbon monoxide (CO) and carbon dioxide (CO_2) production, specific extinction area (SEA), smoke toxicity index and specific optical density. Measured peak values of these parameters are often considered as a basis upon which to rank a set of materials in

terms of the best to worst performance that might be encountered in a real fire scenario; however, scaling or extrapolation of the small-scale test results to estimation of material performance in larger fires or real fire scenarios is not scientifically predicated to date. Nonetheless, all of these parameters are important in this study since together they provide indicators of the fire performance of the various rigid PUR foams under study.

Amongst the parameters measured in the cone calorimeter, heat release rate (HRR) is regarded as the single most important fire property. As a result, its measurement and control has generated great interest amongst fire researchers [78]. It provides an indication of the potential size of a fire, the rate of fire growth, the time available for escape or fire suppression, and to some degree perhaps even the release of smoke and toxic gases, which have been suggested to increase with increasing HRR and other parameters that might be used to define fire hazard [79]. Since heat release rate serves as the driving force for many other properties of a fire, it is commonly linked to an overall measure of fire hazard.

There are three useful measures derived from measurement of the heat release rate of a material versus time after exposure to the incident flux. These are the peak heat release rate, the time to peak heat release rate and the average heat release rate. The peak heat release rate (pHRR) is defined as the maximum heat release rate measured at any time during the test period. It provides a measure of the anticipated intensity of a fire that would result due to involvement of the material under test in a real fire scenario. Therefore, from the perspective of energy output, the lower the pHRR value, the better the performance of the material in the case of fire.

The time to peak heat release rate is the time between ignition and the peak in the measured HRR curve. It provides a measure of the speed of fire growth; or of how quickly a fire involving the material of interest might

43

develop to its most intense stage [60, 78, 80]. On the other hand, the average heat release rate (Ave. HRR) is defined as the integral of the heat release rate over the entire period during which heat is released by the burning sample during the test.

The time to ignition (t_{ig}) is similarly an important indicator of relative flammability of a material since it relates to the minimum time during which the specimen is exposed to a given level of incident heat flux before it ignites and burns, with or without a piloted ignition source. The time taken to ignite a polyurethane foam sample, for example, is a function of several key factors such as imposed heat flux, the cell structure, chemical composition, level and nature of fire retardant additive and geometric configuration of the material [81]. High incident heat flux, or low thermal inertia or weak chemical bonds in a material usually result in faster times to ignition, with consequently greater flammability hazard from the point of view of shorter times to ignition and potentially less time for occupants to escape.

By way of example of the above measures, Figure 2.3 shows traces of the HRR versus time curves obtained during one of the author's experimental studies with two different polyurethane foam samples, one non-flame retarded and the other flame retarded. Sample *a1* is non-flame retarded with a time to ignition of around 6 seconds. Following ignition, is the measured HRR which rapidly increases to a peak value and subsequently decays slowly over time. Sample *d3*, which is flame retarded, took 74 seconds to ignite but once ignited, the HRR again grew rapidly, this time to a higher peak value than that seen for sample *a1*, and again decayed over time. The figure underscores the difference in ignition times and measured HRR profiles between two specific non-fire retarded and fire retarded foam samples. In terms of life safety, the foam with the longer ignition time should allow occupants more time to escape; however, there may be toxic

gases emitted during the long pre-ignition period and, in the case shown in Figure 2.3, the ignition delay also comes at the cost of a higher peak heat release rate, albeit persisting for a shorter time than the peak values of HRR measured for the non-fire retarded material. The generation of the HRR occurring over the burning period defines the average HRR and also helps put the overall fire hazards of the two classes of materials into perspectives.
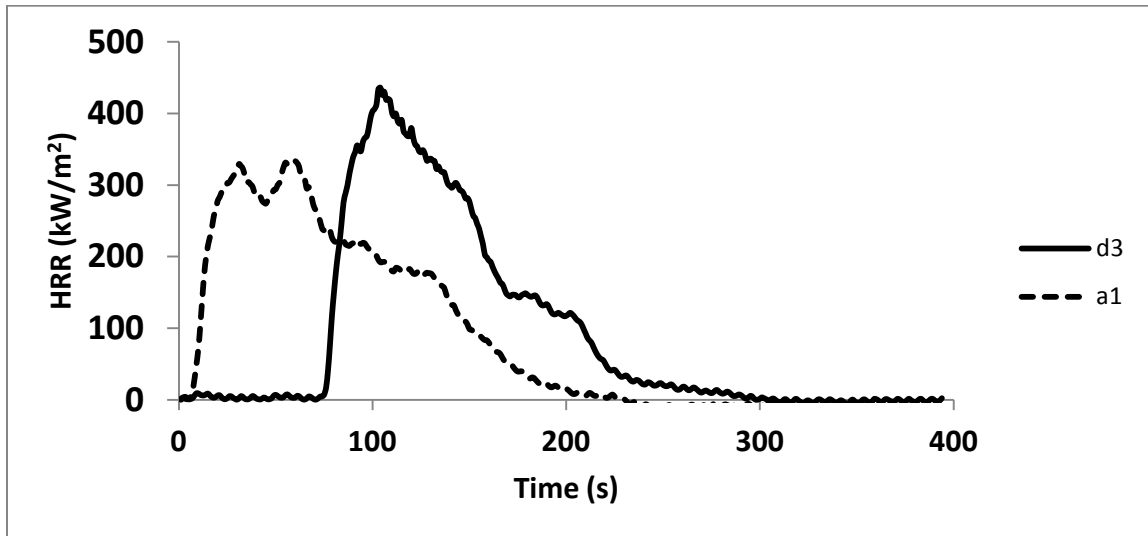
Figure 2.3: Comparison of HRR profiles and times to ignition between non FR (*a1*) and FR (*d3*) foam samples

2.6 Combustion Products

Once a fire occurs, flames, heat, smoke and toxic gases are produced, accelerate upwards within the fire room due to buoyancy and spread along the ceiling, finally exiting through any openings out of the room. Any occupants in the building, depending on their location with respect to the fire compartment, may be exposed to the combined effects of these products. In reality, very few fire fatalities are due to direct contact with the flames from the fire; instead, exposure to hot and potentially toxic combustion products is by far more dangerous. Approximately 76% of fire fatalities are attributed

to inhalation of toxic combustion products, such that the generation of smoke in the event of fire in polymeric materials, particularly in enclosed places, is a matter of great concern [7]. At the same time, the compositions of the toxic products that are directly responsible for fire deaths are not well known because analysis of the post fire environment is difficult and detailed pathological examination of fire victims can rarely be conducted within the time frame required to conclusively determine which combination of toxic gases might have been inhaled [82].
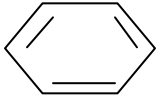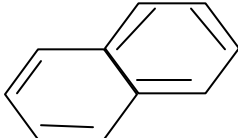
The hazard from the gases produced during a building fire depends not only on the types, density and irritant properties of the gases in the smoke plume, but also on several other factors. These include the combustion properties and chemical composition of the fuel, as well as the quantity of material involved, its configuration and proximity to other combustibles, the source of ignition, the ventilation conditions and the fire temperature, and the volume of the initial fire compartment and any adjacent spaces to which the combustion products may spread. Independent of how the gases are generated, however, most combustion products produce at least one of two major toxic effects when thermally decomposed: (1) asphyxia or narcosis, which causes depression of the central nervous system leading to incapacitation, unconsciousness and death; or (2) irritation, often of eyes and respiratory tract, which causes immediate impairment of vision and acute discomfort. In order to predict the likelihood of these hazards ensuing from exposure to combustion products from materials of certain formulations, more detailed study is needed to understand the impacts of different levels of FR agents on smoke production and nature of gases that may be evolved due to incorporation of FRs at different levels of concentration in a single base foam formulation. Since smoke obscuration, particulate inhalation and toxic gas inhalation occur simultaneously, it is often difficult to state clearly whether any single factor is primarily

46

responsible for the death of a victim. Therefore, in studying the lethality of combustion products, the effects of smoke and toxic gases are generally studied in combination. In the following two Sections, smoke generation and the principal fire gases of interest in the present study are discussed.

2.6.1 Smoke Products

Smoke is a major combustion product in any given fire scenario. It is comprised of a range of airborne solid and liquid particulates that are evolved when a material undergoes pyrolysis or combustion [83]. Smoke aerosols vary widely in appearance and structure, from light colored, for droplets produced during smoldering combustion and fuel pyrolysis, to black solid, carbonaceous particulate or soot produced during flaming combustion [84]. The combustion of natural or synthetic organic materials produces carbon dioxide and water resulting from complete combustion and other gases such as lower molecular weight aliphatic and aromatic hydrocarbons and carbon monoxide resulting from incomplete combustion.

In general, aliphatic structures generate less smoke during combustion than do aromatic ones [85]. It is believed that polycyclic aromatic hydrocarbons (PAHs) are a key intermediate compound in soot formation and a general trend has been established for sooting tendencies of hydrocarbons, which increases from the least to the highest tendency to form soot in the order: alkanes-alkenes-alkynes-low molecular weight aromatics-polycyclic aromatic hydrocarbons [86-87].

n-alkanes	e.g. $CH_3(CH_2)_4CH_3$	[n-hexane]
iso-alkanes	$(CH_3)_2CH.CH(CH_3)_2$	[2,3 dimethyl butane]
Alkenes	$CH_3.CH = CH_2$	[propene]
Alkynes	$CH_3.C =CH$	[propyne]
Benzene Series		[Benzene]
Naphthalene Series		[Naphthalene]

Increasing soot

Smoke can reduce or obscure visibility and cause disorientation, thereby inhibiting both the escape of trapped victims and the rescue actions of fire fighters. The particulates can also be inhaled, causing further irritation and injury to those who may be trying to escape. In parallel to observations on the production of toxic gases from fires discussed above, the smoke production rate and physical properties of smoke depend upon oxygen availability and ventilation conditions, external heat flux applied to the fuel of interest and the specific materials burning and, as with the gaseous products, will vary in composition with time [88].

Smoke density can be measured by both static and dynamic methods. The cone calorimeter, used also for HRR as discussed above, is a dynamic system in which the pyrolysis and combustion products from the material of interest are carried away continuously by a flowing stream of air. Smoke

density in that stream is measured by the change in light obscuration across the gases in the exhaust duct at discrete times and the results are integrated over the duration of the test. Consistent with use of this apparatus for measurement of other fire performance parameters, the smoke density values from the cone calorimeter represent potential smoke production under well ventilated fire conditions. In contrast, the smoke density chamber is a static method in which the optical density of smoke is measured via light obscuration as smoke accumulates within the sealed test chamber as a function of time over the test period. In this way, it is used here to simulate conditions of smoke production representative of those that might be encountered in a poorly ventilated fire situation to allow assessment of material performance across a range of conditions that might be encountered in a typical fire scenario.

In assessing smoke production of a burning sample, specific extinction area (SEA) and specific optical density (Ds) are the two parameters commonly measured; the first in the cone calorimeter and the second in smoke density chamber test respectively. For the cone calorimeter, the specific extinction area (SEA) is a measure of the instantaneous amount of smoke being produced per unit mass of specimen burnt. It varies as a function of time for the duration of the test [89]. An averaged value for smoke production is used since peak values of SEA are particularly sensitive to instantaneous fluctuations in specimen mass loss and therefore, the longer time averaged value is more representative for overall assessment of smoking tendency of a material and therefore fire performance. Depending on the rates of fire growth and smoke production, the lower the average value of smoke density, the easier it is expected to be for people to escape from a fire situation and therefore the better the performance of the material.

In a smoke density chamber, the accumulation of smoke is measured by the obscuration of light from a 6.5 Volt, 2.75Amp tungsten filament lamp positioned to shine a beam vertically through the chamber. The result is expressed in terms of specific optical density (D_s) of the environment as a function of time which indicates the smoking propensity of a given quantity of material as it pyrolyzes and burns in an oxygen limited environment.

2.6.2 Principal Fire Gases

Equally important to smoke generation during pyrolysis and burning of a material is the identification and quantification of the gases produced during various phases of the fire in both ventilated and vitiated conditions. By the very nature of fire, it is a dynamic event in high temperature and sooty environments; generating different fire effluents under different fire ventilation conditions. The gases of particular importance to FR and non FR rigid polyurethane foam fires are CO, HCN, nitrogen oxides, HCl, volatile organic compounds and CO_2, all of which are produced in most building fires [90]. Tables 2.2 and 2.3 contain listings of components previously identified during thermo-oxidative pyrolysis and combustion of rigid polyurethane foam respectively; Table 2.4 contains a compilation of exposure and toxicity threshold values for some key gases generated from FR and non-FR polymeric materials such as rigid PUR foam involved in residential fires. In other work, common gases generated during combustion of polyurethane foams have been identified as carbon dioxide, carbon monoxide, hydrogen chloride, nitrogen oxides, hydrogen cyanide, hydrogen sulphides, acrolein and formaldehyde [9]. The condition under which thermal degradation occurs affects the nature of gaseous products generated even from the same material.

Table 2.4: Common fire gases from polymeric materials involved in residential fires [42]

	Gases From Typical Polyurethane Fires	Lethality of Gases
1	Ammonia (NH_3)	1000 ppm fatal within 10 minutes
2	Hydrogen Chloride (HCl)	1500 ppm fatal within several minutes
3	Phosgene ($COCl_2$)	25 ppm fatal within 30 minutes
4	Acrolein (CH_2CHCHO)	30-100 ppm fatal within 10 minutes
5	Oxides of Nitrogen (NO_x)	200 ppm fatal within 10 minutes
6	Carbon Monoxide (CO)	10,000 ppm exposure fatal within 1 minute
7	Carbon Dioxide (CO_2)	70% concentration fatal within several minutes
8	Hydrogen Cyanide (HCN)	450 ppm fatal within 9 to 13 minutes
9	Hydrogen Sulphide (H_2S)	400-700 ppm dangerous in 30 minutes
10	Sulphur Dioxide (SO_2)	500 ppm fatal within 10 minutes

For instance, in the study that Michal conducted [91], he evaluated the generation of CO from a number of polymeric materials, including rigid polyurethane foam, under different oxygen concentrations in order to simulate real-fire conditions in which the O_2 concentration in the atmosphere can vary widely. It was found that the amount of CO generated from rigid polyurethane foam decomposed in the flaming mode under limited O_2 conditions in a combustion chamber set at temperatures between 500 and 800^0C varied from 0.012 - 0.015% (120-150ppm).

Another study conducted by Bott et al. [92] found that small quantities of CO and HCN were generated from decomposition of highly cross-linked isocyanate-based rigid polyurethane foam under nitrogen and air atmospheres in a tube furnace over a temperature range of 300-750°C. The volatile gases were analyzed using Draeger tubes, infrared (IR) and mass spectrometric (MS) techniques. The results obtained in air and nitrogen atmospheres show that the generation of CO and HCN are dependent on the amount of air introduced and temperature.

All of the interactions between the combustion processes and the global fire environment must be considered together during identification and determination of the concentration of combustion gases from polyurethane foams. In order to better investigate these complexities, it is necessary to assess the gases generated under controlled thermal exposure in both well ventilated and poorly ventilated conditions using a single formulation of base polymer mixed with specific quantities of key additives of interest. Such studies have only rarely been undertaken for any polymer to date [25]. Instead of undertaking in-depth studies into the details of potential toxic gas generation from a matrix of material formulations exposed to various heat flux and fire ventilation conditions, many researchers have used measurements of the concentrations of only one or two major combustion gases as indicators of the potential toxicity of a material in the event of a fire [6]. These measurements commonly include carbon monoxide and carbon dioxide, which are then related back to smoke production tendency [58], or are sometimes coupled with identification or concentration measurements of other species such as unburned hydrocarbons, volatile organic compounds, oxides of nitrogen or others frequently probed during research on engines or other controlled combustion processes [93].

While most studies are focused individually on the identification and time-averaged concentrations of gaseous products from thermal decomposition and combustion, the current study takes a further step over the existing work by determining the key fire gases at the three characteristic stages of fire development (pyrolysis, steady burning and post-fire), under different ventilation conditions and for varying levels of fire retardant added to the same base foam resins. With this in mind, the reasoning and importance behind measurements of each of the broad categories of gaseous species is briefly discussed below with reference to whether or not it is currently

included as part of the cone calorimeter test method used in the present study.

2.6.2.1 Reduced Oxygen Concentration (O_2)

One important factor in a fire environment is the absence of oxygen, rather than the release of oxygen due to burning or pyrolysis of polymeric materials. The rate of burning, the combustion efficiency and the yields of specific products are influenced by the percentage oxygen in the surrounding atmosphere and the rate at which depleted oxygen is replenished. As the oxygen supply to the fire decreases, the levels of CO and other potential toxic gases increase as the fire progresses. Because of its primary role in the cone calorimeter test, oxygen consumption is directly measured during burning of each sample and is used in HRR calculations.

2.6.2.2 Carbon dioxide (CO_2)

Carbon dioxide (CO_2) is the end product of the complete combustion of carbonaceous material and thus must be considered in any fire situation. It is, for the most part, the most abundant product generated during combustion of hydrocarbons under well ventilated conditions [17]. It is used as an indicator of the efficiency of combustion, which, in turn, is sometimes linked to whether burning occurred in well or poorly ventilated conditions. Normal air contains about 300ppm CO_2 ($0.03\%CO_2$) by volume and since it is an important constituent of the physiological process; it is not ordinarily considered to be a toxic gas. Nevertheless, CO_2 can be dangerous in situations where a person is breathing in an atmosphere containing higher than normal CO_2 levels. Because of its primary role in determination of heat release rates, the carbon dioxide yield is directly measured during the cone fire testing and generally presented as amount of CO_2 produced (kg) per kg of fuel burned (kg/kg).

2.6.2.3 Carbon monoxide yield (CO)

Carbon monoxide is generated during combustion of organic substances and, because it is a partial oxidation product, the concentration of CO is sometimes related to incomplete combustion of the material. The incomplete or inefficient combustion of any carbonaceous material will result in greater production of CO than does efficient and complete combustion [17]. Analogous to the use of heat release rate as one of the most important parameters by which to describe thermal hazard and rank fire performance of various materials, potential toxic effects from materials are often ranked in fire performance testing via measurement of only a single species such as carbon monoxide. This is perhaps well justified when one considers that experience has shown that the largest percentage of fire injuries and deaths are due to the generation and inhalation of carbon monoxide [6, 94], although deaths primarily due to HCN have been on the increase [95]. At about 1500ppm of CO, human death can occur within one hour of exposure [96]. Although carbon monoxide presents a severe threat to occupants of a building on fire, it is not well understood how much the generation of this gas is affected by variations in the quantity of FR or other chemical additives in a polymer, nor whether changes in CO concentration can be correlated to increases or decreases in many of the other key toxic species produced during different fire situations [97]. Nonetheless, the amount of CO produced is measured directly in cone calorimeter fire testing as amount of CO produced (kg) per kg of fuel burned (kg/kg).

2.6.2.4 Smoke Toxicity Index (CO/CO$_2$)

The CO/CO$_2$ weight ratio has been used by many fire researchers as a measure of smoke toxicity during fire performance tests since CO is known to be the most abundant toxic fire gas responsible for fire death [6].

Therefore, the greater the ratio, the lower the combustion completeness, and hence, the greater is the potential toxicity of the smoke and consequently the more dangerous the material [59]. However, during incomplete combustion in either flaming or non-flaming modes, many other compounds such as hydrogen cyanide (HCN), oxides of nitrogen (NOx), hydrocarbons, oxygenated organic compounds and nitrogen-containing organic compounds can be produced [62]. Since relatively small amounts of HCN and NO can be lethal, in-depth study into the evolution of effluent fire gases during decomposition and burning of rigid polyurethane foams should go beyond measurement of only the CO/CO_2 weight ratio. Therefore, smoke toxicity index is used as a complementary indicator of the fire environment. With respect to the present study, it will be particularly helpful to understand how this parameter might be directly correlated to variations in the quantity of FR or other chemical additives in PUR foams or to other key toxic species produced during different fire situations.

2.6.2.5 Nitrogen Oxides (NOx)

Nitrogen oxides are generally produced at highest concentrations during high temperature hydrocarbon combustion. Nitrogen oxides have been detected in experiments involving the flaming combustion of rigid PUR foam. In a normal oxygen environment, nitrogen in the combustion atmosphere will undergo oxidation to form nitrogen dioxide. Therefore, any change from pyrolysis to flaming combustion may convert the nitrogen containing decomposition products to nitrogen oxides under high oxygen and temperature conditions [62]. Since they have been found to be toxic [17], it is important that they be measured in combustion processes even though these gases are not measured as part of the standard cone calorimeter test method. Recent work using Fourier transform infrared spectroscopy (FTIR) to analyze fire effluents has shown that nitrogen oxides in fire effluents may

be predominantly nitric oxide (NO) and that, this gas may be relatively stable at low concentrations and temperatures of inhaled fire effluents [98-99].

It is therefore, of interest to examine how the concentrations of nitrous compounds vary amongst materials with different levels of FR under the wide range of thermal and ventilation conditions that might be encountered in fire situations. There are many other potential toxic gases produced during pyrolysis and combustion under different conditions, such as HCN and SO_2 which are not considered in the present work, although they have been the subject of previous studies [25,100].

2.6.2.6 Organic Compounds

Measurement of the unburned total hydrocarbons during combustion of a fuel is potentially of interest as a global indicator of potential hazard since the concentration of total unburned hydrocarbons (UTH) in the hot gases relates to the efficiency of decomposition and combustion of the fuel. Existence of unburned hydrocarbons, even if specific species are not identified in detail, indicates the potential existence of toxic hydrocarbon combustion intermediates as well as the possibility for the hot gases to re-ignite, portending serious danger to a trapped victim or to a fire fighter. Although general characteristics of burning of rigid polyurethane foam in air have been studied over a wide range of temperature and ventilation conditions, however, few detailed analyses of the composition of the combustion products have been done. It has been observed that thermal degradation and combustion of polyurethanes do produce a mixture of saturated and unsaturated aliphatic hydrocarbons and aromatic compounds having a wide range of molecular weights, including alkenes, acids, alcohols, aldehydes, nitriles and polycyclic aromatic hydrocarbons (PAH), each contributing to the overall fire environment [17]. Specific lower molecular

weight species such as propene, acetone, acrolein, formaldehyde and acetaldehyde have been seen along with aromatics such as benzene, toluene and xylenes [25,101-102]. For the most part, however, interest has centered on assessment of generation of only a subset of the common toxicants, such as HCN and CO and NO_x [62].

More detailed investigation of combustion products has been conducted in fires fueled by materials such as wood cribs, cotton towels and hydrocarbon pool fires with much less work available for even these same species in fires involving rigid polyurethane foams as fuel [103-104]. Although detailed analysis of combustion products is not widely developed for polyurethane foam fires, such detail is of interest since, apart from the potential toxic nature of the volatile organic compounds, information about the identity and quantity of the various volatile organic compounds that are generated from various foam formulations under different fire conditions will potentially provide more insight into the effects of differing types and quantities of FR additions on the molecular mechanisms of degradation of the polymer systems.

Stauffer *et* al. [105-106] investigated the effects of increasing levels of flame retardants on the smoke and toxic gases produced by polyester resins which are typically used in polyurethane base foam formulations. As samples were decomposed in the NBS Smoke Chamber, they observed that as the quantity of brominated flame retardant increased, the production of CO_2 declined, while the production of CO, HBr and total hydrocarbons increased. They also found that, based on the amount of material decomposed, O_2 consumption also decreased with increasing bromine concentration in the substrate. While the exact nature of the decomposition products depended on the specific polyester under test, they concluded through pyrolysis under

vacuum or in an inert atmosphere that the polyesters decomposed into a large number of high and low molecular weight fragments. Further, increasing the temperature of pyrolysis increased the amount of low molecular weight fragments at the expense of the higher molecular weight fragments. The use of air as the decomposition atmosphere also resulted in decreased production of high molecular weight fragments with increasing temperature [107].

Other studies have shown that measured quantities of lower molecular weight degradation products decrease with increasing addition of phosphorous-based and expandable graphite flame retardants, thereby leading to enhanced flame retardancy of a polymer system [54]. In addition, it has been shown that expandable graphite FR addition appears to improve fire performance because aromatic units are retained in the polymer matrix even with addition of low concentrations of 15% EGFR [60]. At the same time, only the smaller units such as aliphatic oxygenated functional groups are volatilized during decomposition and combustion of EGFR rigid polyurethane foams [54].

To build on existing knowledge, the current work will examine the impacts of varying levels of different fire retardants on fire behavior, smoke development and composition of gases evolved during pyrolysis and combustion of rigid polyurethane foam of consistent base foam formulation. The combined results will increase our understanding of molecular mechanisms of decomposition and combustion of fire retarded rigid PUR foams under differing thermal exposure and ventilation conditions.

2.7 Gas Generation Methods

One reason that there have been few detailed studies of gases generated during thermal pyrolysis and burning of materials is that characterization of fire gases and toxicity testing are accompanied with great challenges. Extreme care must also be taken to control as many parameters as possible during testing in order to obtain consistent results over time. Nonetheless, over time many ways have been developed to approach a field as complex as fire effluent characterization. Figure 2.4 summarizes the different fire performance test methods and analytical gas detection methods that are employed around the world to assess toxicity of effluents from materials used in transportation applications [108].
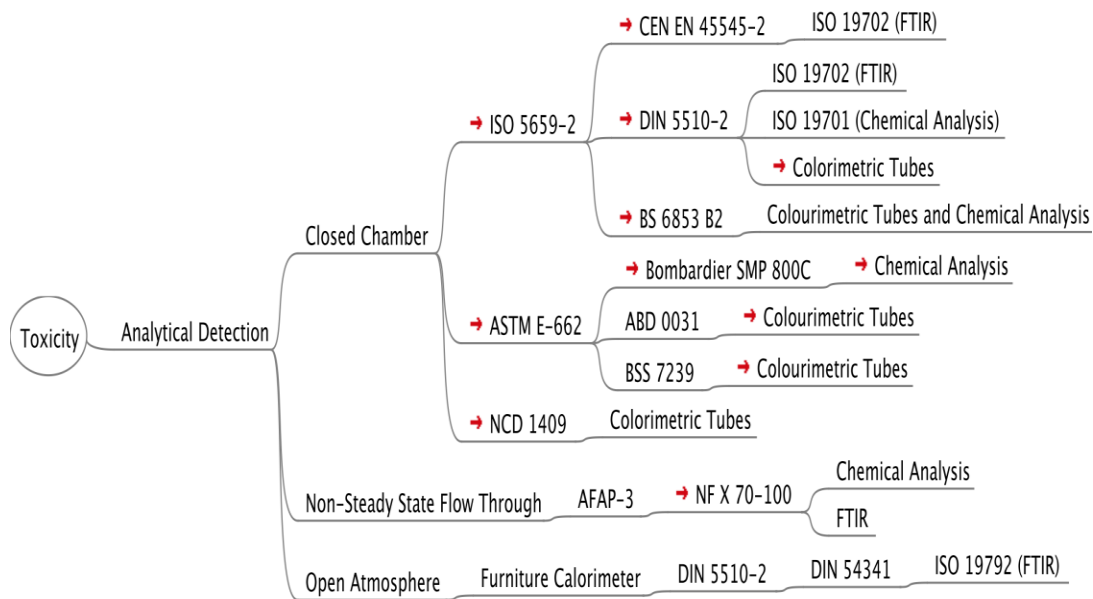
Figure 2.4: Key Fire Toxicity Test Designs [108]

As can be seen from the figure, various methods have been adopted over the years to both generate the fire effluents and to identify and measure concentration of the gaseous products that are evolved during thermal

decomposition and combustion of the samples. It can be seen from Figure 2.4, that fire gases are usually analyzed using one of three broad categories of analytical detection schemes: colorimetric tubes, Fourier Transform IR Spectroscopic analysis or using a complex suite of analytical chemistry techniques, including gas chromatography, mass spectrometry and other more complicated methods. These are consistent with the main techniques outlined in the literature [29, 101, 107]. While methods such as FTIR and GC-MS permit the use of multiple detection schemes for more comprehensive characterization of fire gases, there are significant differences in the effectiveness and efficiency of these analytical techniques when applied to analysis of combustion gases. There are also many divergent views which hold sway on which toxic gas measurements are most appropriate, or how to conduct such measurements, and how well each test method might simulate real fire scenarios [95, 109]. With due consideration of all the above factors, the gas analysis methods used in the current study are discussed in Section 3.4, following a more complete description of the rigid polyurethane foam formulations studied and the fire performance test methods utilized.

Chapter Three: Experimental Apparatus and Techniques

Two main categories of equipment were used in this study, namely: fire performance test systems and gas analysis systems. Standard fire performance tests were conducted using the cone calorimeter and smoke density chamber which are available at the University of Waterloo Live Fire Research Facility (UWLFRF). Gas analysis was performed using a variety of different analytical techniques such as dispersive and non-dispersive infrared analysis, chemiluminescence, flame ionization detection, gas chromatography and mass spectrometry to monitor the concentration of various combustion products (CO, CO_2, NOx, UTH and VOCs) that evolve from flame retarded rigid polyurethane foams. Due to numerous challenges associated with chemical analysis of fire gases, no one analytical technique was found to allow for a full quantitative and qualitative analysis of all the combustion products that were present during these tests. This chapter provides information on the materials and sample preparation, as well as background on the fire performance tests and gas analysis systems used in the research.

3.1 Materials and Sample Preparations

The base foam used for the samples studied in this research was a methylene diphenyl isocyanate (MDI)-based rigid polyurethane foam intended for application as building insulation. Specific details of the base foam are of a proprietary nature since it was a commercial product obtained from a local foam manufacturer; however, Table 3.1 does present the global chemical composition of the virgin foam.

In addition to the isocyanate, the foam contains 40 parts Mannich polyol to 60 parts polyester polyol, as well as the catalysts and surfactants necessary for production of the sample. The Mannich polyester polyols are a group of

aminic polyols with an aromatic structure containing a high content of tertiary nitrogen, and are therefore extremely reactive in the foaming process [110]. They are used because they react with increased compatibility with isocyanates to obtain rigid polyurethane foams with good physico-mechanical, thermal and superior flammability performance [110]. The use of Mannich polyols comes with some trade-off, however, since while their aromatic content tends to promote char formation [111-112], higher portions of Mannich polyol relative to polyester polyol will also lead to increased smoke generation from burning foam samples [112].

Table 3.1: Base rigid polyurethane foam formulations

Materials	Relative Amount
Resin mix:	
i). Polyester ⎫ *Polyols* ii). Mannich ⎭	60 parts ⎫ 40 parts ⎭ = 100 parts polyol
iii). *Water*	3-4 parts pphp (parts per hundred polyol)
iv). *Catalysts*	1-2 parts pphp (parts per hundred polyol)
v). *Surfactant*	0.5-1 parts pphp (parts per hundred polyol)
Isocyanate:	Polymeric MDI 100-120

For the current research, this base foam was used to custom-fabricate four different classes of material. Most studies to date have examined FR concentrations of between 5-30%wt [23, 30]. For the foam samples considered here, examination of FR concentrations between 0-30%wt in increments of 10% were recommended by the foam manufacturer. Of that range, preliminary studies indicated that concentrations of 0, 10, 20%wt

would form a practical range; being a manageable number of tests from the research perspective.

a) Non Fire Retarded **(NFR)** base foam samples contain no fire retardant additives and therefore serve as the control and reference foam formulations for comparison with samples containing 10% and 20% fire retardant additives.

b) Brominated Fire Retardant **(BFR**) foam samples containing 10% and 20% brominated fire retardant additives in the base foam. This class of material is intended to represent a conventional halogenated fire retardant system in which bromine acts as a gas phase combustion inhibitor by interfering with reaction intermediates and slowing the combustion process [29].

c) Phosphorous Fire Retardant **(PFR**) foam samples containing 10% and 20% phosphorous-based fire retardant additive in the base foam. Phosphorous is a non-halogenated flame retardant additive that has been used in rigid polyurethane foam for many years and is known to be active in the condensed and/or vapour phase. In the condensed phase, it promotes formation of a cross-linked reinforcing network of carbonaceous structures and surface char which restricts the transfer of heat to the interior of the foam and obstructs the outward flow of combustible gases generated during thermal degradation of the polymers [29, 54]. Consequently, fewer volatile and combustible vapours are available to support combustion of the PFR sample. In addition, PFR can also volatilize and form active radical species such as PO_2*, $PO*$, and $HPO*$ which act as scavengers of the highly reactive $H*$ and $OH*$ radicals, further decreasing the efficiency of, or even inhibiting those reactions that drive hydrocarbon combustion [47].

d) Expandable graphite fire retardant **(EGFR)** foam samples containing 10% and 20% expandable graphite intumescent additives in the base foam. Upon exposure to heat flux, expandable graphite forms a carbonaceous polymeric layer at the burning surface which inhibits the diffusion of oxygen and heat into the polymer matrix and the outflow of combustible vapours, again inhibiting combustion of the material [54].

Samples of each of the above formulations were prepared using hand mixing techniques and cast into molds of dimension 260 x 260 x 60mm. As a result of this preparation method, it was difficult to obtain homogeneous density through the entire foam slab. From the resulting slabs, specimens of 100 x 100 x 25mm and 75 x 75 x 25mm were cut for cone calorimeter and smoke density tests respectively. Measurements of the dimensions and mass of each sample showed that the foam had a high average density relative to commercial products, ranging from 60 to 68kg/m^3.

3.2 Fire Performance Test Methods

Samples were tested in the cone calorimeter and smoke density chamber in order to determine their general fire performance parameters, such as total heat release, peak heat release rate, smoke density and other parameters discussed in Section 2.5. At predetermined times during the fire performance testing, gas samples were collected and analyzed, on and off-line, to identify key compounds contained in the product gases at those stages of decomposition/burning. The layout and theory behind each of the performance test methods is discussed in the next sections followed by more detail on the sampling methodology and analysis techniques employed.

3.2.1 Cone Calorimeter Test Method [ASTM E 1354]

The cone calorimeter fire performance test method prescribed in ASTM E 1354 was used in this work for assessing the fire behaviour and exhaust gas

generation from samples of each material under well ventilated conditions. This method facilitates the study of ignition and burning characteristics (i.e fire performance) of a material in a fashion which mimics some of the complexities of full scale burning behavior of a polymeric material using tests conducted at the bench scale. The cone calorimeter, therefore, is not just an apparatus for measuring the rate of heat release from a material; it has become an important tool for characterizing some aspects of the combustion chemistry of materials and products [113].

The cone calorimeter test apparatus was first designed in 1982 to what is now known as the National Institute of Standards and Technology [114]. Since that time, the cone calorimeter has become commercially available and its popularity has grown due to its flexibility and wide range of uses. Figure 3.1 shows a detailed schematic of the FTT cone calorimeter used for this study and housed at the University of Waterloo Live Fire Research Facility.
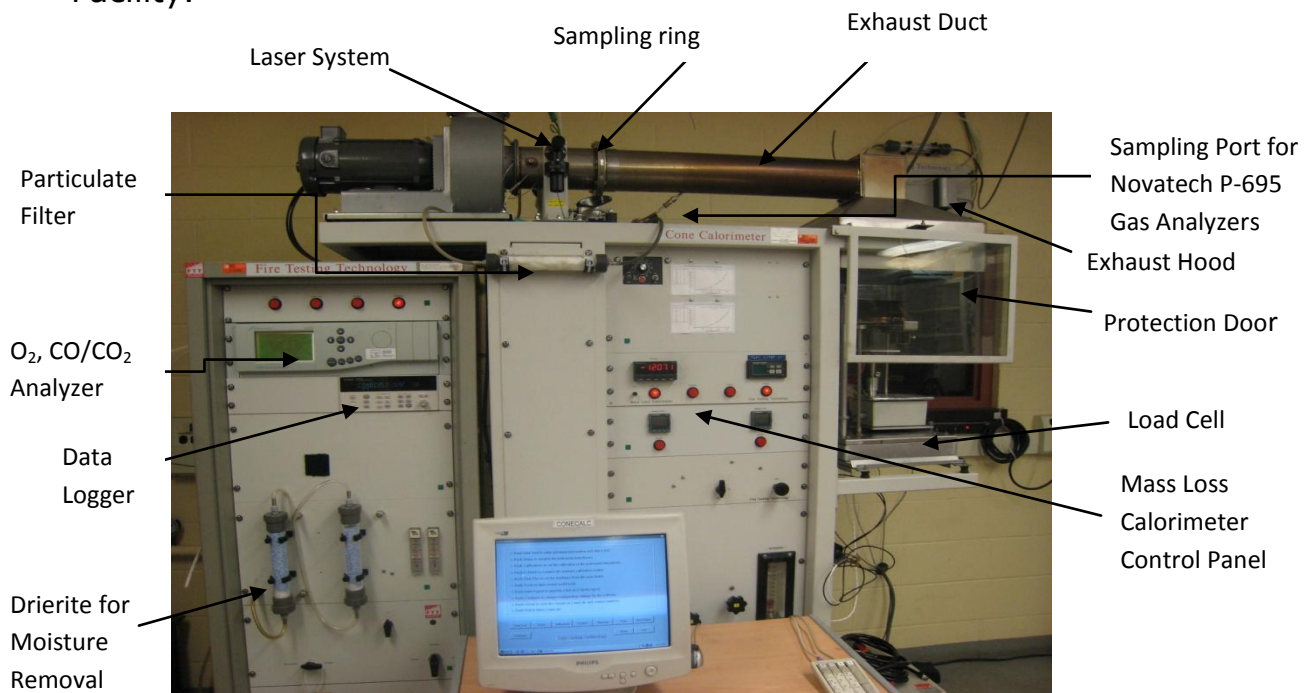
Figure 3.1: Details of an FTT cone calorimeter with relevant sections identified [ASTM E1354]

It consists of a fan and controlled exhaust system, a conical electrical heater, a load cell, an electric ignition spark plug, a laser smoke obscuration measurement system, gas analysis and data collection systems. The cone heater imparts a uniform radiant flux of up to 100kW/m^2 onto the test sample which decomposes and forms vapours that are then ignited and burned under ambient conditions. The mass of the sample is measured throughout a test using the load cell and the rate of mass loss of the sample can be calculated. The products of combustion are collected by the exhaust system and concentrations of O_2, CO and CO_2 are measured in real time using a paramagnetic gas sensor for measuring O_2 concentration and IR absorption principle for measuring CO/CO_2 concentrations.

Operating procedures, sample preparation and calculations are fully described in the standard test method for assessing fire performance of materials using the cone calorimeter, ASTM E 1354 [76], with key information briefly reiterated below. With supplementary gas collection and analysis equipment, aspects of the composition and potentially, toxicity of the smoke and fire gases, may also be determined. Since identification of compounds in the sampled gases forms an integral part of the present research, methods used in that portion of the analysis are discussed in Section 3.4.

Based on measured values of CO, CO_2 and O_2 in the exhaust gases and the duct flow rate, the HRR of a test sample is determined using equation (7).The heat release rate is a function of E, the heat of combustion per unit mass of oxygen consumed (assumed to be 13.1MJ/kg O_2), φ, the oxygen depletion factor defined in equation (8), $\dot{m}_e$, the mass flow rate in the exhaust duct defined in equation (9) and determined from the pressure drop

across, and temperature, at an orifice plate in the exhaust duct, and C which is the orifice plate calibration constant.

$$\dot{Q} = 1.10 \ (E)(\dot{m}_e) \ (X^i_{O_2}) \left[\frac{\varphi}{1.105\varphi + (1-\varphi)} \right] \tag{7}$$

$$\varphi = \frac{X^i_{O_2}(1 - X_{CO_2} - X_{CO}) - X_{O_2}(1 - X^i_{CO_2})}{X^i_{O_2}(1 - X_{CO_2} - X_{CO} - X_{O_2})} \tag{8}$$

$$\dot{m}_e = C \sqrt{\frac{\Delta P}{T_e}} \tag{9}$$

By introducing the oxygen depletion factor, φ, into equation (7), the relative contribution of CO_2 and CO production are accounted for in the calculation of HRR, while the water vapour in the exhaust is neglected.

A helium-neon laser beam is passed through the exhaust duct and attenuation of the beam is measured as a function of time to determine the smoke obscuration and therefore smoke production potential of the material under test. An extinction coefficient, k, which is a direct measurement of the concentration of smoke particles in the duct, is determined from the attenuation data as:

$$k = \frac{1}{L} \log_e \left(\frac{I_o}{I} \right) \tag{10}$$

The extinction coefficient, k, depends on the path length, L [m] which is the diameter of the exhaust duct, as well as the intensity of the obstructed light beam, I_o, and measured light intensity, I. As such, it varies with the concentration, and the light scattering and absorbing characteristics of the smoke. In a dynamic flow system such as in cone calorimeter, the optical

smoke density is measured continuously as it passes through extract duct at a linear flow rate that is monitored continuously. Using the cross sectional area of the duct, the smoke volumetric flow rate, $\dot{V}$ at the smoke meter [m³/s], corrected to ambient temperature is calculated. By combining this with the instantaneous fuel mass loss rate $\dot{m}_e$ of the specimen under test [kg/s], the specific extinction area (SEA) is obtained:

$$SEA = k\frac{\dot{v}}{\dot{m}} \left[m^{-1} . \frac{m^3 . s}{s . kg}\right] \qquad (11)$$

Specific Extinction Area (SEA) is the parameter often quoted in literature for the assessment of smoke production of a burning material. The unit of smoke measurement in this parameter, [m²/kg] is not immediately self-evident; but can be visualized from the simplified view of light attenuation shown in Figure 3.2; where only a few smoke particles are shown [114]. Smoke particles are treated as spherical particles released from a burning sample which obscure a beam of light travelling across a flow-through geometry such as in the exhaust duct of cone calorimeter.
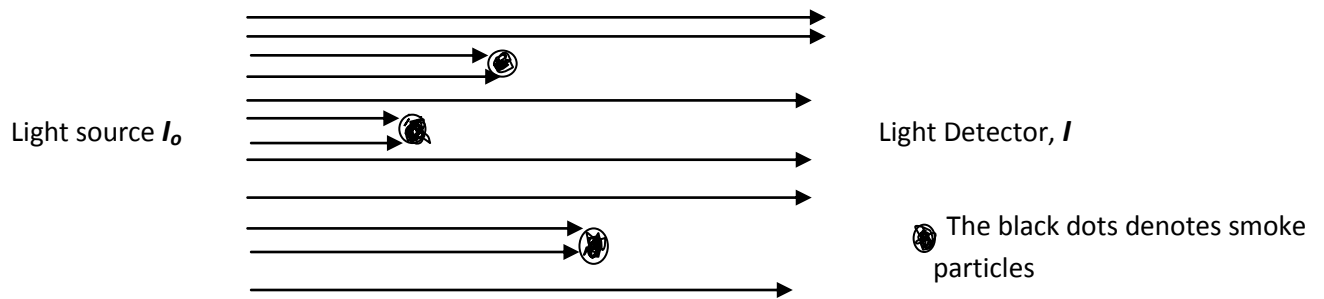
Figure 3.2: Illustration of simplified view of smoke extinction area [115].

As smoke particles are assumed to be uniformly distributed, the attenuation of the light beam becomes a function of the overall effective cross sectional area of the smoke particles normalized by the mass of the test sample [115]; or SEA is visualized as the area of obscuration defined as the sum of

the projected areas of all the smoke particulates caused by 1kg of sample mass burnt. Therefore, the SEA unit is expressed in m^2/kg.

The total smoke production, TSP [m^2] can also be defined using the smoke production rate, SPR [m^2/s] as:

$$TSP = \int_0^t SPR\,dt \quad \text{where SPR} = k.\dot{V} \qquad (12)$$

Therefore, the total smoke production normalized to the mass loss is defined as the specific extinction area (SEA). Since the parameter varies over the test period, an average value is used here [11]:

$$\text{Ave. SEA} = \frac{Ave\ RSP}{Ave\ \dot{m}} = \frac{TSP}{TML} \ [m^2/\text{kg}] \qquad (13)$$

where TML = the total mass loss

The specific extinction area, considered as the smoke obscuration area per mass of sample pyrolyzed, is proportional to the '*mass optical density*', a term that is commonly used for smoke visibility analysis. Since the burning rate of a fuel depends on the fire growth rate, the smoke hazard will also invariably depend on fire growth. Therefore, the total amount of smoke produced in a fire scenario will depend on SEA and the mass burning rate of the material.

In the current experimental study, samples of non-fire retarded (NFR) and fire retarded (FR) rigid foams from each of the four categories outlined in Section 3.1 were mounted in the cone calorimeter in a horizontal orientation and their top surface was exposed to a uniform heat flux of 50kW/m^2 to represent generalized fire conditions [70]. Unlike the standard test method, but to maintain consistency of method in the present results, the electric spark igniter was not used in any of the tests because it interfered with the

intumescing surface of the EGFR samples. Otherwise, data were recorded and analyzed following the procedure defined in the ASTM 1354 test standard. Three specimens of each formulation were tested and the averaged results are compared to assess repeatability. Averaged values across each formulation were reported as appropriate. Key flammability parameters such as heat release rate (HRR), total heat release (THR), time to ignition (t_{ig}), percent mass remaining (PMR), and specific extinction area (SEA) were determined. Supplementary gas concentration measurements and analysis equipment allowed further investigation into the composition of fire effluents generated from the samples during this test.

3.2.2 Smoke Density Test Method [ISO 5659]

The smoke density fire performance test method prescribed in ISO 5659 was used in the experimental work to conduct an assessment of the fire behaviour and exhaust gas generation from samples of each material under poorly ventilated conditions. The information obtained in this method is complementary to that obtained using the cone calorimeter under well ventilated conditions. In the smoke density tests, under the action of incident heat flux, each sample decomposes and forms vapours which are then ignited and burned, initially under ambient conditions. As the sample decomposes and burns, smoke fills the chamber and the ambient environment becomes less and less well ventilated over time. Smoke density is measured through determination of the level of attenuation of a laser beam by smoke accumulated in a closed chamber during pyrolitic non-flaming decomposition or flaming combustion of the specimen over time.

The smoke density chamber is a widely recognized method for measuring smoke and has often been used to simulate poorly ventilated compartment fire environments as well as for characterizing the combustion chemistry of materials and products [117]. The original test procedure was the National

70

Bureau of Standards (NBS) smoke chamber method, standardized in the United States as ASTM E662 standard test method [118], and first published in 1975. This test was designed to determine the smoke generating characteristics of plastic materials used in aircraft, construction, train and subway interiors [119-121]. The ASTM E 662 equipment consists of a vertically-oriented radiant heater with a 3-inch diameter circular opening. The specimen is mounted vertically and parallel to the radiant heater. In 1998, a new protocol, ASTM E 1995, was developed to incorporate a variety of changes to the apparatus and test methodology. The most significant change was the replacement of the NBS-style radiant heater with a horizontally-oriented cone heater [122]. The horizontal orientation allows the specimen holder to include a load cell, identical to that used in the ASTM E 1354 cone calorimeter. This standard does not, however, supersede ASTM E 662, and both apparatus configurations remain viable options to date. The current experimental work follows the ISO 5659-2 test method, which consists of horizontally–oriented radiant cone heater and load cell, similar to ASTM E 1354. Figure 3.3 shows the FTT smoke density chamber [123] which is housed at the University of Waterloo Live Fire Research Facility. There are two major components of the equipment namely: the smoke chamber and the laser attenuation/data collection system.

The smoke chamber consists of an airtight closed chamber of fixed volume having internal dimensions of 914 mm x 610 mm x 914mm and front-mounted door with a glass window from which the burning sample may be observed. Inside the chamber is a cone heater which is identical to that in the cone calorimeter described in Section 3.2.1, as well as a load cell, an electric ignition spark plug, and a laser smoke obscuration measurement system.

Figure 3.3: Detail of the FTT Smoke Density Chamber [ISO 5659]

The load cell allows continuous measurement of mass loss of the sample during the test so that the rate of mass loss can be calculated. The laser attenuation system consists of a collimated light beam, of path length 914mm and diameter 51mm, passing vertically through optical windows at the bottom and the top of the chamber. The intensity of the light is continuously measured by a photomultiplier (PM) tube in the form of electric signal, the current of which is proportional to the relative optical intensity data (or percentage transmission), T which is collected at fixed intervals of one second throughout the test and registered on a personal computer using FTT SmokeBox software.

Two parameters are typically measured namely; D_s which is an instantaneous measure of the optical density at a particular instant in time and the maximum optical density, D_m, which is used primarily for ranking the relative smoke production of a material and in identifying likely sources of severe smoke production. Operating procedures, sample preparation and calculations are fully described in the ISO 5659-2 standard test method

[124] for assessing fire performance of materials with the key information briefly reiterated below. The specific optical density D_s at any given time is calculated as follows [125]:

$$D_s(t) = G.log_{10}\left[\frac{100}{T(t)}\right] \qquad\qquad (14)$$

where T is light transmittance, %, read from the photosensitive instrument. If the smoke is produced from an exposed surface area, A, of the test specimen and passes through the light path length, L, and is collected in a closed chamber of volume, *V,* the optical density of the generated smoke should be directly proportional to both *A and L,* and inversely proportional to *V.* Therefore, the geometric constant, G $= \dfrac{V}{AL}$

By using the standard sample holder in the FTT Smoke Density Chamber, the exposed specimen area, A, is fixed at 65mm x 65mm (i.e 0.004225m^2), and the light path length, L, through the smoke is 0.914m in the fixed volume of the smoke chamber of 0.5096m^3.

$$\therefore G = \frac{V}{AL} = 132 \qquad\qquad (15)$$

And therefore, equation (14) can be written as:

$$D_s(t) = 132. \, log_{10}\left[\frac{100}{T(t)}\right] \qquad\qquad (16)$$

This test method should be used to compare the smoke generated by different materials under test, thus the values of specific optical density are only characteristic of the specific specimens and test conditions and cannot directly be generalized to different situations.

In the smoke density performance testing conducted in this research, samples of non-fire retarded (NFR) and fire retarded (FR) rigid foams from each of the four categories outlined in Section 3.1 were mounted in the smoke density apparatus in a horizontal orientation to minimize the possibility of melting or dripping of the material during the test [126]. The top surface of each sample was exposed to a uniform heat flux of $50kW/m^2$ with spark pilot igniter to represent generalized fire conditions [118]. Data were recorded and analyzed following the procedure defined in the ISO 5659-2 test standard. Three specimens of each formulation were tested and the averaged results are compared to assess repeatability. Averaged values across each formulation are reported as appropriate. Two parameters, the optical density (D_s) and the maximum optical density (D_m) were determined. Supplementary gas analysis equipment allowed further investigation into the composition of fire effluents generated from the samples during this test.

3.3 Gas Sampling Methodology

Gas sampling involves collection of representative samples of analytes from the gases evolved during each test such that they can be transferred to the gas analysis system(s). Figure 3.4 shows the flow chart for the combination of different gas measurement techniques used in this study. The cone calorimeter system has provision for measurement of O_2, CO and CO_2 concentrations in the exhaust gases, since they form the basis for measurement of heat release rate. Other gas species concentrations are measured at predetermined times during each of the fire performance tests using external gas analysis equipment to provide further details of the composition of the fire gases.

Exhaust Duct from **Cone Calorimeter**

On-line gas measurements

SDC

Sorbent tubes

Off-line VOCs measurements

Servomex 4900 Gas Analyzers
[O_2, CO_2 & CO] measurements

FTIR Gas Analyzer
(Miran 205B)

Novatech P-695 Analyzers
UTH (Baseline 8800H analyzer)
NOx (TML 41H) Analyzer
O_2/CO_2/CO (Servomex 4900C)

TD-GC/MS
TD (Dynatherm ACEM 9300)
GC (Agilent 6890)
MS (5973)
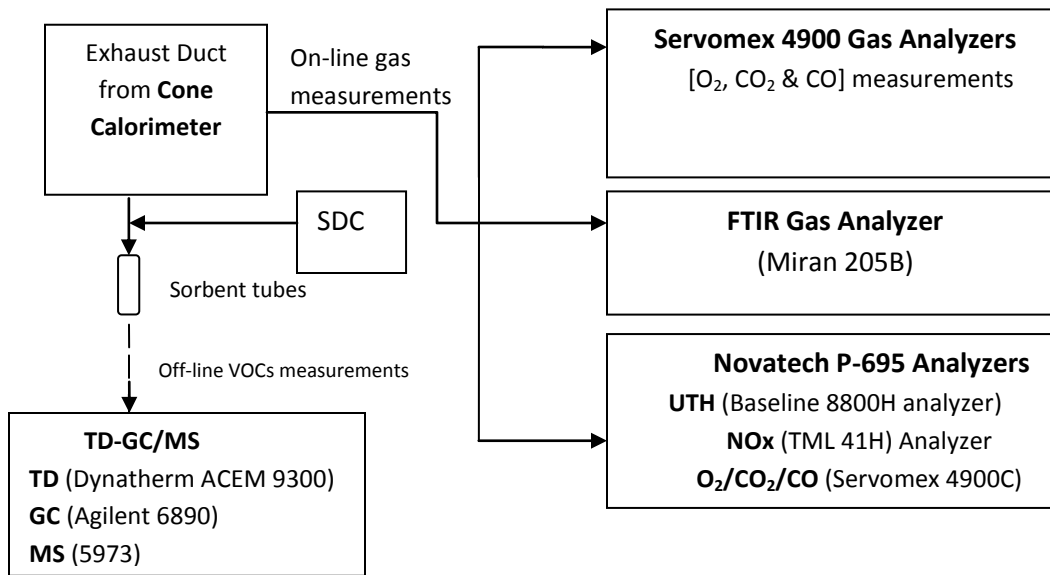
Figure 3.4: Flow chart of the combination of different techniques used for gas measurements

During cone calorimeter tests, the sample gases are drawn into an FTIR gas cell and a Novatech P-695 gas analyzer system to facilitate measurement of NO_x and unburned hydrocarbons in real time. During both cone calorimeter and smoke density testing, gas samples are pumped onto sorbent tubes through a manifold system for off-line measurement of volatile organic compounds using Thermal Desorption-Gas Chromatography/Mass Spectrometry (TD-GC/MS). Due to differences in the sampling methods required for gas analysis using each system; specifics of each sampling method are discussed in turn below.

3.3.1 Cone Calorimeter Sampling Method

The schematic diagram in Figure 3.5 shows the combined experimental configuration used during cone calorimeter testing, including the different gas sampling methods and measurements. Gas samples are withdrawn from the calorimeter exhaust duct at a fixed position through a port sampling ring

arrangement. From the duct, the sample passes through a $0.3\mu m$ HEPA filter to remove particulate and a sorbent drying agent to remove moisture from
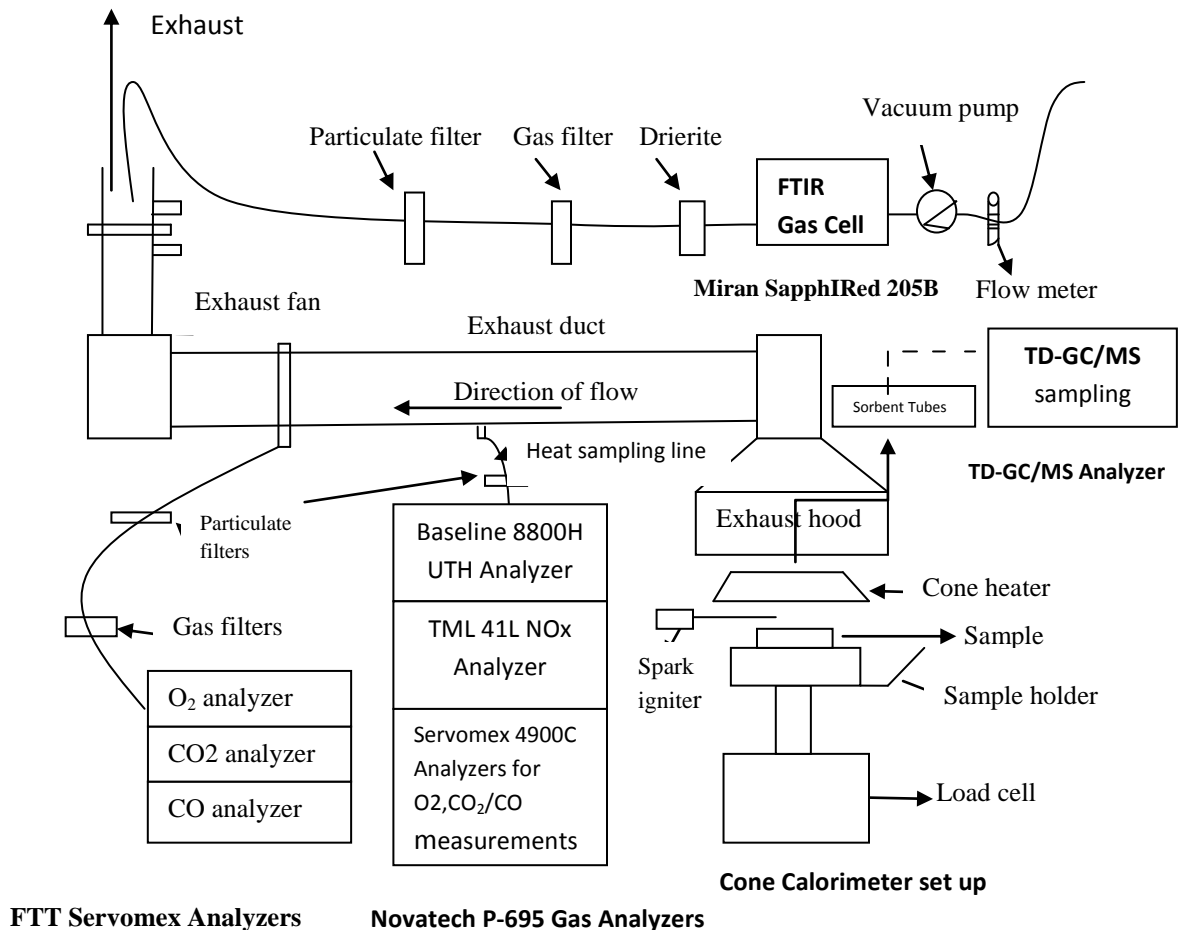
Figure 3.5: Schematic diagram of combined experimental configurations for cone calorimeter testing

the sample stream. Temperature and pressure differential across an orifice plate are measured in the exhaust stack and are used to approximate the volume flow rate of gases in the stack which is held constant at 24 l/s across all experiments. The built-in gas analyzers provide measurements of the volume fractions of oxygen, carbon dioxide, and carbon monoxide in the sampled gas in real time, at a sampling rate of one sample/second.

In day-to-day calibration, methane gas is used to generate HRR for calibration purposes. Before each set of samples was tested, the cone calorimeter was calibrated according to the ASTM standard using a regulated flow of methane gas to ensure proper operation of the instrument and to also compensate for minor changes in mass flow determination. In addition, ethanol and PMMA calibration samples are regularly tested to recalibrate the entire cone calorimeter system for O_2, CO, CO_2 measurements which are used for the calculations of HRR and other fire performance characteristics.

Calibration of smoke measurements on the cone calorimeter is conducted each day before test. For zeroing, smoke laser is turned off to represent the highest level of smoke obscuration; and once values are stabilized, the transmission reading is 0%. For balancing, smoke laser is turned ON, allowing the values to stabilize, the light transmission is approximately 100%.

During cone calorimeter testing, additional gas samples are taken using 3 seconds sampling windows during three different stages of fire development. Stage *I* samples are collected entirely during non-flaming oxidative pyrolysis of the foam sample after application of the heat flux to the sample before ignition occurs. Stage *II* samples are collected as close to the time of peak heat release rate as possible to represent the behavior of the material during more fully developed fires. Finally, stage *III* samples are collected during the final decay phase of the fire when HRR drops to about 40% of its peak value to learn more about gases that might be found in post-flashover and post-suppression environments. Assessment of the similarities and differences in gas compositions at these times will provide enhanced data and understanding of gases that might be found during characteristic phases of a full fire situation.

3.3.2 Smoke Density Chamber Sampling Method

In the smoke density chamber testing, a metered flow of gas sample is drawn from the bulk of evolved gas from the top of the cone heater onto 3 separate sorbent tubes, one for each stage of fire development, and later analyzed using the TD-GC-MS gas analysis equipment shown in Figure 3.5. Gases are sampled from inside the closed chamber to take advantage of the fact that there is no dilution of the combustion products in this test. A 3-second sampling window is again used, with samples timed to probe each stage of fire development. In these tests, Stage *I* represents the pre-ignition phase, while stage *II* corresponds to the time when the specific optical smoke density in the chamber is approaching its peak value; and stage *III* occurs when the optical density in the chamber decays to 40% of the maximum value of measured optical density.

Before each test, inside surfaces and support framework are cleaned with suitable materials such as soft cloth and ammoniated spray detergent to avoid possible interactions between residues from sample to sample. The two optical windows are cleaned with suitable solvent using ethyl alcohol and soft tissues in order to ensure accuracy of results. The photomultiplier (PM) control unit is calibrated by putting the carousel in the "*Dark Current*" position to ensure that no light is transmitted through to the photomultiplier tube; thus signaling the highest levels of smoke obscuration. When in the "*Clear*" position, the carousel is adjusted such that all the light is transmitted through an open aperture onto the photomultiplier tube signaling 100% light transmission [123]. The cone heater flux meter is calibrated in accordance with ASTM E 1354 standard [76].

3.3.3 Novatech 695 Sampling Method

The Novatech *P-695* system is interfaced to the cone calorimeter for species concentration measurements including O_2, CO_2, CO, total hydrocarbons and nitrogen oxides. The gas analysis system is plumbed to allow zeroing and calibration of each analyzer with appropriate gas mixtures. This is intended to set common zero reference values to allow baseline comparisons between gas concentration data from the three different measurement systems. At the start of testing each day, all the gas analyzers are calibrated before measurements are undertaken. The Servomex 4900 gas analyzers are calibrated as discussed in Section 3.3.1. The NOx gas analyzer is zeroed with nitrogen gas and calibrated with 400ppm of NO, while UTH analyzer is zeroed with dry air and spanned with 2076ppm of CH_4.

Representative gas samples from the cone calorimeter exhaust stream are drawn by vacuum pumps through a heated sampling line into the Novatech gas analysis system. The sampling line contains an integrated particulate filter to remove soot and heavy combustion products and is heated to 165°C in order to minimize sample gas losses. The sampling system collects gas samples and outputs concentration data continuously at a 1Hz sampling rate throughout each test. The advantage of using the *Novatech* P-695 system is its capability to measure unburned hydrocarbons and nitrogen oxides in real time which cannot be measured with the built-in gas analyzer on the cone calorimeter testing apparatus.

3.3.4 FTIR Sampling Method

For FTIR analysis, representative samples of gas are continuously drawn from the cone calorimeter exhaust stream at 14 l/min through the exhaust duct using a vacuum pump (Fig 3.5 above). The sampling train consists of Teflon tubing incorporated with double filters and drierite units to remove

soot and water vapour before being passed into the 12.5m path length FTIR gas sampling cell. The filters and drierite combination protects the FTIR optics from condensation and damage that could arise if soot or corrosive compounds such as HCl were allowed to pass into the gas analysis cells. The sample gas flows through the cell in a batch sample mode in which the analyzer internal pump pulls a sample into the gas cell for about 20 seconds to fill up the cell. The pump is then shut down while each component is analyzed at its defined wavelength. It takes about 60 seconds to analyze a batch sample while the resolution of each spectrum is 4cm^{-1}. After the data is displayed, the cycle is repeated [137].

3.3.5 GC-MS Sampling Method

With the aim to gaining additional understanding of the dynamic environments that are developed during both cone calorimeter and smoke density testing of fire retarded rigid foams, a new approach to sample collection was also designed based on sorbent tube sample collection followed by off-line analysis using a Thermal Desorption Gas Chromatography Mass Spectrometry (TD-GC-MS) method [101,128]. Gas samples are withdrawn at a location above the conical radiant heater which is set as consistently as possible during both cone calorimeter and smoke density chamber testing. Due to natural fluctuations in the generation of gas across the surface of a sample, spatially averaged samples of the gas are collected through a conical port with a circumference of 18mm shown in Figure 3.6.

In the initial stages of the research, several different port sizes and locations were tested; the final location and size was optimized to ensure the most representative and relatively repeatable gas samples were captured for gas analysis. The sample lines are insulated and kept as short as possible to minimize losses and residence time effects in the lines. Using a vacuum

pump, gas samples are drawn through a manifold system at a rate of 0.9 l/min onto fast flow 6mm I.D sorbent tubes for off-line measurements of volatile organic compounds.

Figure 3.6: Detail of the interior of the UWLFR Smoke Density Chamber

Each sorbent tube consists of three, layered adsorbent materials namely: carbopack C, carbopack B and carboxen 1000 in a 60/80 mesh, arranged in order of increasing adsorbent strength from sample inlet to sample outlet as shown in Figure 3.7. This choice of adsorbent materials helps to capture a wide range of n-C_7 to n-C_{20} compounds adsorbed onto the carbopack C, and n-C_5 to n-C_{14} adsorbed on carbopack B while the light hydrocarbons, n-C_1 to n-C_4, are adsorbed on the carboxen 1000 [129]. Even at the relatively fast flow rates used, breakthrough was avoided. After some iteration, a 3 second sampling window (mentioned above) is chosen for collection of samples during each of the three stages in the fire performance tests. A solenoid switching system is used to direct the sample into each sorbent tube at the

appropriate time. After collection, off-line gas analysis was conducted using the TD-GC-MS analysis method [130].
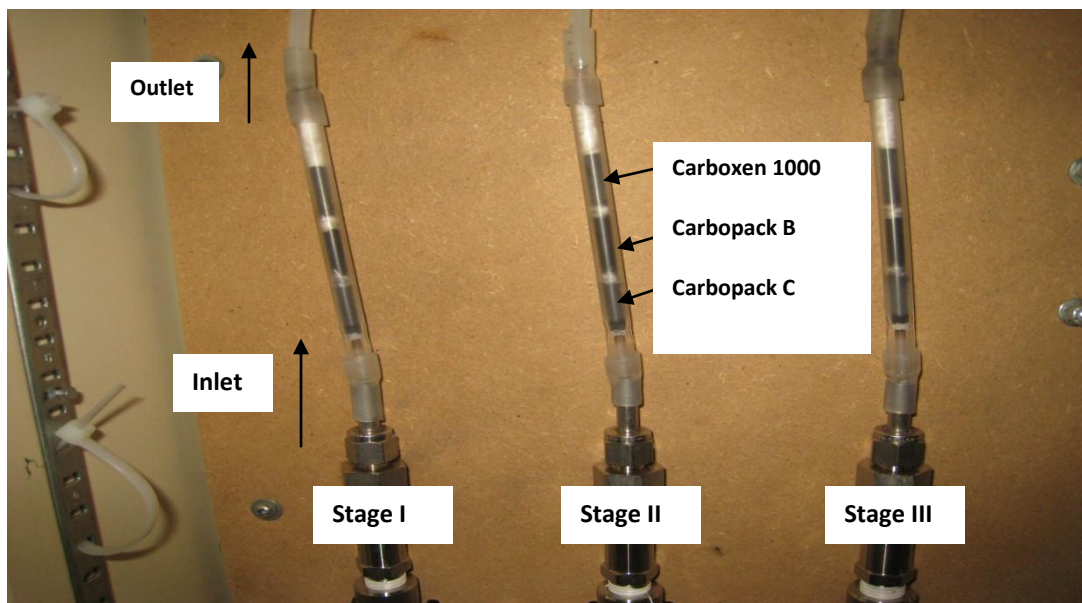
Figure 3.7: Arrangement of multi-bed layers of adsorbent materials and sampling stages

3.4 Gas Analysis Techniques

In order to identify additional combustion gases over those measured as an integral part of cone calorimeter testing and, where possible, to measure their respective concentrations, the gas analysis systems described above were applied. In addition to the TD-GC-MS analysis in Section 3.3.5, solvent extraction GC-MS was also attempted; however, the solvent peak masked key compounds of interest so this method was quickly abandoned.

Each of the analytical techniques, when applied individually, provides information by which to identify and quantify gaseous products generated during fire testing of rigid polyurethane foams. In this experimental study, the Novatech and FTIR methods were first applied during cone calorimeter

testing to identify gaseous products in the exhaust and the data was integrated to better understand the performance of PUR foams under fire conditions. For comparative purposes, the newly developed TD-GC/MS method was then applied to extend identification of products in cone calorimeter tests, as well as to study and identify products in the gases generated during smoke density testing of the same foams. Each of the gas analysis systems/techniques as applied in this study is discussed further in the following sections.

3.4.1 NOVATECH Gas Analyzers

The *Novatech P-695* gas analysis system consists of a model *8800 Baseline* flame ionization detector (FID), a *TML 41* chemiluminescence instrument, and *Servomex 4900* infrared and paramagnetic detectors. The *Novatech P-695* system was designed for monitoring gases during full-scale fire testing, but adapted here for on-line concentration measurements of major combustion gases present in the exhaust stream of cone calorimeter tests. The three analyzers are explained in more detail below.

3.4.1.1 Servomex 4900 Series Analyzers [O2, CO2 & CO]

Servomex 4900 series analyzers, similar to those used in the cone calorimeter, are installed in the Novatech to provide O_2, CO_2 and CO concentration measurements. Oxygen concentrations were determined using paramagnetic sensor technology, while CO and CO_2 concentrations were measured, respectively, via gas filter correlation and single wavelength IR non-dispersive photometric methods. The *Servomex 4900* IR CO/CO_2 and O_2 analyzers in the Novatech P695 provided valuable data for comparison against gas concentrations measured using the cone calorimeter gas analyzers.

3.4.1.2 Model 8800 Heated Total Hydrocarbon Analyzers

The Model 8800H Total Hydrocarbon Analyzer measures the total concentration of hydrocarbons in the gas stream using an electronically flow controlled Flame Ionization Detector (FID). As a small sample of gas passes through the flame produced by a hydrogen and air mixture in the detector, organic or hydrocarbon based gases in the sample are ionized and the freed electrons are continuously collected on a biased electrode, producing an electrical signal proportional to the total amount of organic compounds that are burned in the flame. Since the current measured corresponds approximately to the proportion of reduced carbon atoms in the flame, the response of the detector is determined by the number of carbon atoms (ions) hitting the detector per unit time. Therefore, saturated hydrocarbons such as methane, ethane and propane which contain only carbon and hydrogen atoms possess high combustion efficiencies and respond more on the detector than hydrocarbons possessing substituted functional groups or heteroatom compounds which decrease the detector's response. The current measurement is reported as a concentration by the analyzer. To relate the signal output to the actual concentration, it is necessary to define the concentration range on the instrument when the analyzer is in the auto-ranging mode. In the present application, concentration range is from 0-2070ppm where gas analyzer is zeroed with air and calibrated with 2070ppm methane to standardize the sensitivity setting of the analyzer.

The analyzer is not capable of identifying specific hydrocarbon species; so more detailed identification and analysis of specific species requires the use of complementary gas analysis methods which form the extended scope of the present study.

3.4.1.3 Model TML 41 Nitrogen Oxides Analyzers

The TML 41 Nitrogen Oxides Analyzer measures the chemiluminescence which occurs in a reaction cell in which nitrogen oxide (NO) in the sample gas reacts with ozone (O_3) in a two-step reaction process shown in the equations below:

$$\text{reaction cell}: \quad \begin{array}{l} NO + O_3 \longrightarrow NO_2{}^* + O_2 \\[1em] NO_2{}^* \longrightarrow NO_2 + hv \end{array} \qquad (17)$$

In the first process, NO and O_3 collide and chemically react to produce O_2 and $NO_2{}^*$ which retains a certain amount of excess energy from the collision. The NO_2 molecule quickly returns to its ground state, thereby releasing the excess energy in form of quanta of light (hv) with wavelengths between 600 and 3000nm such that the relationship between the amount of NO present in the reaction cell and the intensity of light emitted is linear.

The NO_2 in the gas sample is not detected via the chemilumescence process since NO_2 does not react with O_3 to undergo chemiluminescence. In order to measure the concentration of NO_2, then, the analyzer periodically switches and sends the sample gas stream through a converter cartridge filled with Molybdellum (Mo) chips heated to a temperature of 315°C. The NO_2 in the sample gas is converted to NO according to equation (18);

$$xNO_2 + yMo \longrightarrow xNO + Mo_yO_z \quad \text{(at } 315^{\circ}\text{C)} \qquad (18)$$

and is routed back to the main reaction cell where it combines with the original gas sample and undergoes the chemiluminescence reaction described in equation (17) to provide a measure of the total NO_x content in the sample. The concentration of NO_2 is then calculated as the difference between the measured amounts of NO_x and NO.

3.4.2 MIRAN 205B Fourier Transform Infrared Spectrometer

The MIRAN 205B SappIRed FTIR was interfaced to the cone calorimeter at UW Live Fire Research Facility in an attempt to use Fourier Transform Infrared spectroscopy (FTIR) to assess the overall composition of gases evolved during testing of rigid polyurethane foams [131]. FTIR is a powerful analytical tool that has been widely used in laboratory and industrial gas analysis for many years, in applications such as determination of gas-phase compositions during thermal degradation and combustion [132], emissions monitoring and car exhaust research and toxic fire gas monitoring [97, 133].

Standard FTIR instrumentation allows for real-time measurement of fire gases that have characteristic spectral bands in the infrared region of the spectrum. It is based on the principle that every gaseous molecule, with the exception of monatomic (He, Ne Ar etc) and homopolar diatomic (H_2 O_2, N_2 etc) molecules, has a unique set of rotational and vibrational frequencies that absorb infrared energy in a characteristic manner, thereby giving each gas molecule a unique IR spectral fingerprint. Once the spectrum of a given gas sample has been measured, individual gases can be identified and quantified based upon the spectral location and magnitude of the measured absorption peaks, given that the spectrometer has sufficient resolution that the individual absorption lines in the spectrum can be discerned. With systems having appropriate resolution and time response, FTIR has been shown to be a powerful method for fire gas analysis over a wide range of tests and operating conditions [132,134-136].

In the MIRAN 205B SapphIRe FTIR, gas samples from the cone calorimeter exhaust stream flow through the sample cell and are analyzed to produce an FTIR spectrum with 4 cm^{-1} resolution across the spectral range from 709 to 1298 cm^{-1} (14.1-7.7 µm). Due to the size of the sampling cell and flow rate of the system, a 20 second purge and refresh time is required in a batch

sampling mode; where samples are captured and then analyzed off-line. A full spectral scan takes approximately 60 seconds to complete so that results obtained are integrated over the gases present during the 20 second period. Once the spectral data is obtained, it is analyzed using the 'Thermomatch' software [137], which correlates the measured spectrum against a library of 120 known spectral signatures in order to identify the compounds present. A typical FTIR spectrum, as measured by the MIRAN system is shown in Figure 3.8. If the spectra from the FTIR library do not provide an acceptable match to the measured spectrum, analysis of the locations of individual peaks in the measured spectrum may still provide some information about the composition of sample gas. In the present work it was found, however, that even though many molecules contain strong absorption signatures in the wavelength range scanned by the MIRAN instrument, the sampling methodology and long scan time required by the instrument greatly limited the quality and resolution of the results that could be obtained. Therefore, FTIR provided only time-averaged concentrations of gases that might be present in the cone calorimeter exhaust stream, picking up only some of the gases that had relatively high concentrations and persisted for some time during the test, as shown by the result in Figure 3.8.

As would be expected, spectral signatures for CO, CO_2, nitrous oxide ($2222cm^{-1}$) and unburned total hydrocarbons ($3000cm^{-1}$) are readily identified in the fixed band pass region, while spectral lines associated with IR absorption of toluene and HCN are identified in the fingerprint region. The high concentrations of CO_2 found in the combustion gases cause spectral interference and make identification of other gases difficult.
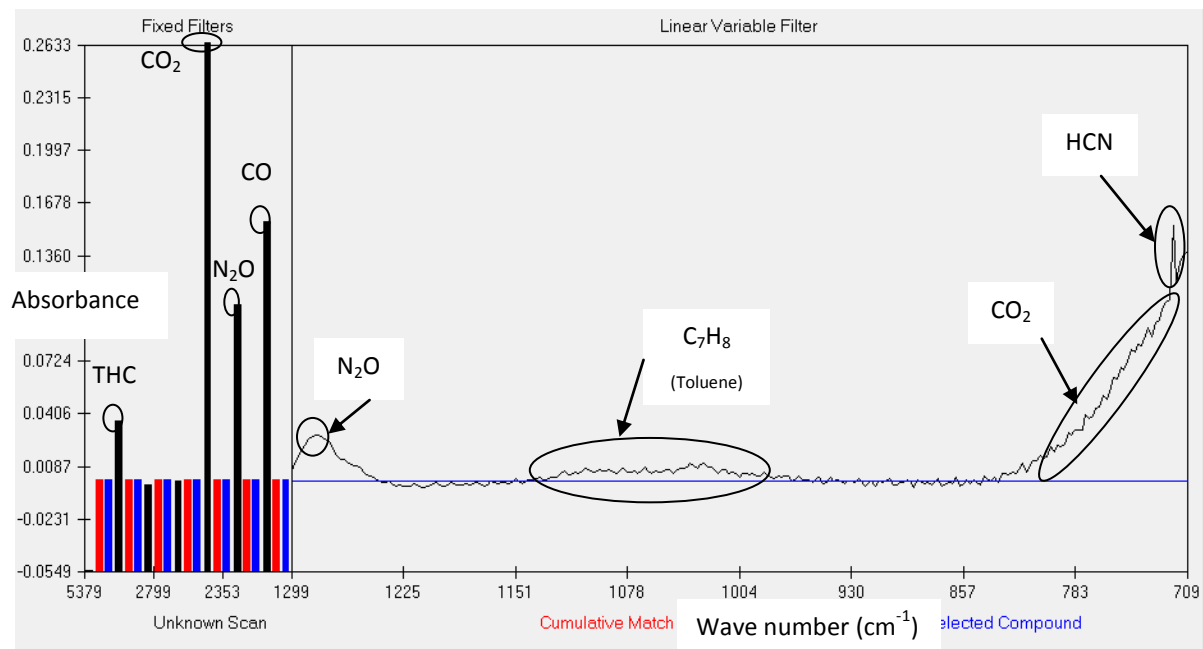
Figure 3.8: FTIR spectrum taken over 380s after ignition

It can be seen from Figure 3.7 that the strong absorption of carbon dioxide interferes with the HCN peak which occurs at 714cm^{-1}. Even after many iterations on both sampling and analysis methodology, FTIR spectra obtained using the *Miran 205B* FTIR system did not yield consistent results that would aid in identification and characterization of the gases generated during the different stages of cone calorimeter and smoke density testing of the rigid polyurethane foams outlined above. As a result, use of other gas analysis techniques, specifically those based on gas chromatography and mass spectrometry, were explored. The method developed in this work is described below.

3.4.3 Gas Chromatography-Mass Spectrometry (GC-MS)

More detailed characterization of the volatile organic compounds produced during decomposition and burning of NFR and FR rigid polyurethane foams was performed using sorbent tube sampling with off-line analysis using

Thermal Desorption-Gas Chromatography/Mass Spectrometry (TD-GC/MS). Gas chromatography interfaced with mass spectrometry (GC/MS) has long been one method of choice for identifying volatile organic compounds in complex mixtures such as are found in combustion and fire gases [138-139]. It can be used for real time characterization of the gases or can be coupled to a sampling methodology that allows off-line GC-MS analysis. In the off-line method used here, a representative sample of the gases is first collected on an appropriate adsorbent material and later desorbed again and transferred into the gas chromatography (GC) and mass spectrometry system in which the various fire gases are separated and identified.

Analytical thermal desorption (TD) was first introduced as an accessory to GC/MS systems in the early 1980s to provide an alternative to solvent extraction for the measurement of semi-volatile organic compounds (S-VOC) in air. Today, TD-GC/MS is recognized as one of the standard techniques applicable for environmental and workplace air monitoring and odor/emissions profiling [140], although to the author's knowledge, it has not been widely applied in research related to identification of fire exhaust gas components. The thermal desorption technique is especially useful in detecting trace levels of volatile and semi-volatile compounds [140]. It also offers significant advantages over standard solvent extraction methods for volatile organic compounds (VOCs) due to the shorter sampling times required and higher extraction efficiency because the sample is not diluted by solvent during desorption from the sampling medium. In addition, since the sample is thermally desorbed from the sampling medium, there is no interference from a solvent and ultra-low detection limits of parts per billion (ppb) or parts per trillion(ppt) are possible [140]. Universality of the method to a wide range of VOCs (polar to non-polar gases to semi-volatiles) makes it an excellent candidate method for combustion gas sampling in complex chemical environments [138-140].

In this work, the volatile and semi-volatile organic components of the fire gases collected on the three layer custom-packed solid adsorbent system described in Section 3.3.5 were transferred to a Dynatherm ACEM 9300 thermal desorption system directly interfaced to an Agilent 6890 gas chromatography and 5973 mass selective detector(MSD). The organics were thermally desorbed from the sampling tube into a sorbent trap system via a rapid heating over approximately 10 seconds from $35^{o}C$ to $300^{o}C$ while the sample tube is held for 3 minutes at the final temperature to ensure complete desorption of the targeted volatile compounds [141]. From a main trap, the desorbed components were re-collected on a heated focusing trap and transferred to the inlet of the Agilent 6890 gas chromatography and 5973 mass spectrometry under a constant flow of helium carrier gas for chromatographic separation and mass spectral identification.

The two-stage desorption process delivered the analytes onto the GC column more rapidly and in a much narrower band than would otherwise have been possible, thereby improving chromatographic results. In addition, the inlet port of the gas chromatography could be operated in either split or splitless modes; the splitless mode was employed in this work due to the low concentrations of many organic vapours because of the heavy dilution of exhaust combustion gases in the well ventilated cone calorimeter test [140]. Chromatographic separation was carried out on an HP-1ms fused silica capillary column, 60m x 0.32mm I.D x 1.0µm film thickness (Agilent Technologies). Carrier gas was helium at a constant flow of 0.9ml/min; while the GC oven was programmed from $40^{o}C$ for 5 minutes to $300^{o}C$ at $5^{o}C$/min. At the end of the analysis sequence, the total GC run time was 58 minutes.

After chromatographic separation, each component of the sample was ionized in a quadrupole MS analyzer by means of an electron impact (EI) with an ionization voltage of 70eV. Mass fragments ranging from 40-300amu were collected and were separated in a mass filter according to their mass to

charge ratio. Agilent MSD Productivity Chemstation software was used for data acquisition and analysis [142]. The mass spectrum of each gas, which is a plot of the number of ions detected (abundance) versus the mass of each ion, forms a unique fingerprint which enables positive identification of a wide range of volatile organic compounds (VOCs) for quantitative or semi-quantitative measurements.

Measured spectral signatures are compared to those listed in the National Institute of Standards and Technology (NIST) mass spectral library version 2.0 which is available on Agilent GC/MS systems [143]. Using the library, specific organic compounds were identified on the chromatograms using peak recognition and matching, as well as calculated values of the Kovats Retention Index [144], which is characteristic of each compound. In order to aid the analysis and assess repeatability of the analysis process, a known quantity of an internal standard, 1, 4-dichlorobenzene-D4, was also added to each sample prior to desorption to facilitate positive identification of peaks via their measured retention times. Once the thermal desorption conditions for VOCs extraction were optimized, samples from 3 different test runs of the same material were injected in order to evaluate the repeatability of the analytical method. In this way, the method was verified to have good linearity, reproducibility and accuracy for the VOCs identified in this work [145].

3.4.4 Repeatability and Uncertainty Measurements

Three test runs of each class of material were conducted in the cone calorimeter and smoke density chamber and results were averaged for all tests. Heat release rate (HRR) is regarded as the single most important fire parameter which serves as the driving force for many other fire properties. And since it is commonly linked to an overall measure of fire hazard and the peak HRR used to represent the worst case scenario during flaming

combustion of a specimen in the cone calorimeter, it is used here to demonstrate test to test variability. Figure 3.9 shows the repeatability of three tests and the averaged test result of HRR versus time of the base foam. Results of repeatability of fire retarded samples are shown in Appendix 3.1.
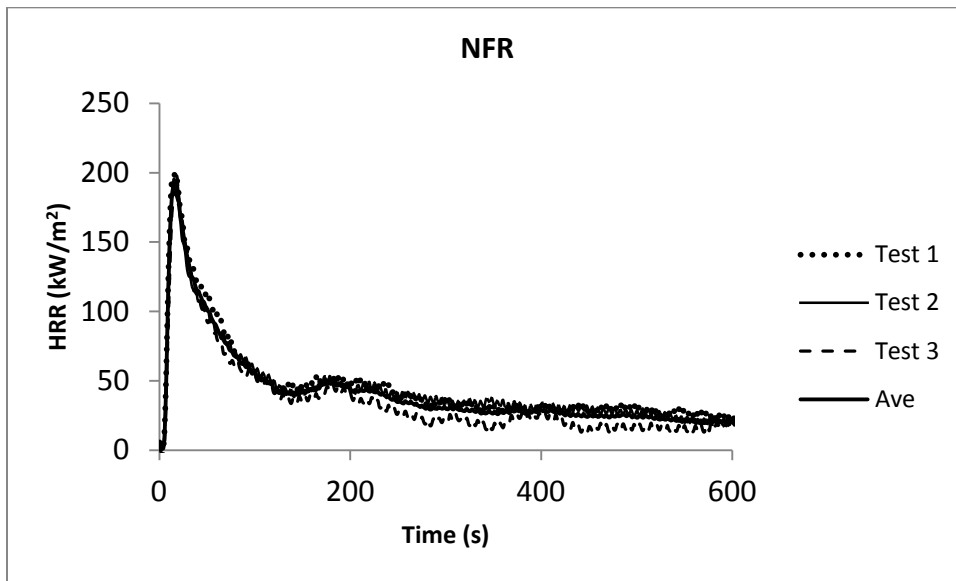
Figure 3.9: Averaged HRR curve for NFR sample

The NFR control sample and all the FR system formulations are subjected to repeated testing; and variability in the fire performance indices is quantified for the four classes of material samples tested. Table 3.2 shows the variability in the peak heat release rates of all the samples. For example, the sample mean of peak HRR for the NFR control sample with a sample size of n =3, is determined as 198 kW/m^2 while there is 95% confidence level that the true mean peak HRR falls between 196 kW/m^2 and 200 kW/m^2 while the coefficient of variation which is defined as the ratio of standard deviation to the sample mean of peak HRR is calculated to be 0.0087.

Table 3.2: Variability of **peak HRR** of the NFR and FR samples

Sample Material		Sample Size n	Mean of pHRR $\bar{x}$ [kW/m^2]	Standard Deviation, s [kW/m^2]	Margin of Error	95% Confidence Interval for $\bar{x}$	Coefficient of Variation
NFR		3	198	1.73	1.96	198$\pm$1.96	0.0087
BFR	10%	3	180	16.26	18.40	180$\pm$18.40	0.0903
	20%	3	146	8.54	9.66	146$\pm$9.66	0.0585
EGFR	10%	3	160	7.52	8.51	160$\pm$8.51	0.0470
	20%	3	148	5.15	5.83	148$\pm$5.83	0.0348
PFR	10%	3	176	2.35	2.66	176$\pm$2.66	0.0133
	20%	3	191	19.08	21.59	191$\pm$21.59	0.0999

Of all the samples tested, the NFR samples showed the least test to test variation, while 10%BFR and 20%PFR samples show significant variations in results across the three tests. Although, the confidence limit on the pHRR may be narrowed by increasing the number of tests conducted on each sample material, the number of tests in this research was constrained by the size of the sample materials supplied and therefore did not allow for repeated testing beyond three samples. A similar outcome is observed with time to ignition, average HRR and total heat release (THR) for the same test results.

For smoke development of sample materials tested under the cone calorimeter, the least sample to sample variation is observed for NFR and PFR samples for the average CO and CO_2 production and the highest variation is seen in BFR and EGFR samples (Appendices 3.2 and 3.3 respectively). Also, the least amount of variations is observed in average specific extinction area (SEA) parameter for 10%EGFR and PFR samples, while significant variation is noted in the 20%EGFR sample (Appendix 3.4). There is less variability in 20%EGFR sample in non flaming mode with respect to the maximum specific optical density under smoke density chamber testing, whereas the highest variation occurs in 10%BFR sample tests under flaming combustion (Appendix 3.5). For the unburnt total

hydrocarbons (UTH) gas analyzer used in this study, repeatability of test results specified by the manufacturer lies within $\pm 1\%$ of the selected range for gas measurements [127]; while the accuracy of nitrogen oxides gas analyzer is within 0.5% of gas measurement [169].

Chapter Four: Results and Discussion

Fire performance, smoke and gas production of NFR and FR rigid PUR foams were investigated using the cone calorimeter test method to simulate well ventilated decomposition and burning conditions and the smoke density chamber test method to simulate decomposition and burning in oxygen limited environments. By sampling gases produced under flaming and non-flaming conditions, various oxidative-pyrolysis and combustion products evolved from different samples were analyzed with the gas analysis systems and techniques outlined above. The results of fire performance characteristics of the various samples are presented in Section 4.1, followed by Section 4.2 in which the smoke development under different test methods and burning conditions are discussed. Results related to evolution of major combustion gases are outlined in Section 4.3 with the main volatile organic compounds (VOCs) identified from the pyrolysis and combustion products of the samples at various stages of the fire performance testing discussed further in Section 4.4. The Chapter closes with general remarks on the entire set of data in Section 4.5.

4.1 Performance Parameters

Non-fire retarded (reference) and fire retarded samples were tested in the cone calorimeter with an incident radiant heat flux of $50kW/m^2$ to simulate their fire performance under well ventilated combustion. The base foam described in Section 3.1 was employed throughout; concentrations of brominated, phosphorus and expandable graphite fire retardants were added to that foam in concentrations of 10% and 20% by weight to produce the fire retarded test specimens. Key experimental conditions, such as incident radiant flux, ventilation and specimen geometry were kept constant while the main fire performance parameters, namely: HRR, THR, MLR, t_{ig}, EHC,

SEA, CO and CO_2 production were measured. Due to well documented evidence there can sometimes be issues with repeatability of cone calorimeter tests; the results presented here represent averages of three different experiments. Results across each set of material samples were found to be reproducible to within $\pm$ 10%, consistent with levels reported in the literature [146-147].

A typical plot of the variation in heat release rate (HRR) with time for the NFR polyurethane base foam is shown in Figure 4.1. After an initial delay period of 3s, the material began to decompose with very low levels of measured heat release, but it did not immediately ignite. Following this induction period, the material ignited and there was a rapid rise in measured heat release rate to a peak value due to combustion of volatile gases evolved from the sample. As the fuel was consumed, the HRR decreased progressively with time.
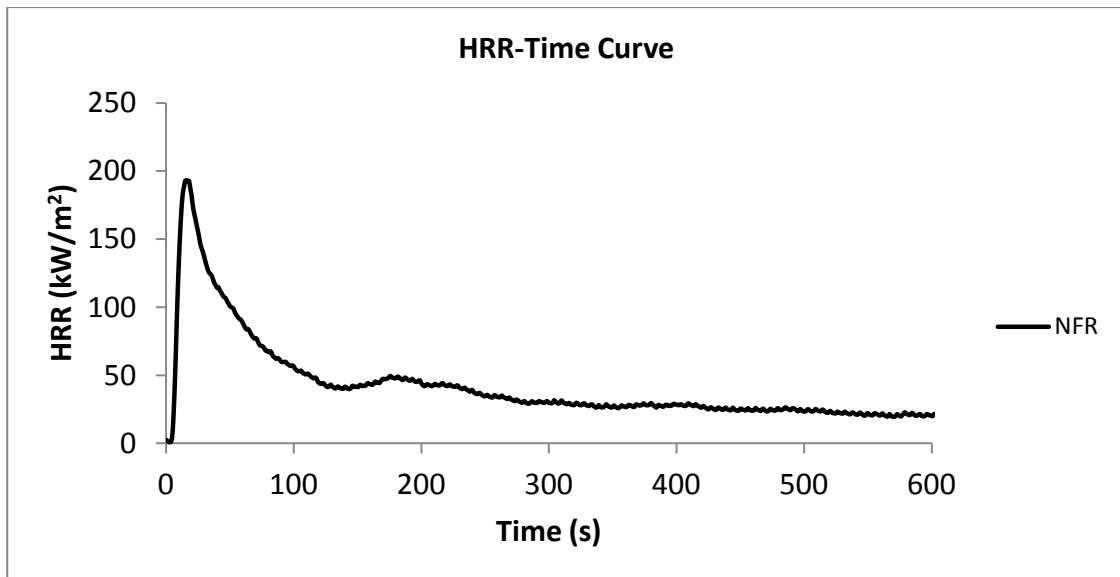
Figure 4.1: HRR-time curve for NFR sample

Figures 4.2 and 4.3 contain comparative plots of the heat release rates with time for the NFR control sample and fire retarded samples for 10% and 20% concentrations of each FR agent respectively. The initial growth periods of the HRR-time curves for all FR samples are similar to that of the NFR specimen; however, each sample is characterized by a different value of peak HRR.
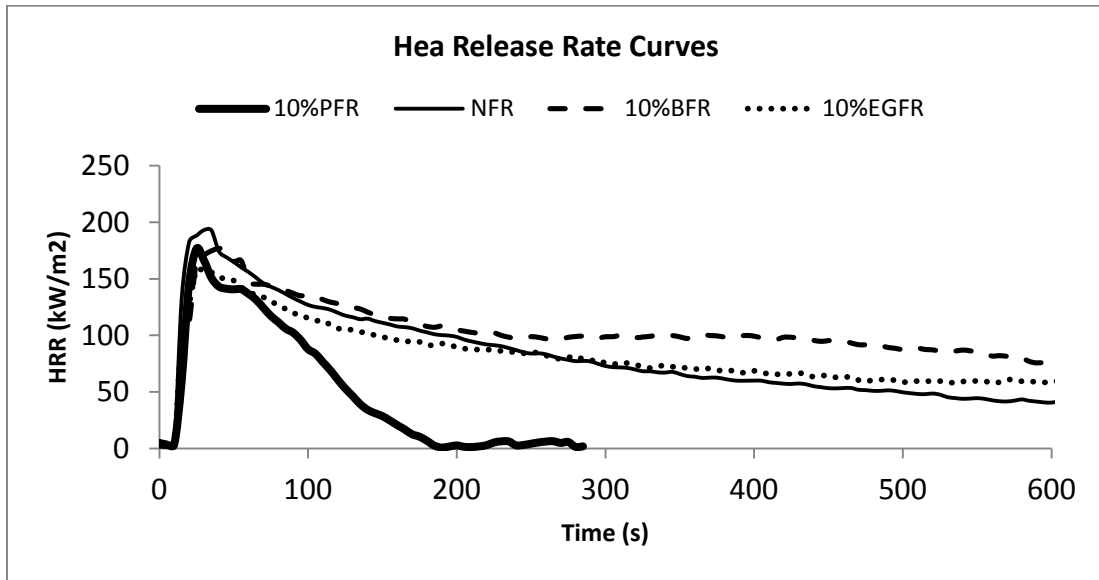
Figure 4.2: HRR versus time curves of NFR and 10% FR samples

Figure 4.2 shows that the highest peak HRR value was recorded for the NFR sample; closely followed by that of BFR and PFR samples. The lowest peak HRR value was recorded by 10%EGFR sample. Figure 4.3 shows sample with 20% FR loading. The plot indicates that the highest peak HRR was recorded for the NFR sample, followed by the 20%PFR system, while 20%BFR and EGFR samples have the lowest values.

Following the peak HRR, the decay curves for each class of FR agent exhibit similar trends for varying concentrations of the same FR additive except for the PFR system in which the plot for 20%PFR sample shows a broader peak

compared to the 10%PFR sample, indicating relatively higher HRR for 20%PFR sample for a longer duration with a subsequent rapid decay in HRR; however, both PFR samples also burned out in a much shorter period of time compared to other samples tested. All other classes of FR agents follow similar trends to one another.
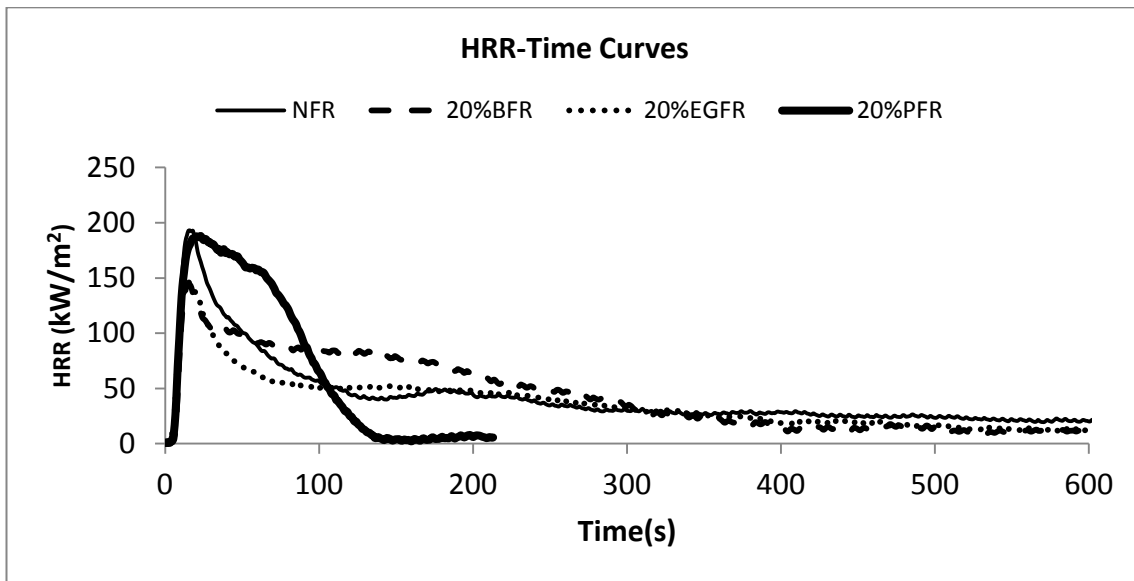
Figure 4.3 HRR versus time curves of NFR and 20% FR samples

To complement the HRR-time curves in Figures 4.2 and 4.3, Table 4.1 shows a summary of the key fire performance data obtained in the full set of cone calorimeter tests for the NFR control sample and fire retarded samples for different levels of FR agent additions. These will be discussed together below. More detailed cone calorimeter test results are included in Appendix 4.1a. Results in Table 4.1 indicate that all samples ignited within 6 seconds of exposure to an incident heat flux of 50kW/m^2. This suggests that addition of the two different levels of the three FR agents to the NFR base foam studied here did not significantly increase times to sustained ignition (t_{ig}) compared to the NFR specimen. Comparison of ignition times listed for the 10% and 20% BFR agent lends credence to the view that addition of higher

concentrations of BFR additives extend the time to ignition and thus reduce the ignitability of a material.

Table 4.1 Summary of cone calorimeter results under well ventilated conditions @50kW/m^2:

Fire Performance Data	NFR	10%BFR	20%BFR	10%EGFR	20%EGFR	10%PFR	20%PFR
Time to Ignition, t_{ig} (s)	3	3	6	2	3	6	4
Heat Release Rate, Peak HRR (kW/m2)	198	180	146	160	148	176	191
Time to Peak HRR t_{PHRR} (s)	16	22	16	14	13	20	19
Fire Growth Rate, FIGRA (kW/m^2.s)	12	8	9	12	11	9	10
Average Heat Release Rate, Ave HRR (kW/m^2)	34	45	43	45	41	66	114
Total Heat Release, THR (MJ/m^2)	30	31	30	21	23	15	15
Percentage Mass Remaining, PMR (%)	10	7	17	30	43	34	33

In contrast, slight reductions in ignition times were observed with incorporation of EGFR or with increasing levels of PFR agents into the base foam; both of which would appear contradictory to expectation. Although only very small changes in ignition time were observed at the concentrations of EGFR used in the samples tested here, the results are consistent with what has been observed by other researchers [116,148-149]. Early ignition of intumescent FR systems is postulated to be due to rapid initial thermal degradation of the material which produces fuel vapors composed especially of low molecular weight hydrocarbons that initiate ignition [148], while the intumescence action develops after ignition and promotes subsequent improvement in the fire performance [116]. In the case of the phosphorous

fire retardant, there appears to be an increase in ignition time over that of the base foam when 10% PFR is added; however, a small decrease in time to ignition is then observed for the addition of 20%PFR agent such that the ignition time appears very comparable to that of the NFR base foam material. While these results potentially will have to be confirmed through examination of intermediate concentrations of PFR addition across a range of NFR base materials in future, it appears that there may be an optimum level of PFR loading in terms of ignition delay for this foam formulation.

In all cases investigated here, the time to ignition remains very short because, independent of FR additive used, the 50 kW/m^2 incident heat flux used in this study promotes rapid decomposition and vapourization of the base foam which masks much of the impact of the FR additives on the overall time to ignition. While similar results have been seen in previous work on similar foams [57], 50 kW/m^2 incident heat flux is not an unreasonable level of flux in a real fire situation so was continued across all tests conducted in this work.

Both average heat release rate (HRR) and peak HRR are key measurements used in assessment of the fire hazard of materials and products, with HRR providing an averaged view of potential thermal hazard and the peak HRR representing the worst case situation in a real fire scenario [58]. For all the foams and FR combinations, the peak heat release rates occurred within an average of 18 seconds after ignition of the samples. As would be expected, Figures 4.2, 4.3 and Table 4.1 indicate a general reduction in peak HRR values with increasing concentration of FR addition to the base foam. The addition of 10%EGFR agent reduces the peak HRR value by 20% compared to the base foam. For the 10%BFR and PFR additives, the data indicates a decrease of about 10% in the peak HRR. Also, the addition of 20% of either BFR or EGFR additive reduces the HRR by 25% relative to the NFR control

sample. In contrast, little reduction in peak HRR over that of NFR sample is observed when 20% phosphorus FR is added.

One measure that has been proposed to determine how quickly a fire may develop to its most intense stage and consequently result in potentially untenable conditions for occupants is obtained by dividing the peak HRR measured in the cone calorimeter by the time taken to reach the peak HRR i.e. taking the slope of the HRR growth curve [26,150]. This value is known as **FI**re **G**rowth **RA**te index (**FIGRA**). It is interesting to note that although the EGFR samples exhibit the lowest peak HRR values, they exhibit rates of fire growth, as measured by the FIGRA parameter, almost as high as those of the NFR base material. In contrast, the BFR and PFR samples exhibit comparable, but lower fire growth rate indices despite the fact that they have differing peak HRR values. The fact that the peak HRR value of 10%EGFR is comparable to that of 10% BFR and lower than that of 10%PFR, while its FIGRA value is still higher than in both cases would suggest that each flame retardant interrupts the burning process to a different extent and potentially also at different times during fire development.

The longer delay of about 20s in time to peak HRR after ignition for BFR and PFR samples compared to the EGFR material accounts for lower FIGRA values obtained in those samples. This is in agreement with the notions that there is an initial rapid thermal degradation of EGFR system promoting early energy release while both BFR and PFR work to interrupt the chemical chain reactions thereby delaying the release of energy from the material. As a result, changes in the peak HRR of NFR and FR materials of the classes studied here should be interpreted with extreme caution if they are to be the sole measure used in ranking the relative fire performance amongst different materials [26].

Although, the values of average HRR for BFR and EGFR foams are similar, but they are higher than NFR sample by 30%, while those of PFR samples are 2-3 times higher than that of NFR sample and the total heat release (THR) for the PFR samples is only half as large as the other materials. This can be explained through examination of the HRR-time curves shown in Figures 4.2 and 4.3 as well as the information in Table 4.1. The PFR systems have peak HRR values which are comparable to that of the NFR sample, and are relatively higher than those of other FR samples tested, while the PFR samples burn over a much shorter period than any of the other materials tested. By definition, the average HRR is the integral of HRR over the sample burning period. Therefore, because NFR, BFR and EGFR samples burned over much longer periods than the PFR samples, the calculated values of average HRR were twice as high for the PFR foams.

The lower measured values of THR and the high percent mass remaining for the PFR samples relative to the other samples indicate that a lower percentage of the PFR samples burned during the cone calorimeter tests than for any of the other samples. Similar reasoning may partially explain the intermediate values of THR observed for the EGFR samples; however, the high mass remaining for the EGFR samples is more likely indicative result of the higher initial relative mass of the EGFR samples due to the EG additives (Appendix 4.1) and the fact that the EGFR itself will not be lost via volatilization as might be the case for BFR or PFR agents.

The above observations can be explained by considering the differences in the mechanisms of FR action between BFR, EGFR and PFR additives. These are discussed in turn. Peak HRR values are reduced in samples containing brominated FR agents, since these additives are designed to inhibit the gas-phase combustion chemistry, effectively decreasing the efficiency of

combustion and therefore the amount of heat generated during burning of the samples. Although BFR samples burned for long periods of time at fairly low levels of HRR until the sample was almost entirely consumed, the lower values of peak HRR coupled with the delay in times to peak HRR occasioned by gas phase inhibition of the BFR system account for the lower FIGRA values compared to the reference sample.

On the other hand, EGFR intumescent foam samples are characterized by lower peak HRR values, medium THR values and high values of mass remaining after the test. While these appear to be somewhat contradictory, they are all consistent with the nature of the FR agent used. The trends seen here, as well as in results reported for other intumescent FR systems [58, 151], can all be related to the way in which an intumescent char layer forms on the surface of the pyrolyzing/burning sample. Figure 4.4, is an image taken during cone calorimeter testing of a 10%EGFR specimen and shows the intumescing carbonaceous char layer that forms across the surface of the sample under the action of heat.

Figure 4 .4: 10% EGFR under the action of 50kW/m^2 heat flux in cone calorimeter testing

For the 10%EGFR, the HRR curve seen in Figure 4.5 exhibits two peaks; with a steep increase to the first peak resulting from vapourization and burning of the material immediately after ignition followed by a decay and subsequent lower peak. Upon ignition, a protective carbonaceous layer begins to form immediately as a result of intumescent action of the EGFR additive.
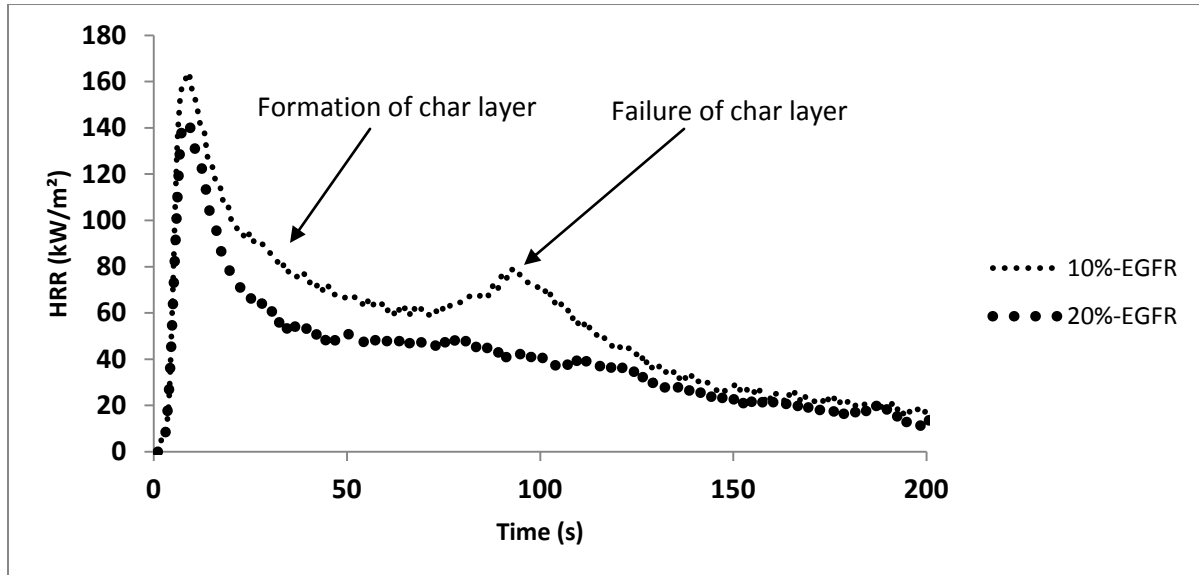
Figure 4.5 HRR-time curves for 10% and 20% EGFR samples

After a short time, this char layer creates a physical barrier which insulates the sample surface from the radiant flux of the cone heater, thereby reducing the formation of flammable vapours as well as limiting the availability of oxygen and diffusion of pyrolyzed products into a reacting zone. In effect, this limits the efficiency of combustion and reduces the observed HRR relative to the NFR sample [53], thus leading to the rapid decline in HRR at around 40 seconds. With continued exposure of the sample to the incident flux, the carbonaceous char layer begins to degrade; allowing heat to penetrate to the sample surface and some oxygen to mix with combustible vapours again. This gives rise to the second broader,

significantly lower, and longer secondary region of elevated HRR around 100 seconds on the HRR-time curves.

In essence, the first peak corresponds to burning before the formation of the protective char layer, while the second one corresponds to burning due to failure of that layer. This observation is in agreement with the literature [116, 151]. Interestingly, the second peak is not as well defined in the 20%EGFR plot, which probably comes about due to the increased level of FR agent which also increases the depth and integrity of the carbonaceous char layer that forms over the burning sample. The measured values of THR suggest that only slightly less foam was burned compared to NFR and BFR samples. The initial FR additive and expanded residual char layer left behind after extinction of the flames must therefore relate to the relatively high measured values of percent mass remaining at the end of the tests.

Finally, video observations of cone calorimeter tests of the PFR samples prove extremely useful in substantiating the results for those samples. In the early phases of burning, at about 20s after ignition, an initial porous surface char layer is formed across the surface of the PFR sample, but this layer does not effectively inhibit the combustion processes and therefore allows partially oxidized combustion products to pass into the reaction zone. In addition, PFR agents inhibit gas phase combustion reactions to some degree which further inhibit the combustion efficiency. These effects are evident through the gradual decrease in measured values of HRR (after the peak) seen in the PFR plots in Figures 4.2 and 4.3; though values of peak HRR are still comparable to the NFR sample.

At about 80s after ignition, a thickened multi-cellular char layer is formed on the surface of the PFR samples which thermally insulates the surface from the incident radiant flux and promotes extinguishment of the flame as well

as reduced availability of fuel vapour and decreased mixing of that vapour with air. The result is the rapid decline in measured HRR value observed in the plot at this time, as well as the shorter total burning period measured for the PFR samples compared to other systems. The decreased duration of burning of the sample and char formation lead to the high percent of mass remaining (%PMR) after the test period. This is consistent with condensed phase (or char forming) mechanisms of flame retardancy that have been reported for many PFR additives [150].

4.2 Smoke Development and Characteristics

Many fire fatalities and injury are caused by exposure to vision obscuring, corrosive and irritant smoke on one hand, and inhalation of toxic gases on the other. The nature and extent of each depend largely on the prevailing fire conditions as well as the composition of the material being burned. Also, the physical and chemical characteristics of the smoke are governed by many factors in the environment such as mode of decomposition, temperature and oxygen concentration, ventilation of the fire, cooling of the fire gases and the time between the smoke formation and the smoke measurements. Smoke from flaming combustion is quite different from that generated during non-flaming thermal oxidative pyrolysis of most materials [152]. Further, due to coagulation, condensation, evaporation and settling, characteristics of the smoke can change with time and thus, aged cold smoke can be different from young hot smoke [152-153].

In flaming combustion, where the temperature is high, the absence of sufficient oxygen to fully oxidize the fuel tends to lead to the formation of black carbonaceous particulate (soot) composed mostly of aliphatic and aromatic intermediate pyrolyzed products [154]. On the other hand, thermal decomposition in the absence of open flames has been shown to lead to

white smoke which is surmised to consist of high molecular weight fractions that condense as the volatiles mix with cooler air to give an aerosol mist consisting of minute droplets of tar and high boiling point liquids [87]. These liquids tend to coalesce under still air conditions and may eventually deposit on surfaces to give an oily residue. Since both flaming combustion and thermal pyrolysis of samples was investigated during this research, it is of interest in this section to further investigate the nature of smoke observed in the different tests.

In order to assess the impact of the three FR additives on smoke evolution relative to that inherent for the NFR reference sample, smoke density measurements were made using the cone calorimeter and smoke density chamber described in Section 3.2. In the cone calorimeter, the smoke and combustion products are measured in the exhaust duct flow. In contrast, in the smoke chamber, smoke and combustion products are measured as they accumulate in a fixed volume chamber throughout the duration of the test. Independent of differences between the two measurement systems, however, previous studies have suggested that smoke measurements performed in the cone calorimeter often follow the same trends as those measured in the smoke chamber when the sample is tested in the horizontal orientation as it was in this work [126].

Smoke development data are presented here in terms of both peak and average specific extinction area (SEA) from the cone calorimeter and maximum specific optical density D_m from the smoke density chamber tests. Although peak values of the specific extinction area are considered more representative of the worst case situation in a fire scenario, they are particularly sensitive to instantaneous fluctuations in specimen mass loss and therefore, average values of smoke production, measured over longer time periods, are more representative of the overall smoking tendency of a

material and therefore fire performance [126]. Both average and peak values of specific extinction area are discussed here [110]. In the following sections, the results from the cone calorimeter tests are discussed first, followed by those obtained for all samples in the smoke density chamber tests.

4.2.1 Smoke Assessment under Cone Calorimeter Testing

Specific to cone calorimeter testing, in addition to assessing the peak and average values of specific extinction area as a measure of smoke evolution, it is common to examine the production of CO and CO_2 from a sample as well. This is because CO and smoke produced during fire scenarios can often be inherently linked to one another since they are products of incomplete combustion. In order to obtain comparable results, it is important to consider the average CO yields with the normalized smoke production defined as average SEA in equation *(13),* i.e the ratio between total smoke production and total mass loss of sample, since the smoke production rate from the sample often varies over the test period. A peak value of smoke production, on the other hand, may occur only at one point in time during testing and as such provides a sense of the highest smoke production due any combined chemical and physical action of the FR, as well as possible changes in local ventilation or mixing conditions around the vaporizing surface of the sample during the test. Average values are integrated across these variations but are more representative values of SEA to use with the CO/CO_2 ratio in order to assess potential correlations between overall smoke and CO production. Due consideration must be given to such differences as they impact the meaning and interpretation of the results presented below.

In general, it would be expected that the presence of flame retardant additives which work via different mechanisms would result in significantly different levels of CO and smoke yields, with corresponding levels of CO_2

production. For example, FR agents that inhibit combustion reactions would be anticipated to result in significantly increased CO and smoke yields with lower levels of CO_2 evolution, even in well ventilated cone calorimeter tests [59,113,148]. Therefore, the CO/CO_2 weight ratio in the exhaust gases is often used as a measure of '*smoke toxicity index*' intended to represent the extent of complete combustion; the greater this ratio, the lower the completeness of combustion, and therefore the greater potential toxicity of smoke developed; and the more dangerous the material based on this indicator [54]. To examine such relationships for the materials studied here, Table 4.2 contains a summary of the measured values of maximum and average specific extinction area (SEA), average CO and CO_2 yields as well as the ratio of CO/CO_2 production from the NFR sample as well as samples with 10% and 20% of the three different FR additives of interest in this work.

Table 4.2: Smoke Data under Cone Calorimeter (well ventilated conditions)

Smoke Performance Data	NFR	10%BFR	20%BFR	10%EGFR	20%EGFR	10%PFR	20%PFR
Specific Extinction Area, **Peak SEA** (m^2/kg)	2573	3792	4800	2437	3652	4600	4968
Specific Extinction Area, **Average SEA** (m^2/kg)	99	326	494	102	156	867	1132
Total Smoke Production (m2)	1.4	4.7	6.9	2.1	1.8	9.1	10.6
Total Smoke Release (m^2/m^2)	154	537	782	236	207	1034	1198
Average CO Yield (kg/kg)	0.1317	0.1706	0.1327	0.0626	0.0678	0.1021	0.1439
Average CO_2 Yield (kg/kg)	1.91	1.9	1.83	1.94	2.05	1.41	1.15
CO/CO2 Weight Ratio (smoke toxicity index)	0.0691	0.0895	0.0722	0.0322	0.0325	0.0724	0.1258

Relative to the NFR reference foam, measured values of peak SEA increase by 45% and 90% for 10% and 20% additions of BFR respectively. Even more notable increases in value (80% and 90%) can be seen for samples with 10% and 20% PFR additions. In contrast, the addition of 10% EGFR appears to depress the peak value of SEA relative to the NFR and other samples tested. The value of peak SEA again increases for the higher concentration of 20%EGFR, by about 40% compared to the NFR sample. The combined results indicate that foams containing BFR, 20% EGFR and PFR all tend to release more smoke than a non-fire retarded base foam, a trend which is in general agreement with the literature [53,113,155].

Considering values of average specific extinction area (Ave. SEA) which is the total smoke production normalized by the mass loss of a sample over the test period, the addition of 10% BFR and 20%BFR increases the quantity of smoke generated per unit mass of sample by a factor of 3 and 5 respectively over the NFR sample. Smoke produced on a unit mass basis by PFR samples is 10 times more than that measured for the NFR foam. Amongst all the FR materials, the EGFR systems generate the least amount of smoke per unit mass lost, but still have average SEA values higher than that measured for the NFR sample.

Consistent with the increasing level of smoke production discussed above, the addition of 10% and 20%BFR to the base foam results in an increase in the average CO yield by 30% and 10% respectively when compared to the NFR sample. It can also be seen from Table 4.2 that BFR addition has little effect on average CO_2 yield over the NFR sample; but average CO_2 yields decrease by about 40% in PFR samples when compared to NFR which is also consistent with the values seen in THR in Section 4.1 above and has also been reported in literature [25]. There is a notable reduction of about 50%

in average CO yield with the addition of 10% and 20% EGFR, while the average CO_2 yield increases by only 10% with 20% EGFR concentration over the NFR sample [25]. This is of interest since the increase in CO_2 yield is likely due in part to the action of the EGFR system which consists of oxidation of the carbon layer shown in equation (*3*) [25]. As a result of the variations of CO and CO_2 production with the various FR additions, the smoke toxicity index $\left[\frac{Ave.CO}{Ave.CO_2}\right]$ increases by about 30% and 5% with the addition of 10% and 20% BFR respectively and by approximately 5% and 80% when PFR concentration increases from 10 to 20%. On the contrary, EGFR addition actually reduces the smoke toxicity index by 50% with the addition of EGFR agents.

All the results summarized in Table 4.2 are again consistent with the anticipated action of the FR additives used. Bromine FR additives act primarily to inhibit the efficiency of gas phase oxidation reactions, since bromine is known to scavenge H* and OH* radicals [156]. This leads to incomplete combustion and considerable increases in smoke production and CO generation and correspondingly reduced values of CO_2 concentrations [53]. As might be expected, the smoke toxicity index remains fairly constant for BFR samples even as levels of FR addition into the base foam are increased. Finally, the smoke development is consistent with the reduced peak HRR and changes in THR and average HRR discussed above.

In contrast, even though phosphorous does act to some degree to inhibit gas phase oxidation reactions, which may result in some increase in levels of CO versus CO_2 production at some times, the addition of phosphorous-based FR agents into the base foam primarily promotes the formation of a char layer (as discussed above). Over time after ignition, this insulates the foam sample and limits the availability of the oxygen necessary to sustain open

burning of the underlying material. The lack of oxygen to the surface of the sample and the gradual cooling of the sample beneath the char layer result in poorly ventilated combustion favouring partial rather than complete, oxidation of CO to CO_2.

Shown in Figures 4.6 and 4.7 are the plots for smoke production rates of NFR and FR samples. As indicated in Figure 4.7, the overall effect is a significant increase in the smoke production rate of 20%PFR sample occurring over a longer period of time than for any of the other samples and resultant increase in overall CO/CO_2 weight ratio, since the CO_2 yield decreases notably despite the CO yield being comparable between NFR and PFR samples [29].
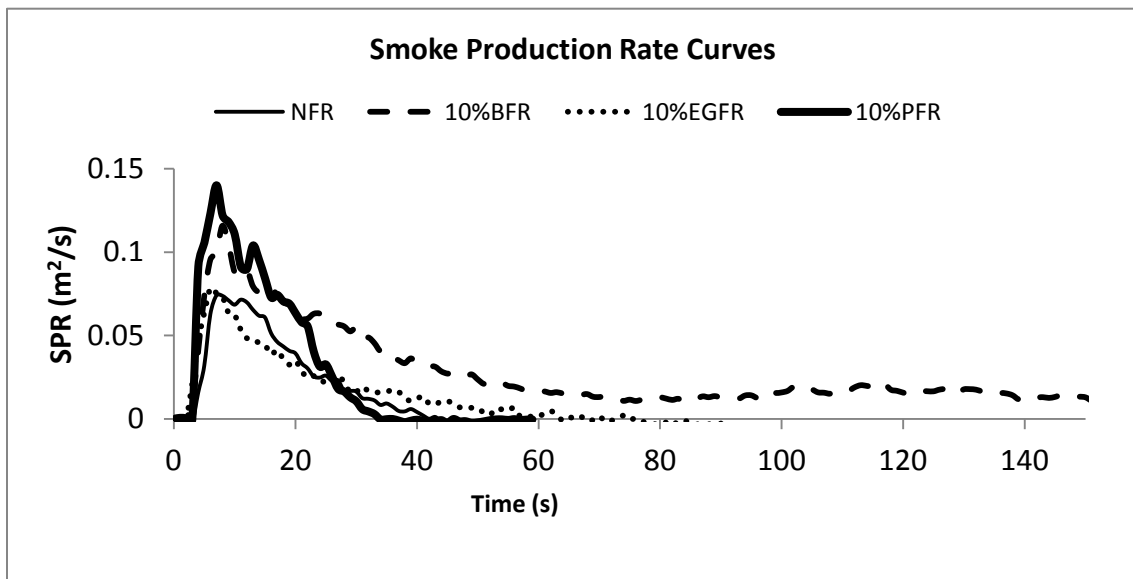
Figure 4.6: Smoke Production Rate Curves for NFR and 10% FR samples
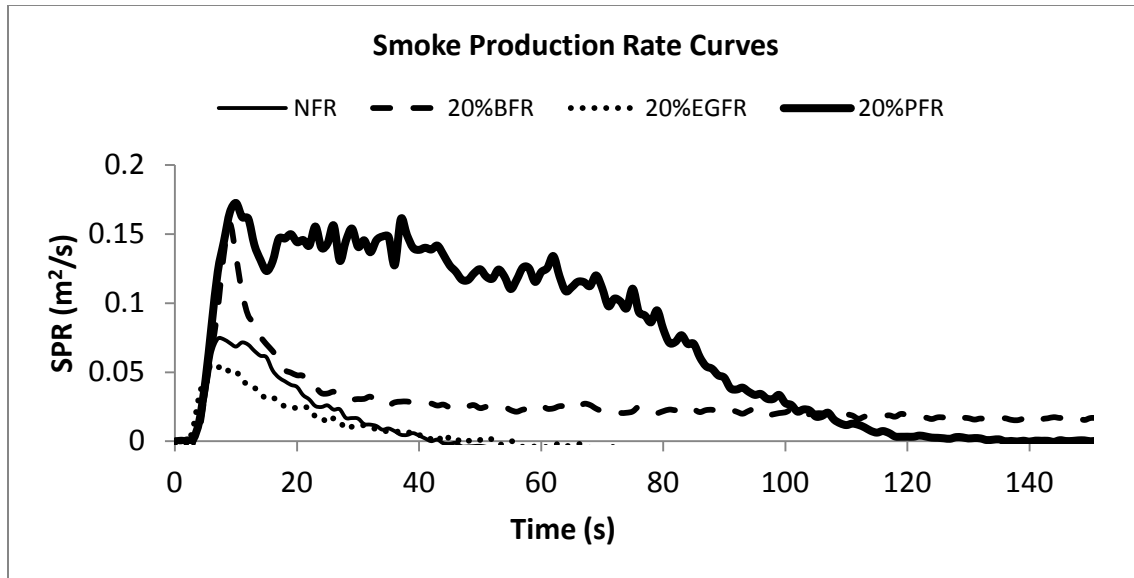
Figure 4.7: Smoke Production Rate Curves for NFR and 20% FR samples

The mechanism by which EGFR inhibits burning of a foam sample is quite different from that of either BFR or PFR which leads to a marked reduction in CO yield, and an increase in CO_2 yield. This combination results in a decrease in the CO/CO_2 toxicity index over that of the NFR base foam. The graphite added to the foam expands due to oxidation of carbon (graphite) by sulfuric acid according to the following reaction as enumerated in equation *(3)* above:

$$C + 2H_2SO_4 = CO_2\uparrow + 2SO_2\uparrow + 2H_2O$$
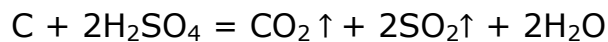
such that CO_2 is generated in large quantities when EGFR samples are exposed to heat. This also initiates a blowing effect that causes an increase in volume of the char structure across the surface of the samples [25, 45, 157].

The thick char layer insulates the underlying polymer from heat and oxygen diffusion thereby thwarting further thermal decomposition [58], such that less sample material is actually consumed. This is consistent with the

decrease in THR and reduced peak HRR discussed above. The rates of smoke production shown in Figures 4.6 and 4.7 are also consistent with the values of average specific extinction area of EGFR samples listed in Table 4.2.

4.2.2 Smoke Assessment under Smoke Density Chamber Testing

Smoke development from all samples was also assessed via testing in the smoke density chamber using the ISO 5659 method with an incident heat flux of 50kW/m^2. In these tests, the samples burned or decomposed in either flaming or non-flaming modes since conditions within the chamber became poorly ventilated as the test progressed. For all cases, smoke density was measured, which reflects the amount of smoke that was accumulated in the chamber with time across the duration of the test.

4.2.3 Smoke development in flaming and non-flaming combustion of the NFR base sample

Before examining the results from smoke density testing, it is important to appreciate possible differences in smoke generation that might result for cases where the sample ignited (flaming) versus those in which it did not ignite and burn (non-flaming). It is well known that particulates (smoke) can be generated through material decomposition, or via smouldering or flaming combustion, although the nature of the particles and their modes of formation will be very different in each case [84]. As a step towards better understanding of any differences that might be encountered in this work; the behavior and smoke development of the NFR control sample were characterized under non-flaming and flaming conditions in the smoke density chamber. In the first case, the incident heat flux was applied to the sample without a pilot flame; while in the second case, the specified pilot flame was used to promote ignition and flaming of the sample.

Figure 4.8 shows plots of measured specific optical density as a function of time for the two cases. Comparison of the traces indicates that the NFR sample which did not ignite (non-flaming conditions) produced twice as much smoke as the one which ignited and burned (flaming combustion). As noted in the literature [158-159], testing of the same material under different burning conditions results in the generation of different amounts of smoke. Generally, more smoke is anticipated to be produced under non flaming conditions compared to flaming combustion consistent with the results here.
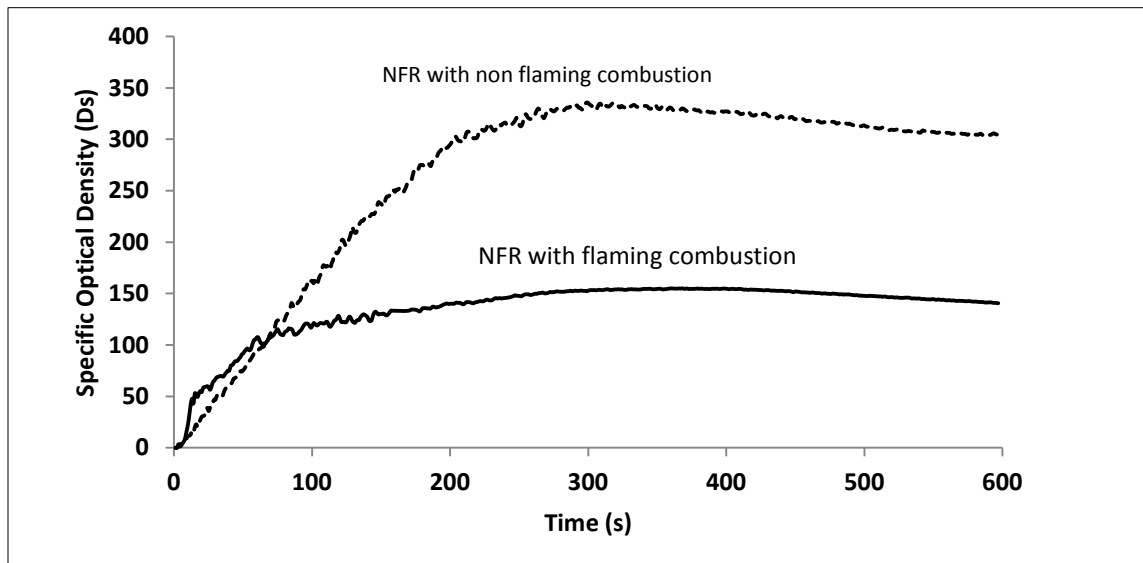
Figure 4.8: Specific Optical Density–time curves for NFR samples in flaming and non-flaming mode

4.2.4 Analysis of specific optical density of samples in flaming and non-flaming combustion

Since both flaming combustion and non-flaming pyrolysis of samples were seen during smoke density tests, the nature and quantity of smoke produced under these various situations will be discussed further in this section. Table 4.3 shows the values of maximum specific optical density, determined by

115

averaging measurements from three smoke density tests (incident heat flux 50kW/m² for each sample), with values of the time taken to reach the maximum specific optical density. Also included in the Table are the percentage mass remaining and different colors observed for each sample under different fire conditions. The measurements taken for all the samples are seen to differ markedly from the peak specific extinction area (SEA) values obtained from the cone calorimeter tests summarized in Table 4.2.

While the NFR, 10%BFR and PFR samples ignited and burned throughout the test period, the 20%BFR*, 10%EGFR* and 20%EGFR* samples thermally decomposed, but did not ignite nor flame during the smoke density tests contrary to cone calorimeter tests in which all the samples were ignited and flamed as they burned.

Table 4.3: Smoke Data in Smoke Density Chamber (poorly ventilated conditions)

Smoke Performance	Flaming Conditions				Non-flaming Conditions		
	0% NFR	10% BFR	10% PFR	20% PFR	20% BFR*	10% EGFR*	20% EGFR*
Max. Specific Optical Density, D_m	166	231	486	437	453	437	324
Time to Max. D_m (s)	340	246	125	113	280	256	239
Percent Mass Remaining (%PMR)	45	37	35	36	36	41	49
Color	White	Black	Black	Black	Brownish Yellow	White	White

The NFR generated white smoke, while BFR and PFR samples produced black smoke, although, the smoke from the PFR sample appeared much darker as reflected in the high value of smoke density index. On the other hand, samples with 20%BFR* and EGFR* evolved notable quantities of off-gases which were brownish yellow for BFR and white for EGFR. These gases are typical of pyrolysis for BFR, and perhaps smouldering for EGFR.

The black smoke as observed from 10%BFR sample is due to the generation of partially oxidized products that lead to increased soot formation when bromine inhibits chemical reactions in the burning sample. The thick black smoke generated during burning of the PFR system was again consistent with formation and thickening of a surface char layer that affected heat transfer, decomposition, mixing and thus efficiency of combustion of the sample. This may appear contradictory to the high peak HRR values recorded for PFR system, especially with 20% concentration as shown in Table 4.1. However, this can be explained by examining the timeline which characterizes the PFR mechanism of flame retardation. Figure 4.9 shows the sequence of events that occur in the 20%PFR sample upon exposure to incident heat flux. There is a delay in time to ignition until about 6s followed by a rapid increase in HRR reaching its peak value at about 20s.
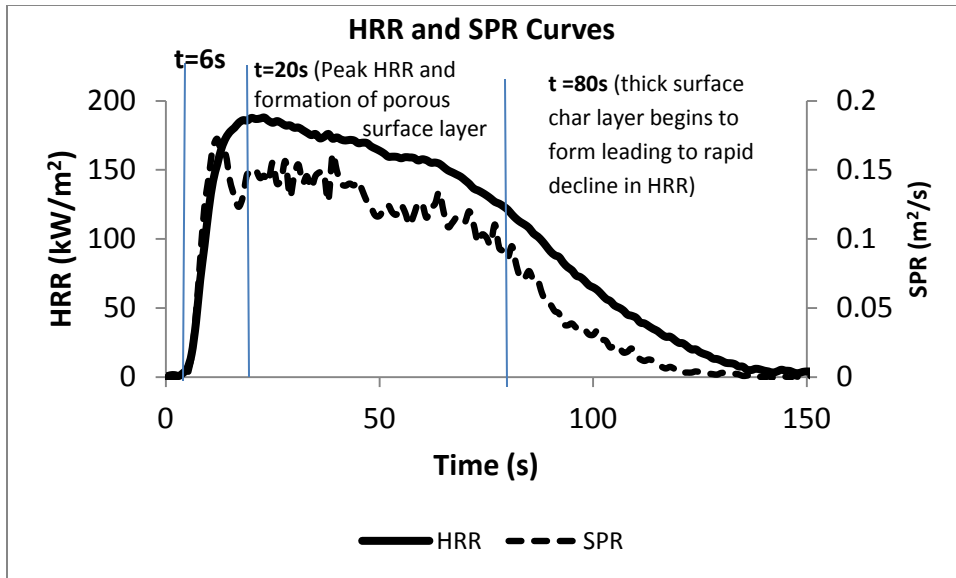
Figure 4.9: Timeline of char formation of 20%PFR surface sample

Between 20 and 80s after ignition, the formation of a porous surface char layer begins. This allows partially oxidized combustion species to escape to the reaction zone [145], thereby sustaining high measured values of HRR for a period of time. At about 80s after ignition, the surface char layer begins to thicken up, creating a more effective physical barrier which then prevents heat and mass transfer and oxygen diffusion to the polymer matrix; thus slowing down combustion efficiency of the burning sample. This latter event accounts for the generation of thick black high smoke and high CO production characteristic of the PFR samples tested here.

Overall, the results indicate that the addition of 10%BFR to the base material results in a 40% increase in value of the maximum specific optical density relative to the control NFR sample. This percentage is much higher than that seen in well ventilated tests between the two materials as shown in Table 4.2; with a noticeable decrease in the time to reach the peak value. As in the case with cone calorimeter testing, addition of PFR to the samples results in even more significant increases in the value of the peak specific optical density (over 150%) and the peak values in smoke evolution are

again reached much more quickly than for either the NFR or 10% BFR specimens.

Considering test samples that did not burn, smoke production of 10%EGFR* compared to 20%BFR* sample shows little difference in the measured values of maximum specific optical density under non-flaming, thermal decomposition in the smoke density chamber; in contrast to the variations recorded during cone calorimeter testing as shown in Table 4.2. All the samples also appear to have reached their maximum specific optical density values at about the same time after application of the incident radiant flux. Similar to the cone calorimeter test results, the maximum value of D_m for the 20%BFR* is higher compared to that of 20%EGFR* sample. However, in sharp contrast to results in the cone, smoke generation is reduced by 25% as the EGFR concentration is increased from 10 to 20% in the present results. Overall, black smoke leads to more obscuration than white smoke and samples which generated black smoke have higher measured values of smoke density than the control sample as indicated in Table 4.3.

It would be expected that smoke evolution from a sample during flaming combustion would be directly linked to the sample mass loss as a function of time. To check whether this is consistent for the samples studied here, Figure 4.10 contains plots of mass loss with time measured during smoke density testing of those samples which ignited and flamed. It can be seen from the plots that the PFR samples show the highest rates of mass loss in the first 80 seconds after ignition consistent with the formation of porous
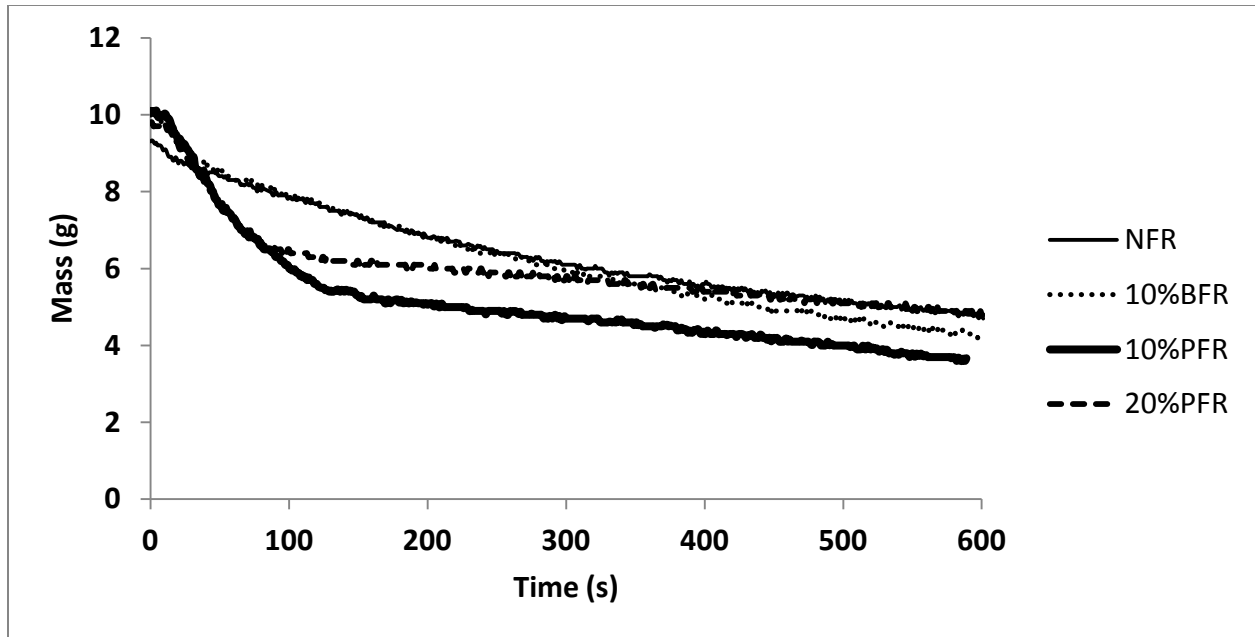
Figure 4.10: Mass Loss versus time of flaming samples in smoke density chamber

surface char layer (discussed earlier under cone calorimeter testing in Section 4.1), more complete fuel vaporization and combustion, and higher HRR. Following this period, the mass loss decreases significantly for the remainder of the test as the carbonaceous char layer builds up creating a more stable structure. This implies less combustion due to less vapourization and burning of the material, and hence more smoke is produced. This is again consistent with the time taken to reach maximum specific optical density at 125 and 113 seconds for 10% and 20% PFR samples respectively as shown in Table 4.3 above. Once at the peak, the samples remain at relatively high levels of smoke production compared with other samples as shown later in Figure 4.13. The 10%BFR sample on the other hand, exhibits a mass loss rate similar to that of the PFR samples for the first 25 seconds after ignition which then decreases to a rate similar to that for NFR for the next 260 seconds. The sample is characterized by high initial smoke production consistent with the higher initial mass loss rate as a result of fuel vapourization and combustion. But the lower total mass loss of sample is

due to the effect of gas phase inhibition of combustion process as the dissociated bromine scavenges the high energy radicals which drive the combustion reactions and thus lowering the reaction temperature. This results into an incomplete combustion which contributes more to the smoke production.

The measured mass loss for those samples that did not ignite is plotted against time in Figure 4.11. The slopes of the lines are again consistent with the ordering of measured values of specific optical density in Table 4.3. Values for 20%BFR* and 10%EGFR* are very similar and the 20%EGFR* sample produces less smoke. The above results demonstrate that, as expected, changes in combustion conditions significantly impact the characteristics and nature of smoke generated by each material. It is therefore of interest to cross plot values of peak SEA as measured in the cone calorimeter against values of maximum values of D_m measured in the smoke density chamber tests for those samples that ignited in both test situations and to determine whether there is, in fact, a correlation between smoke generation potential as measured in the two different situations.
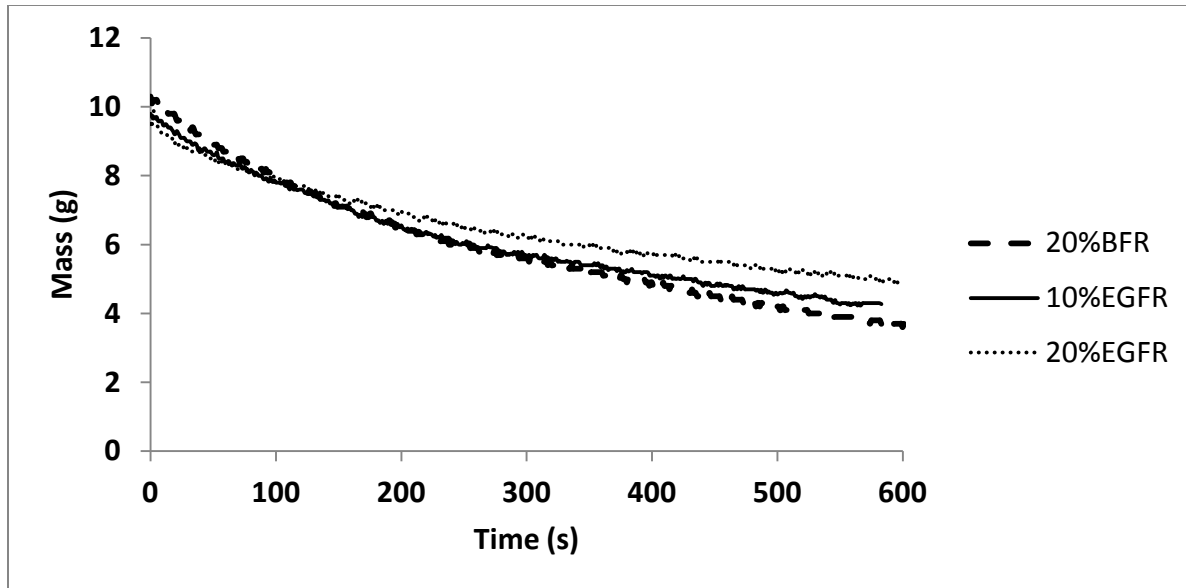
Figure 4.11: Mass Loss versus time of non-flaming samples in smoke density chamber

Figure 4.12 shows a plot of measured values of peak SEA versus maximum specific optical density, D_m. Based on the limited set of results for NFR and FR samples of foam that underwent flaming combustion, it is clear that as measured values of peak SEA increase, so do values of maximum specific optical density, evidenced by the linear regression coefficient of 0.9016. Similar observations have been noted in the literature for smoke measurements on wood-based materials [126]. In the work of Drysdale and Atkinson, whose work involved the testing of wood flooring materials (i.e douglas fir, red oak, interior carpet and resilient floor covering); it was discovered that for similar materials and vent sizes, smoke measurements of the type performed in the cone calorimeter agreed well with static measurements of smoke density by comparing peak specific extinction area values using both methods [160].
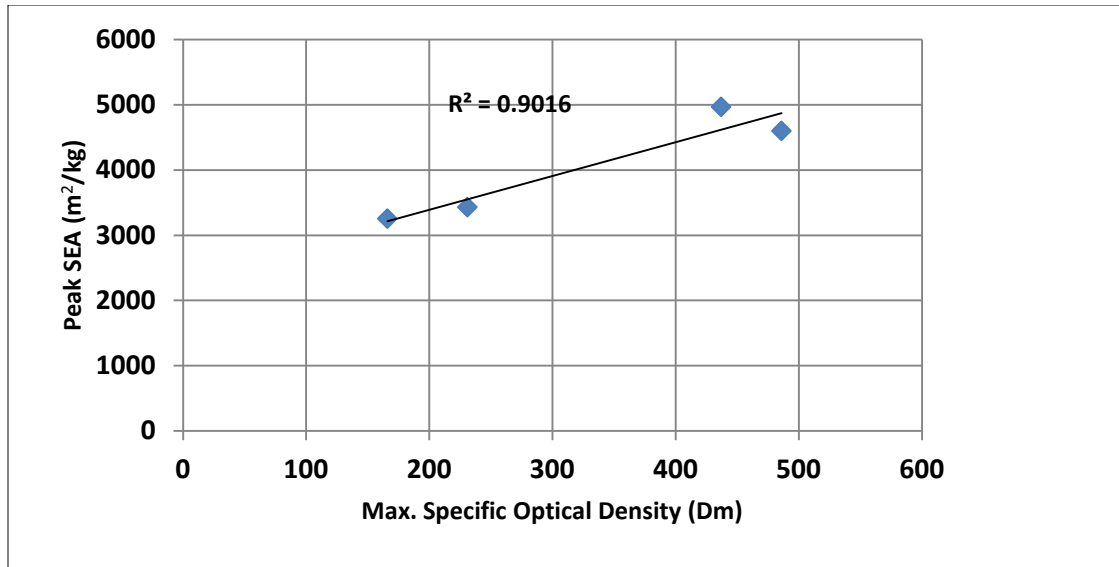
Figure 4.12: Peak SEA versus Max. D_m for samples in flaming combustion

In order to relate the data generated in the smoke density chamber to those collected from cone calorimeter, they translated the data from smoke chamber into specific extinction area, similar to those from the cone calorimeter. To the author's knowledge, such a correlation has not been previously reported for tests conducted with a single base foam and varying levels of BFR, PFR and EGFR additives.

While an initial view of smoke generation from NFR versus BFR, PFR and EGFR samples can be obtained from the global smoke density parameters discussed above, it is also of interest to examine the time dependent evolution of smoke across the various formulations. Shown in Figures 4.13 and 4.14 are plots of measured specific optical density versus time for all the foams as measured in flaming and non-flaming conditions respectively, during smoke density tests. Under flaming combustion, it can be seen that for PFR foams, values of specific optical density increase quickly after ignition to peak values, and then decrease slowly with time in a similar

fashion to cone calorimeter until the thick char layer builds up leading to higher levels of smoke generation.
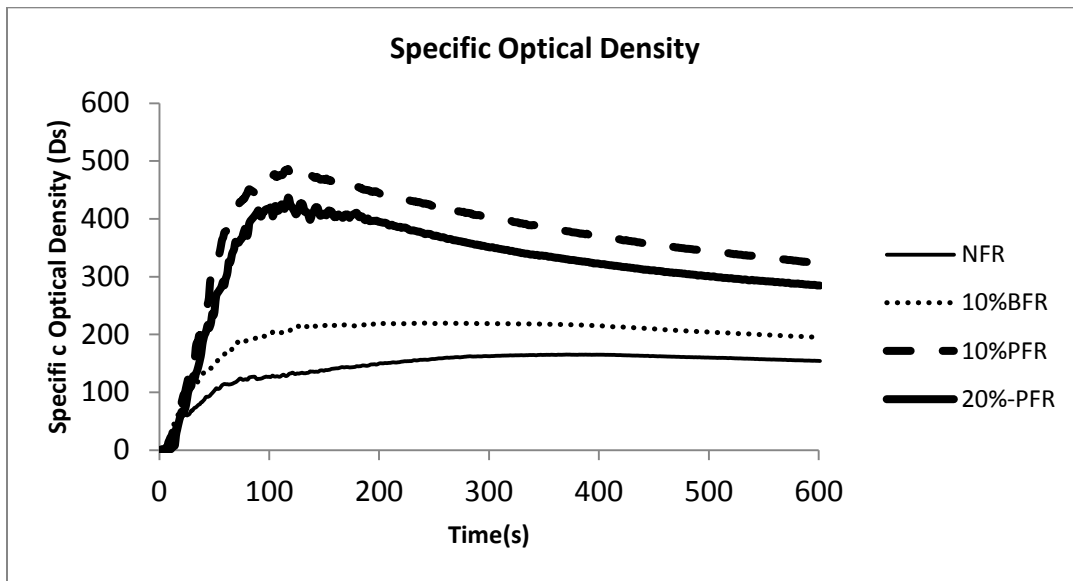
Figure 4.13: Specific optical density-time profile of samples in poorly ventilated flaming conditions

Measured values of specific optical density thus remain at levels higher than for 10%BFR which are again considerably higher than those obtained from the NFR sample. In contrast, smoke generation from NFR and 10% BFR samples increases to a maximum and then continues at fairly constant values until the test is complete. As noted above, the generation of large quantity of black smoke from BFR and PFR samples, in contrast to the white smoke from NFR sample, leads to higher measured values of obscuration. Results are also consistent with previous observations that addition of some fire retardant additives can increase smoke generation from a material [161], so the two effects combined lead to higher values of smoke density for BFR and PFR over the NFR samples studied.

In smoke density testing, the 20% BFR* and both EGFR* materials did not ignite and flame. As shown in Figure 4.14, the initial increase in values of optical density are very similar for 20%BFR* and 10%EGFR* with both

producing significantly more smoke than the 20%EGFR* sample. Following the initial period, however, it appears that smoke production from both EGFR samples decreases very slightly, while that of 20%BFR* continues at a nearly constant rate. Since colour of the smoke does influence the measured values of smoke density, the combined effect of the amount of smoke and colour makes it difficult to know which factor is actually responsible for the values recorded.

Global fire performance results indicate a reduction in peak values of HRR, and therefore a potential improvement in HRR with the addition of FR agents. The yields of CO and smoke increased significantly, especially with BFR and PFR additives. Overall, 20%EGFR addition gives better material performance in terms of peak HRR, THR, CO, smoke yield and smoke toxicity index compared to the other FR agents at all concentrations; reasons for the apparently low ignition times with EGFR additions, however, may merit further investigation from the broader perspective of materials fire safety.
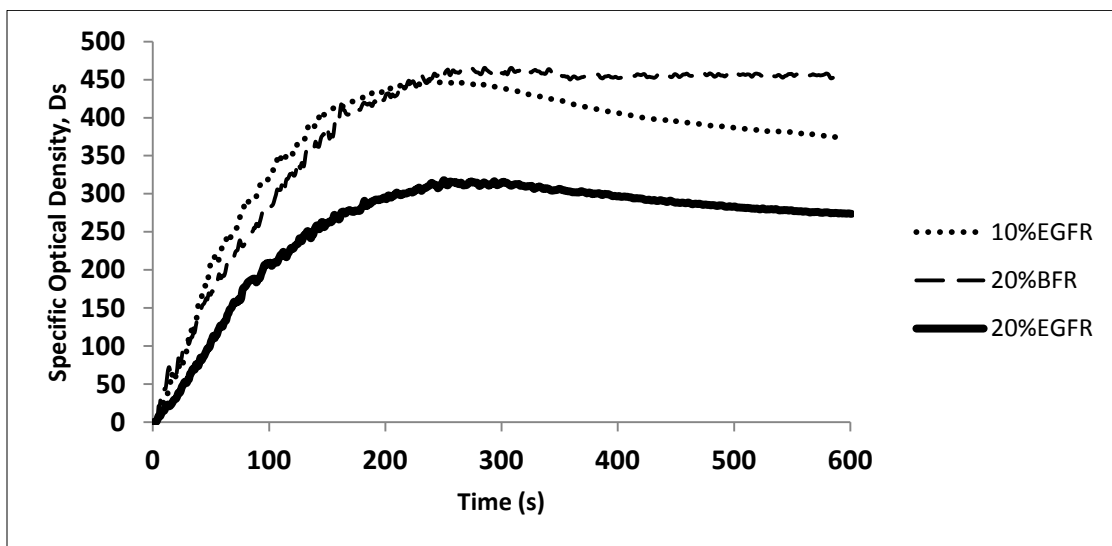
Figure 4.14: Specific optical density-time profile of samples in poorly ventilated non-flaming conditions

4.3 Fire Gases Analysis

The combined effect of inhalation of smoke and toxic fire gases has been recognized as the major contributor in fire fatalities [6, 7]. The identification and measurements of fire gases generated from fire retarded and non-fire retarded rigid PUR foams is one of the prime objectives of this study. This section highlights the major gases produced during decomposition and combustion of the samples in well ventilated and limited ventilation fires. Although, the production of some of the major fire gases from the combustion of rigid polyurethane foam has been studied over the years, few detailed analyses of the gases generated under different ventilation conditions and for varying levels of FR additive have been done. In most cases, interest has centered on a limited range of FR additives, ventilation conditions have been set by the experimental apparatus employed and in many cases only major gases such as CO_2, CO, HCN and a limited number of other compounds considered as key toxic species have been examined [7, 9,12].

As part of this study, the concentrations of the above gases are measured during cone calorimetry testing (well ventilated) for the range of NFR and FR materials discussed above. In addition, concentrations of NOx and unburned total hydrocarbons were measured in well ventilated test conditions and results were corrected for the transport delay and response time of the instruments. Finally, the nature of volatile organic compounds generated during decomposition/burning of the samples in both the cone calorimeter and smoke density chamber are considered. Results for each of these are discussed in turn in the following sections.

4.3.1 Oxygen Depletion

The minimum measured oxygen concentration in a cone calorimeter test will correspond to the peak heat release rate for a given sample due to the theory upon which the test is based. The rate of burning, the combustion efficiency and the yields of specific products, in turn, depend on the percentage oxygen in the surrounding atmosphere and the rate at which depleted oxygen is replenished. For the NFR foam considered here, examination of the HRR versus time or the oxygen depletion versus time curves in Figure 4.15 indicates that during heating and before ignition, up to **Stage I** on the plot, there is little oxygen consumption consistent with the very low levels of heat release from the fuel. After ignition, the HRR grows quickly to a peak value of $200kW/m^2$, while the oxygen concentration decreases equally quickly reaching its minimum concentration value of 20.50% as oxygen is consumed in oxidizing the fuel vapours to CO and CO_2 . The HRR subsequently decays slowly over time as more fuel is vapourized and combusted, in concert with a correspondingly slow increase in the measured oxygen concentration with time.
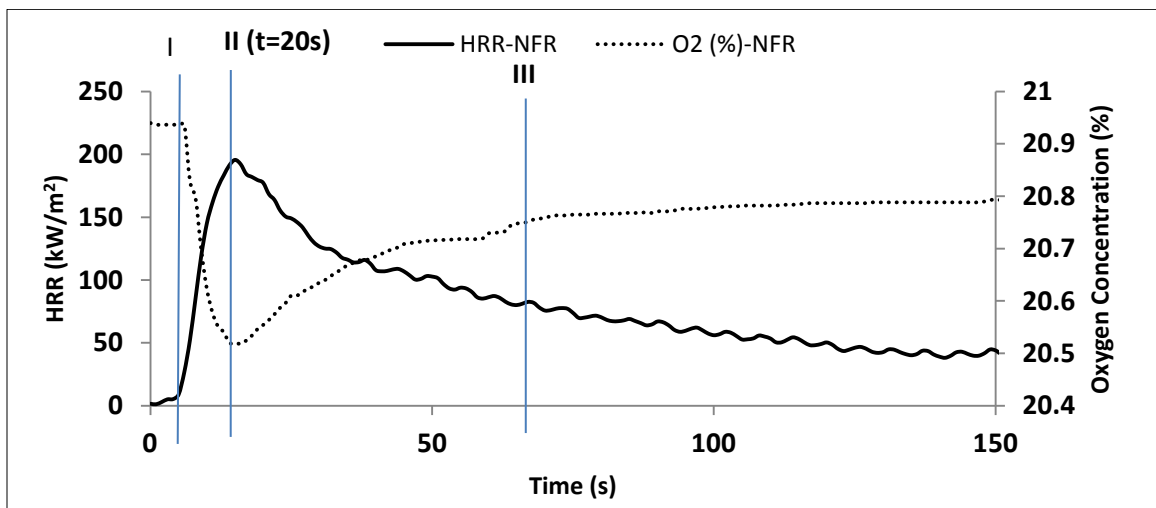
Figure 4.15: HRR and oxygen concentration versus time curves for NFR sample

This plot clearly shows the relation between combustion (HRR) of the NFR sample and measured oxygen concentration in the cone calorimeter test. It is also evident from the plot that the HRR is at its peak value when oxygen concentration is at lowest level. From the plot, it was determined that for this material a typical fire performance test consists of three main stages: thermo-oxidative pyrolysis before ignition (**I**), flaming combustion with maximum heat release rate (**II**) and smoldering or post flaming (**III**) stages. These are chosen as the basis of comparison of results for the FR materials examined in this study.

Representative oxygen depletion versus time curves for all of the 10% FR samples are plotted in Figure 4.16 to facilitate comparison of the burning characteristics to those of the NFR sample shown in Figure 4.15. By about 20s in Figure 4.16, all of the FR samples are burning rapidly and reaching their peak HRR values, leading to fairly similar minimum measured oxygen concentrations of about 20.53%, 20.49%, and 20.45% for NFR, BFR and PFR samples respectively. The highest oxygen concentration was measured for the EGFR sample at its peak HRR when compared with all the other samples suggesting that much less oxygen was being consumed in the oxidation reactions for this material; consistent with the reduced peak HRR value. After the peak, the oxygen concentration for the PFR sample remains low relative to the NFR and other FR systems from about 20–80 seconds after exposure to the heat flux. During this period, the porous surface char layer built up but still allowed oxygen diffusion to the burning matrix. The oxygen concentration then returns to ambient levels much more quickly than any of the other materials as the surface char layer builds up and suffocates the flame.
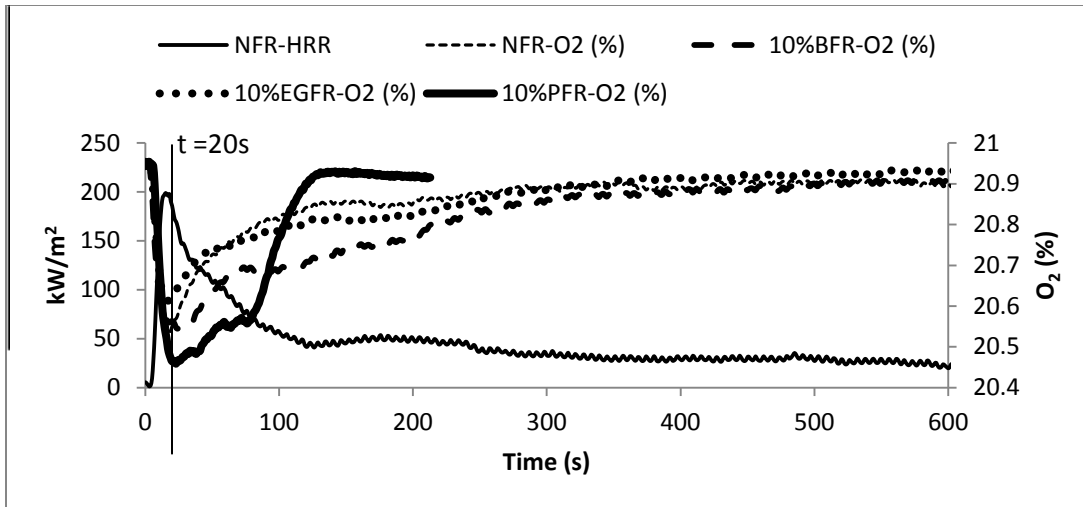
Figure 4.16: Oxygen depletion-time curves for NFR & 10%FR samples and HRR-time curves for FR sample

In comparison, Figure 4.17 contains plots of the representative oxygen depletion versus time curves for 20%FR samples. These indicate higher oxygen concentrations for 20%BFR and EGFR samples, suggesting less oxidation in an integrated sense and also lower heat release rates for those materials (as indeed was reported in Section 4.1).
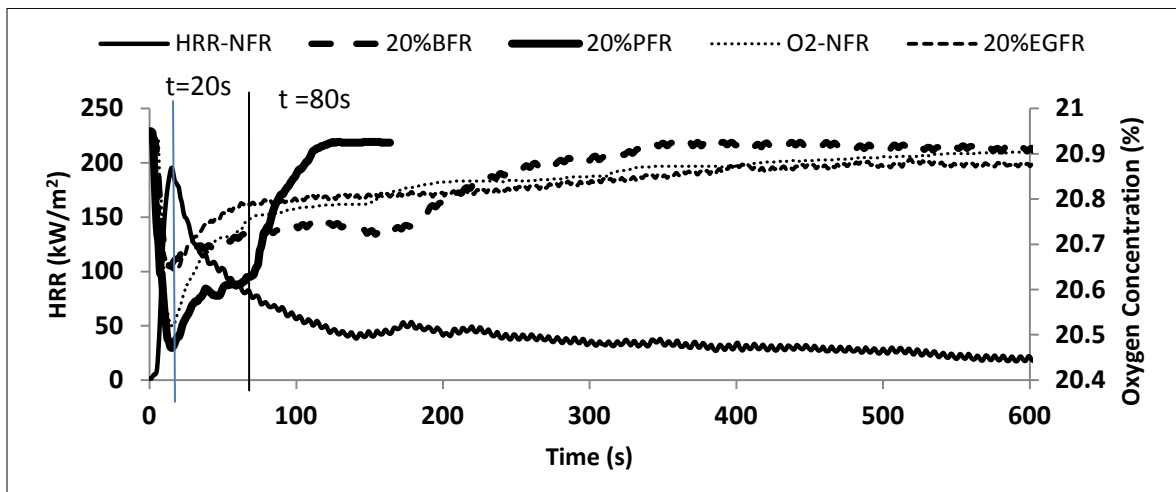
Figure 4.17: Oxygen depletion time curves for NFR & 20%FR samples and HRR-time curves for NFR sample

129

While overall trends in measured oxygen consumption with time are similar for all samples through stages **I** and **II**, the rate at which the oxygen concentration increases back to ambient levels during stage **III** is different amongst the samples depending upon the interactions and different modes of action of FR agents. These will determine whether the samples sustain small flames, smoulder, or extinguish quickly towards the end of the test, as discerned through video records of each experiment.

From Figures 4.16 and 4.17, it can be observed that the 10% and 20%PFR plots have similar shapes, indicating similar combustion behavior which is in agreement with other evidence discussed in previous sections on phosphorous flame retardant action. Oxygen consumption for samples containing BFR is found to be much less than that for the NFR samples, about 20.52% at its peak. In Figure 4.17, oxygen consumption profiles of the 20% BFR and EGFR samples are the same until after the peak HRR. Following this, more oxygen is consumed in burning of the BFR sample than the EGFR before oxygen levels return to ambient towards the end of test. Both materials consumed less oxygen compared to the reference sample, which is particularly in agreement with the lower peak HRR and increased smoke and CO production in BFR sample. Again, this is consistent with the data shown in Table 4.2.

4.3.2 Carbon Dioxide Concentration Measurements

Figures 4.18 and 4.19 show the plots of measured CO_2 concentrations with time for NFR and 10%FR, and 20%FR samples respectively as tested in the cone calorimeter. As would be expected, for all samples, concentrations of CO_2 increase with HRR, but oxygen levels decrease as the CO_2 production increases and the foam is burned. For instance, the superposition of the HRR curve and CO_2 concentration-time curve for the NFR sample (shown in

Appendix 4.2) indicates the two measurements are directly related, where the peak HRR corresponds to the maximum CO_2 concentration. Considering NFR and 10%FR samples, the maximum concentration of CO_2 produced is about 0.5% from the PFR and BFR systems, which are also characterized by the highest levels of oxygen depletion.

Figure 4.18: Carbon dioxide concentration–time curves for NFR and 10%FR samples
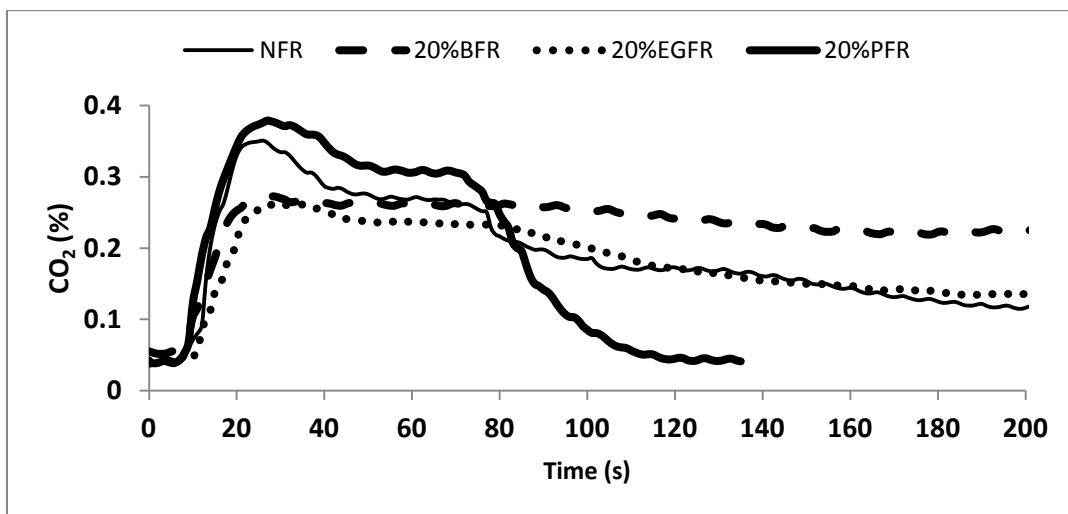
Figure 4.19: Carbon dioxide concentration –time curves for NFR and 20%FR samples

A slightly lower level of CO_2 concentration of 0.33% is seen for combustion of 10%EGFR compared to 0.37% CO_2 produced from the NFR base foam.

Again, this is found to be consistent with the oxygen depletion profiles and peak HRR for NFR and EGFR samples. In contrast, the maximum CO_2 concentrations for 20%FR samples are generally lower than those for the10%FR samples as shown in Figure 4.19. The maximum concentration of CO_2 produced is about 0.37% from PFR samples, a similar concentration to that produced during testing of the NFR base foam. Concentrations produced from BFR samples are about 0.33%, but this level is produced at a relatively higher and constant level than any other materials, particularly in the later stages of test. Again, it can be seen from the figure that the EGFR sample produces lower concentrations of CO_2 (0.22%). Overall, the shapes and peak values on the time traces of CO_2 concentration are all entirely consistent with the oxygen depletion results outlined in Section 4.3.1 above.

4.3.3 Carbon Monoxide Concentration Measurements

Measurements of CO concentrations with time are plotted in Figures 4.20 and 4.21 for NFR and 10%FR samples and NFR and 20%FR samples respectively as tested in the cone calorimeter. As indicated earlier, the CO_2 production is at its peak value for the NFR sample when HRR is at maximum whereas the CO concentrations first peak after the CO_2 peak production (shown in Appendix 4.2b). It is interesting to note that following this initial peak, CO concentrations decrease slightly, perhaps corresponding to changes in the slopes of the O_2 and CO_2 curves as well, but increase again towards the end of the test to levels higher than the original peak, as the burning regime changes to smouldering conditions.

Figure 4.20: Carbon monoxide Concentration-time curves for NFR and 10%FR samples
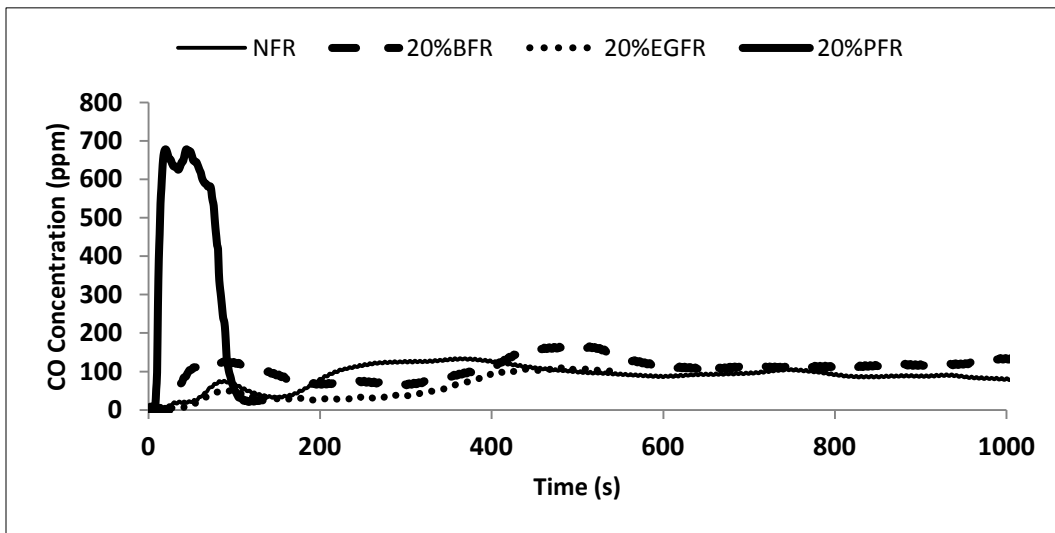
Figure 4.21: Carbon monoxide Concentration-time curves for NFR and 20%FR samples

From Figures 4.20 and 4.21, very similar behavior can be seen for the NFR sample and both EGFR samples, at least early in the test. At some time after the peak CO concentration is reached, however, the CO concentration from the NFR sample actually increases while that from the EGFR sample remains relatively low until near the end of the test when both NFR and EGFR

133

samples are generating similar amounts of CO at a relatively constant rate. To some extent the time evolution of CO concentration from the two BFR samples is also similar to the NFR samples at least in terms of time to peak CO concentration; however the peak concentrations are higher than those seen in the NFR or the EGFR samples.

Following the peak, the CO concentrations generated during testing of the BFR samples then decrease for a period of time and increase again in the later stages of the test. This is consistent with the action of the BFR agent which inhibits the efficiency of gas phase oxidation reactions by scavenging the H* and OH* radicals from the reaction [156] leading to incomplete combustion and considerable increase in CO generation and smoke production, with correspondingly reduced values of CO_2 concentrations [53]. The generally higher CO concentrations measured during testing of the BFR samples is in agreement with the average CO yield of the materials as shown in Table 4.2

The behavior seen for the PFR foam samples is markedly different from that seen for any of the other samples. The CO concentrations increase quickly to levels higher than those seen for samples with any other FR additives (400ppm and 700ppm for 10% and 20%PFR respectively versus 50-200ppm for the other samples) and remain high for a period of time during and after the maximum heat release rate has been reached. The broad peaks are consistent with the trends in HRR and in CO_2 production with time and also with the broad valleys observed in the oxygen depletion results and noted in Section 4.3.1. As discussed above, as the surface char layer builds up on the PFR samples, incomplete combustion sets in, leading to the high CO concentrations seen here; consistent with the time evolution of measured CO_2 concentrations as well as the high average SEA values shown in Table 4.2. The initial high production of CO_2 coupled with the higher CO concentrations measured during the later stage of the fire are unique to the

burning of PFR samples. As with other measurements, the differences observed in the CO concentration-time profiles of different foam samples all point to different FR actions and burning characteristics especially towards the later stage of the fire.

4.3.4 Nitric Oxide (NO)

NO_x has been detected in experiments involving the flaming combustion of rigid PUR foam. Isocyanate is a major component used in formulation of rigid foams and serves as one potential source of nitrogen-containing decomposition products. A change from pyrolysis to flaming combustion may result in oxidation of the nitrogen-containing decomposition products to nitric oxide and nitrogen dioxide species [62]. In addition, NO could be formed by one of the NOx generation mechanisms reported in hydrocarbon combustion literature. The time evolution of nitric oxide under flaming, well-ventilated conditions in cone calorimeter testing is shown in Figures 4.22 and 4.23 for NFR and 10%FR and NFR and 20%FR samples respectively.

From Figure 4.22, it can be seen that the maximum concentrations of NO generated are 18ppm for the NFR sample, 25ppm for the 10%BFR sample and 15ppm for the 10%EGFR sample. Significantly higher levels of NO (70ppm) are seen for the PFR samples, consistent with higher burning rates and overall heat release rates previously discussed. Similar trends are observed with 20%FR agents as shown in Figure 4.23; although in this case, it is notable that addition of 20%EGFR significantly reduces the maximum measured concentrations of NO in the exhaust stream in comparison to the NFR sample. With the addition of 20%EGFR, there also appears to be a delay in the production of NO compared with other samples.
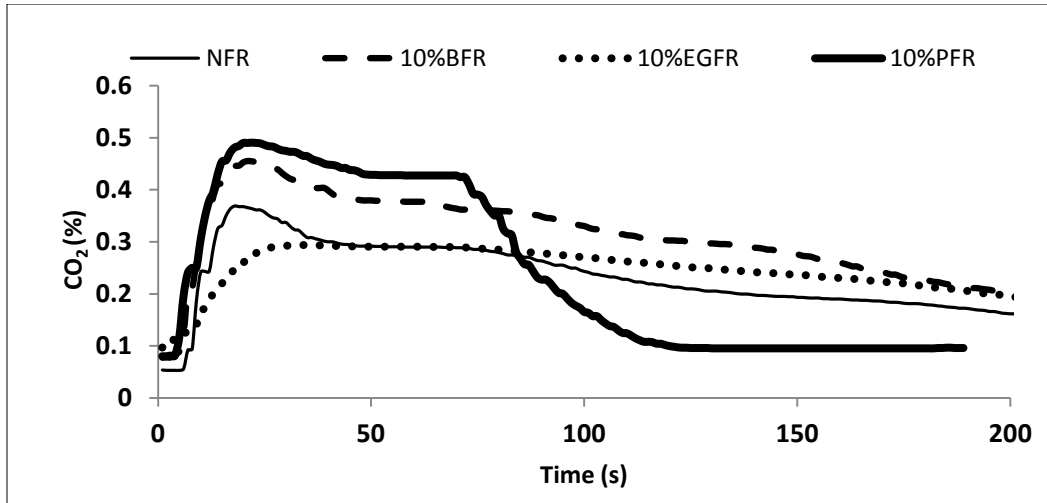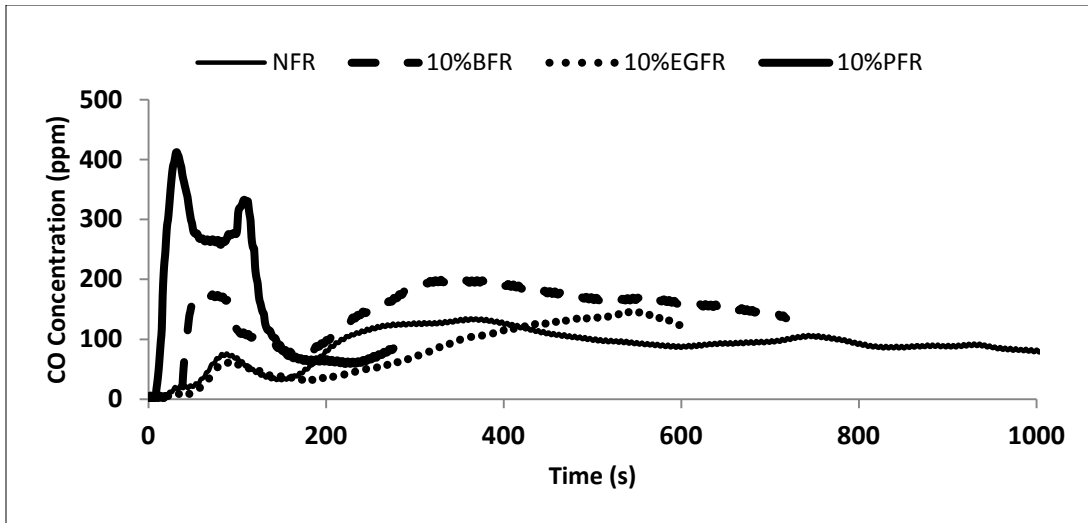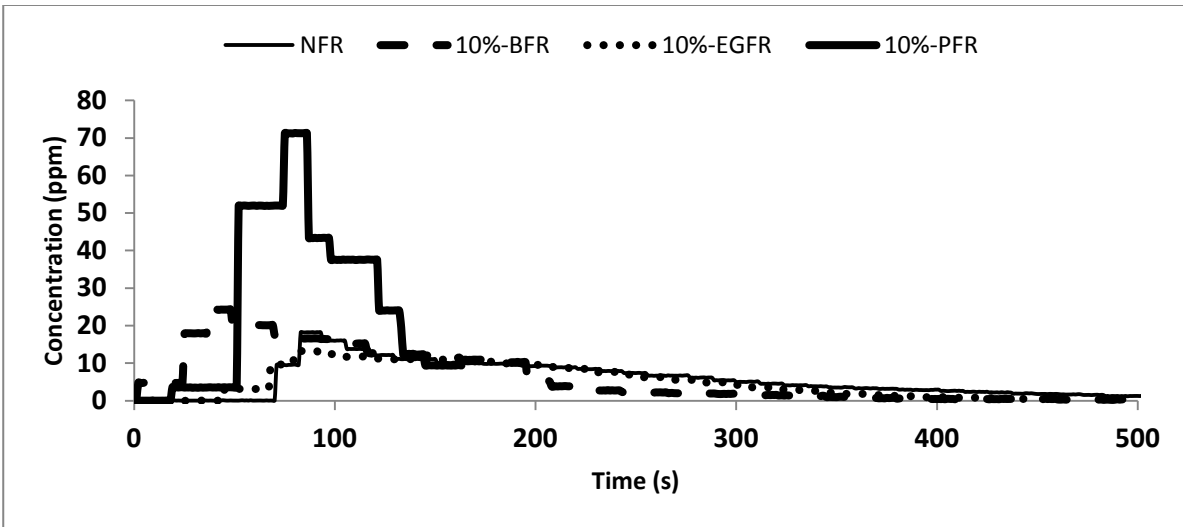
Figure 4.22: NO concentration-time curves for NFR and 10% FR samples
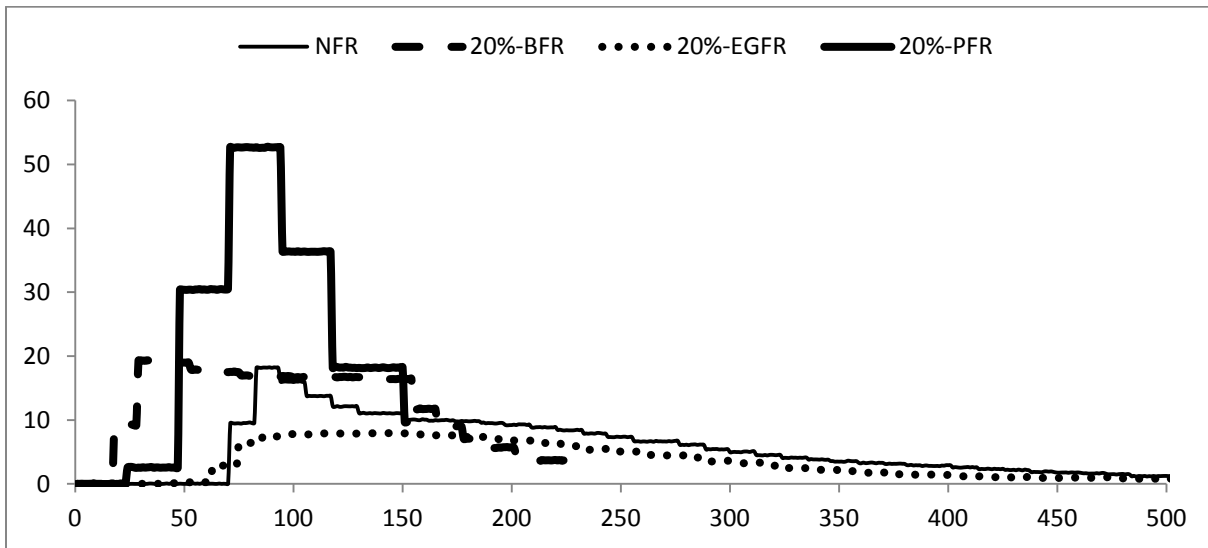
Figure 4.23: NO concentration-time curves for NFR and 20% FR samples

Early formation of the intumescent surface char layer may act as a heat sink in this case, leading to reduced temperatures and reaction rates and slowing down the generation of NO [62,162-163].

4.3.5 Nitrogen Dioxide (NO₂)

Closely linked to the generation of NO in combustion systems is the generation of NO_2. Figures 4.24 and 4.25 show the plots for concentration–time history of nitrogen dioxide (NO_2) as measured for the NFR and 10% FR and NFR and 20% FR samples respectively. Peak values of concentration and time evolution of NO_2 follow similar trends in time and for various FR agents as to those reported above for the NO production. The level of NO_2 generated from the EGFR sample is about half of that produced during testing of the NFR samples which in turn, is less than what is being produced from BFR samples. Again more NO_2 is generated for PFR samples than any other samples in this study, likely due to the higher burning rates of the PFR materials, particularly during the early stage of burning process.
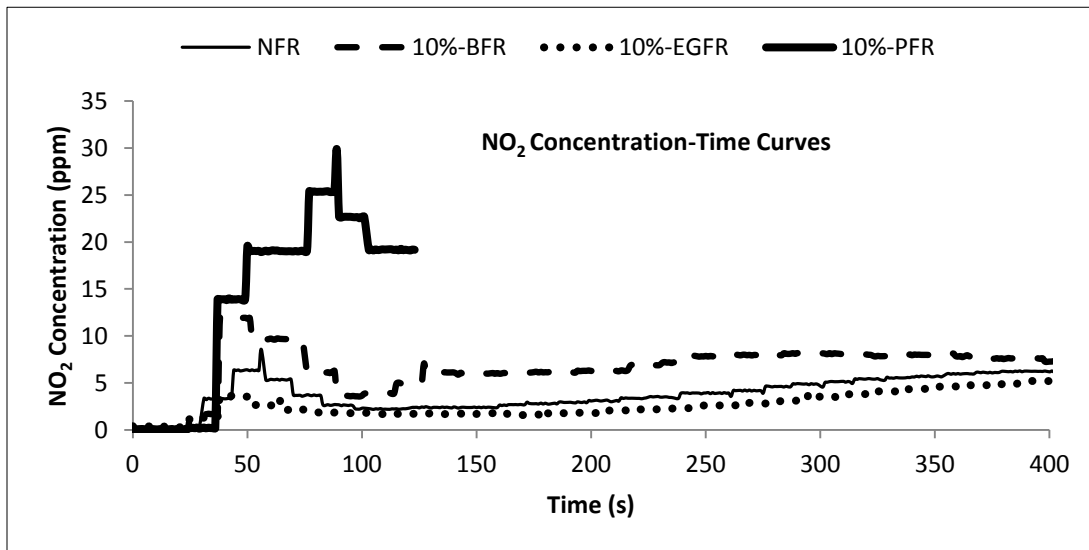
Figure 4.24: NO_2 concentration-time curves for NFR and 10% FR samples

In general, the measured concentrations of NO_2 are less than those seen for NO, consistent with results observed in previous studies [162-163]. This suggests that NOx formed during combustion of rigid polyurethane foams is predominantly nitric oxide (NO) and a lesser amount of NO_2 under the same

burning conditions due to the combined effects of combustion of nitrogen containing products arising from isocyanate group of the base foam formulations and direct formation of nitrogen oxides in the high temperature flame zones.
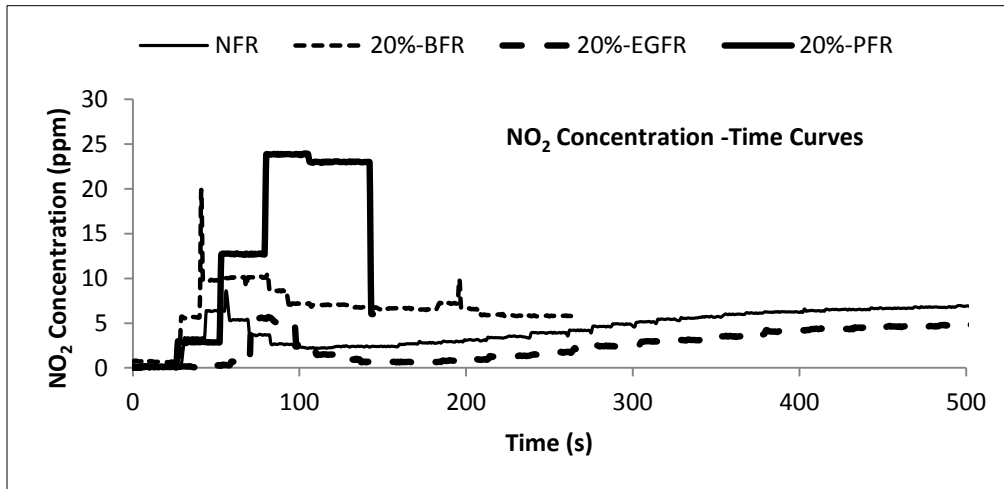
Figure 4.25: NO_2 concentration-time curves for NFR and 20% FR samples

The long shoulders on the NO_x concentration plots, especially for the NFR, BFR and EGFR samples, are indicative of ongoing reactions during the later stage of the fire, consistent also with the time traces of CO and CO_2 concentrations. Previous studies of the decomposition and combustion of rigid polyurethane foam in air have shown that NOx generation is most likely to occur during flaming combustion in high O_2 and temperature conditions [62]. Delays in the onset of formation of NO_x seen for various samples in Figures 4.24 and 4.25, then, mark the change from pyrolysis to flaming combustion. Formation of a surface char layer which deprives the burning material of oxygen and acts as a heat sink, thereby reducing the flame temperature and reaction rates, may contribute to the lower levels of NOx concentrations measured particularly for the EGFR systems.

4.3.6 Unburned Total Hydrocarbons

The generation rate of unburned total hydrocarbon (UTH) and the time to the maximum generation rates were measured and are shown in Figure 4.26 and 4.27 for NFR and 10%FR and NFR and 20%FR agents respectively. The measured values of unburned total hydrocarbons (UTH) reported here reflect the total concentration of all hydrocarbon-based species which are not oxidized during burning of the sample and are therefore carried into the cone calorimeter exhaust stream. For 10%FR additions, the results indicate high concentrations of UTH measured from PFR and EGFR samples, with considerably lower concentrations observed in the case of BFR and NFR samples as shown in Figure 4.26. By increasing FR addition to 20%, PFR samples produce more UTH than NFR samples and samples containing other FR agents as shown in Figure 4.27. From Figure 4.27, 20%FR agents show the highest concentrations of UTH of about 450ppm for PFR samples. While NFR samples generate the lowest concentrations of UTH of about 120ppm, the EGFR and BFR materials produce 180ppm and 250ppm respectively.
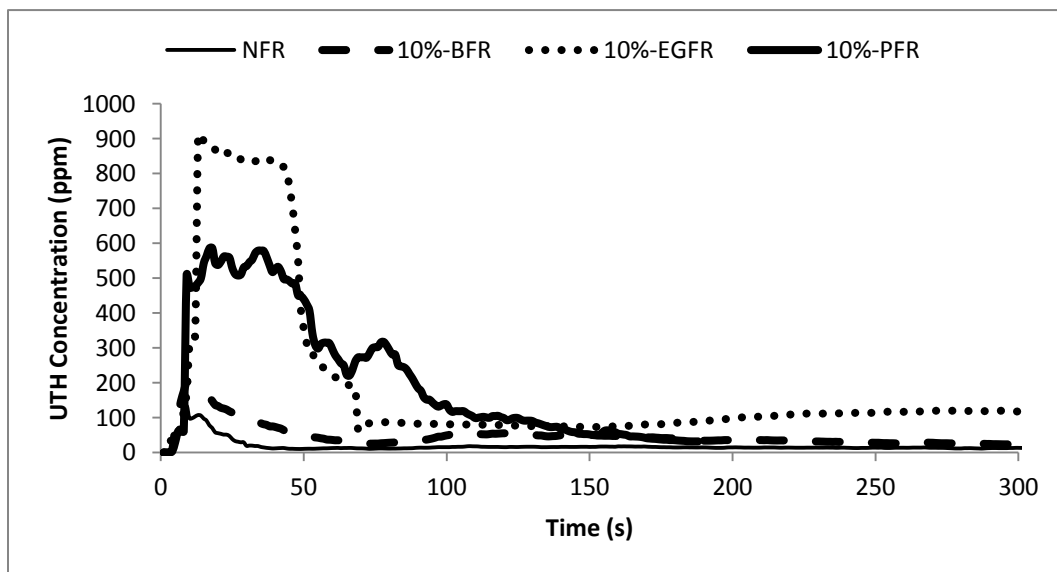
Figure 4.26: UTH concentration–time curves from flaming combustion of NFR and 10% FR samples
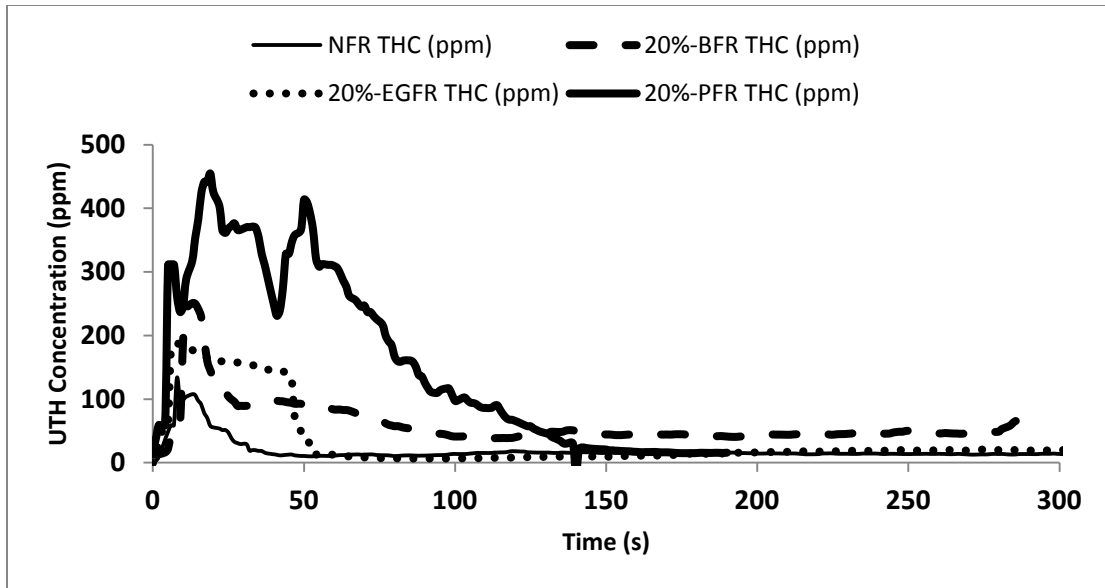
Figure 4.27: UTH concentration-time curves from flaming combustion of NFR and 20% FR samples

The time to maximum concentrations of UTH are generated for all the samples correspond to the times to peak HRR. For both 10% and 20%FR additions, the plots show that generation of unburned total hydrocarbons begins upon exposure of the sample to the incident heat flux and concentrations build up rapidly until they reach the maximum measured values in the free burning phase of the samples (around the peak HRR). Concentrations of UTH then decrease again during the final burning phases of all the tests. Using 20%PFR sample as a case study, the maximum generation of UTH occurs near the time when the peak HRR is measured (t=20s) as shown in Figure 4.28, and the concentration of UTH remains at a high level for a period of time until such a time when a more stable char layer is formed that prevents heat transfer and oxygen diffusion to the matrix leading to steadily lower production rates of UTH species till the end of test.
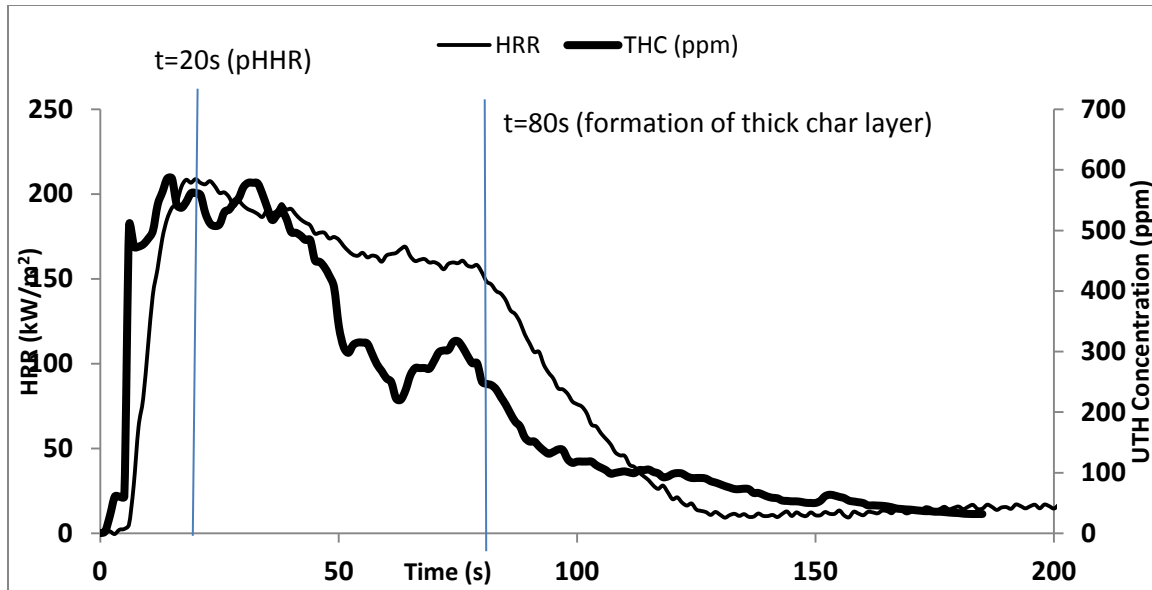
Figure 4.28: Overlay of HRR and UTH time measurements for 20%PFR sample

The shapes and production rates of UTH in both EGFR and PFR samples are particularly interesting. Figure 4.29 shows overlay plots of the UTH concentration with time for both samples of 10% and 20% concentrations of both FR additives. The shapes of UTH time traces for both 10% and 20% EGFR samples appear similar though the peak values are quite different; with the concentrations rising steeply to peak values at about 900ppm and 200ppm for 10% and 20%EGFR samples respectively.

Similarly, plots of measured UTH concentrations with time for 10% and 20%PFR samples are characterized by broad and multiple peaks which may again be explained by the nature of char layer formation on these samples that have been discussed previously. Peak UTH concentrations are also higher, close to 600ppm and 400ppm for 10% and 20% additives respectively when compared to much lower values of 120ppm and 200ppm observed for NFR and BFR materials respectively. Again, this is consistent with the effect of a char layer on combustion of the underlying sample.
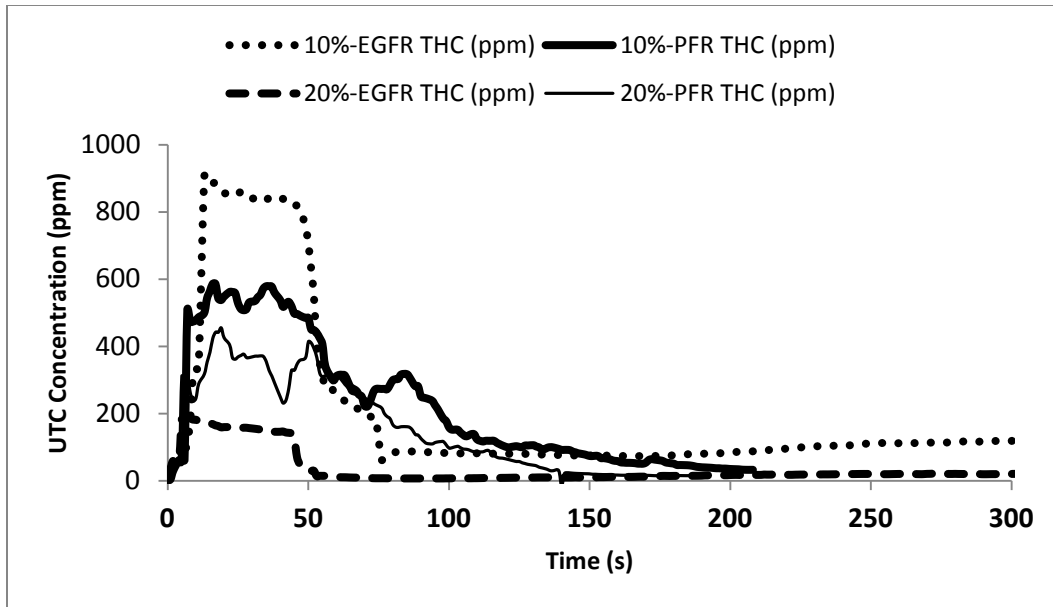
Figure 4.29: Overlay of UTH curves for 10% and 20% EGFR and PFR samples

The high concentrations of UTH measured during testing of the EGFR and PFR samples suggest the presence of rich combustible mixtures, though increasing the concentration of these FR agents in the base foam from 10% to 20% reduces the peak values of UTH concentration generated during burning of EGFR by 80% and PFR systems by 25%. The peak UTH concentration for BFR sample does not appear to be much affected by increasing percentage of the BFR agent. The relatively low production rates of UTH species in both 20%EGFR and PFR samples is consistent with the idea that increasing the level of these FR agents directly increases the amount of char formation which invariably reduces the mass loss rates (MLR) of the samples (see Appendix 4.3); and hence results in low production rates of UTH. This idea is further supported by the fact that the 20%EGFR and PFR consume less oxygen during testing as the concentration of FR agents increases from 10-20%.

142

The combined results indicate that the various flame retardants tested in this research play significant roles in the polymer chemistry and physics of burning behaviour often resulting in some degree of incomplete combustion with commensurate changes in concentrations in UTH gases outlined above.

4.3.7 Volatile Organic Compounds (VOCs)

From the global fire performance results discussed above, HRR characteristics of the rigid base foam changed, and indeed seemed to improve, with the addition of different FR agents. At the same time, yields of smoke increased significantly, especially for 20% BFR and PFR additive loadings. Marked, but consistent, differences are observed in other fire performance characteristics, concentrations of major fire gases and UTH concentrations as measured in the initial phases of testing NFR and FR samples. In the next stage of the research, it was of interest to examine in further detail the nature of the gases generated from each sample during testing in attempts to deduce in more detail how each individual FR additive acted during decomposition and burning of the base foam under study.

To this end, the evolution of volatile organic compounds released from the different materials was studied by collecting sample gases on specific adsorbent materials during well-ventilated cone calorimeter and poorly ventilated smoke density chamber tests. Gas samples were collected using the methods outlined in Sections 3.3.5 at the three stages shown in Figure 4.15. ***Stage I*** represents oxidative pyrolysis, ***stage II*** represents a fully developed fire and ***stage III*** represents a post-fire situation. Analysis of all samples was conducted off-line using the combined analytical technique of Thermal Desorption Gas Chromatography and Mass Spectrometry (TD-GC/MS) (Section 3.4.3). The results form the basis for this section.

The major decomposition and combustion products from NFR and FR samples were identified by GC/MS for each stage of the tests, focusing particularly on VOCs that can be detected in the mass scanning range from $40\,amu$–$300\,amu$. Unstable and reactive compounds present, as well as compounds with masses outside this range, were not detected. For purposes of the discussion here, the major compounds identified were categorized into groups according to their molecular structure, including aliphatic hydrocarbons, ketones, aldehydes, alcohols, nitrogen-containing compounds, halogenated (brominated) compounds, aromatic hydrocarbons and organic acids.

In the literature review in Section 2.4.1, the general decomposition mechanisms of rigid PUR foams under different atmospheres and temperatures as they affected decomposition pathways were discussed. These will determine, to differing degrees, the nature of gaseous products formed during fire performance testing as well. Although, these steps may describe the basic mechanism of dissociation of pure PUR foam in an inert atmosphere under steady heating, and before it ignites, the flame retardant additives, oxygen concentration local to the sample, ignition and combustion of the sample and resultant temperature history, may result in significant variations in quantity and compositions of the gases produced in the tests performed here, as well as in a real fire. Detailed investigation of such effects form a major portion of this research in which representative gases generated during both cone calorimeter (well-ventilated) and smoke density (poorly ventilated) testing of NFR reference foam, as well as 10% and 20% concentrations of each FR additive were identified and compared. Sampling was timed to collect gases in **Stage I** before ignition to capture early thermal decomposition products; in **Stage II** around the time to peak HRR to capture products which might arise during flaming combustion of each

material and in **Stage III** towards the end of burning to capture products representative of post-fire effluents.

Previous results indicate that the aliphatic hydrocarbons, especially propene which is formed by almost simultaneous degradation of urethane groups and degradation of the polyester resin and aliphatic oxygenated functional groups, are the first to evolve during the pyrolysis and combustion of the polymeric structure. The main nitrogen-containing products observed were nitriles and amines [35]. Other gases such as acetaldehyde, acetone, acetonitrile, benzonitrile, 2-ethylhexanol, benzene, toluene, xylene, styrene and benzofuran have been identified from previous studies as well [62, 64, 66]. These will be used as the basis for comparison and interpretation of the results which are discussed in turn in the following sections.

4.3.7.1 Stage I: Thermal Decomposition Products

Results of the major decomposition products identified by GC/MS in the early stage of fire before ignition occurs (**Stage I**), in a well-ventilated cone calorimeter test environment for NFR and 10%-FR agents are summarized in Table 4.4. Gaseous species produced during initial decomposition of the NFR sample include low molecular weight hydrocarbons such as propene, acetaldehyde, acetone, acetonitrile, 2-propenitrile and high molecular hydrocarbon fuels including nitrogen-containing aromatic compounds (benzonitrile and aniline), aromatic compounds (benzene, toluene, styrene, limonene, phenylethyne) and fused aromatic components such as indene.

These gases are typical of those expected from oxidative decomposition of polyurethane foams and other hydrocarbon fuels with readily available air (oxygen) and low temperature conditions [62, 87]. The presence of propene (olefins) and amines supports the dissociation steps depicted in equation *(5)* of Section 2.4.1; while all the nitrogen-containing species such as nitriles

and amines may have come from the isocyanate component of the MDI-based foam formulations.

Table 4.4: Thermo-oxidative products in well-ventilated Cone Calorimeter Testing for NFR and 10%FR samples [Stage I]

Compounds	Group Names	NFR	10%BFR	10%EGFR	10%PFR
Propene	Alkenes	x	x		
Propane	Alkanes		x		
Acetaldehyde	Aldehydes	x			
Hexanal	Aldehydes		x		
Acetone	Ketones	x	x	x	**x**
1,3-Dioxolane, 2-methyl-	Ethers			x	
Hexanoic acid, 2-ethyl-	Aliphatic acids	x	x		**x**
Acetonitrile	Nitriles	x			
2-Propenenitrile	Nitriles	x			
Benzonitrile	Aromatic Nitriles	x		x	**x**
Aniline	Aromatic Amines	x	x	x	**x**
o-Toluidine	Aromatic Amines				x
1-Hexanol, 2-ethyl-	Aliphatic Alcohols		x	x	x
Phenol, 2-methyl-	Aromatic Alcohols		x		x
Phenol	Aromatic Alcohols		x	x	x
Benzene	Aromatics	x	x	x	x
Toluene	Aromatics	x	x	x	x
Styrene	Aromatics	x	x	x	x
Limonene	Aromatics	x	x	x	x
Phenylethyne	Aromatics	x	x	x	x
Indene	Aromatic Fused ring	x			
1,2-Benzenedicarboxylic acid	Aromatic Acids	x	x	x	x

Gases produced from the BFR samples are quite similar to those identified for the NFR sample with the exception of nitriles such as acetonitrile, 2-propenitrile and benzonitrile. The low molecular weight straight chain hydrocarbon gases identified in both samples is indicative of decomposition of the foam to smaller chain organic vapours during initial heating. Contrary to the gases generated during heating of both NFR and BFR samples, the absence of light weight straight chain hydrocarbons in the gases generated during heating of EGFR and PFR samples appears inconsistent with early stage thermal decomposition of PUR foams. This could be explained

however, by the fact that gases may not have been detected if they were present at only very low concentrations in the well ventilated, diluted conditions of the cone calorimeter exhaust stream. The absence of brominated species in the gases generated from samples with 10%BFR may be a result of similar dilution of the product gases.

The higher molecular weight compounds such as aromatic amines, phenylethyne and 1,2-benzenedicarboxylic acid, and common aromatic species that were identified in the gases generated from EGFR and PFR samples are consistent with the anticipated initial thermal decomposition products. Coupled with the absence of low molecular weight gases, it may also be that the higher molecular weight pyrolysis products do not completely break down to the smallest hydrocarbon units due to the action of the FR agents. This may merit further investigation in future.

As opposed to the compounds identified in the gases generated during heating of the reference sample, some aromatic alcohols and amines are evident in the decomposition products of all of the samples that contained FR agents, suggesting that the decomposition pathways shown in equations (4) and (5) were in some way involved when there were FR additives in the samples. In general, the main product groups include alkenes, aldehydes, nitrogen-containing compounds, aromatics and other fragments characteristic of the MDI-based foam, in addition to major gases such as CO and NO discussed in Section 4.3 above [62,69]. Even at 10%FR loading, difference in the thermal decomposition products are certainly observed using the TD-GC-MS system indicating that this method can discern that, as anticipated, different pathways for decomposition are followed depending on the FR additives used. Furthermore, those products which are identified are consistent with other measurements taken in this study as well as with the

different modes of action of various FR additives described in literature [62, 64, 69]. Detailed chemical kinetic analysis of these differences and their justification based on foam formulation, FR and temperature interactions is deferred to future work involving a more quantitative investigation of the chemical species produced.

Table 4.5 shows a list of compounds identified during decomposition of 20%FR samples under the same test conditions as in Table 4.4. The addition of 20%FR agents seems to further alter the chemical structure and characteristics of decomposition gases across FR samples. Gases evolved from NFR sample include low molecular weight hydrocarbons (propene, acetaldehyde, acetone, acetonitrile, 2-propenitrile), alcohols, aromatic nitriles (benzonitrile), common aromatic compounds (benzene, toluene, styrene, limonene, phenylethyne) and higher molecular aromatic compounds (indene, benzendicarboxylic acid).

Table 4.5: Thermo-oxidative products in well ventilated Cone Calorimeter Testing for NFR and 20% FR samples (Stage I)

Compounds	Group Names	NFR	20%BFR	20%EGFR	20%PFR
Propene	Alkenes	x	X	X	X
1,3-Butadiene	Alkenes		X		
Butane	Alkanes				X
Propyne	Alkynes		X		
1-Buten-3-yne	Alkynes		X		
3-Penten-1-yne	Alkynes		X		
Acetaldehyde	Aldehydes	x		X	X
Acetone	Ketones	x		X	X
Methane, bromo-	Brominated		X		
1,3-Dioxolane, 2-methyl-	Ethers			X	
1,4-Dioxane	Ethers			X	
Hexanoic acid, 2-ethyl-	Aliphatic Acids	x			
Acetonitrile	Nitriles	x			X
2-Propenenitrile	Nitriles	x			X
Benzonitrile	Aromatic Nitriles	x			X

Compound	Class				
Benzyl nitrile	Aromatic Nitriles				x
Benzonitrile, 2-methyl-	Aromatic Nitriles				
3,3'-Diaminodiphenylmethane	Aromatic Amines			x	
Benzenamine, 4,4'-methylenebis-	Aromatic Amines			x	x
Ethyl alcohol	Alcohols				x
1-Hexanol, 2-ethyl-	Alcohols	x			
Phenol	Aromatic Alcohols			x	x
Benzene	Aromatics	x	X	X	X
Toluene	Aromatics	x	X	X	X
p-Xylene	Aromatics				x
Styrene	Aromatics	x			x
Limonene	Aromatics	x			x
Phenylethyne	Aromatics	x			
Benzene, 1-isocyanato-4-methyl-	Isocyanates				x
Indene	Aromatic Fused Rings	x			
Biphenyl	Aromatic Fused Rings				x
Benzofuran	Aromatic Fused Rings				x
Carbazole	Aromatic Fused Rings				x
1,2-Benzene, dicarboxylic acid	Aromatic Acids	x			

By comparing gases produced from NFR sample with those generated from each of the 20%FR samples, the BFR sample produces a higher number of low molecular weight hydrocarbons than is seen from either the NFR or other FR samples. These are predominantly alkenes and alkynes which include propene, 1,3-Butadiene, propyne, 1-Buten-3-yne, and 3-Penten-1-yne and because they are all major precursors to soot formation [138], they are consistent with the significant smoke production and high UTH concentrations seen in 20% BFR versus 10%BFR samples (Figure 4.27). The absence of heavy aromatics which might also be expected under sooting conditions may be an issue of resolution of the analysis method or may be indicative of variations in the key kinetic processes at this stage of fire development. Also, contrary to the gases identified for the 10%BFR sample, bromo-methane is identified during early decomposition of the 20%BFR sample.

In contrast to the BFR sample, decomposition of the EGFR foam produces some oxygenated hydrocarbons such as acetaldehyde, acetone, 1,3 dioxolane, 2-methyl and 1,4 dioxane which are potentially reflective of differing paths of decomposition in these samples, as well as some oxidation reactions taking place.

Products collected from PFR samples are markedly different from those of either BFR or EGFR samples and these include nitriles, alcohols, and polycyclic aromatic hydrocarbons (PAHs) species. The presence of these thermal decomposition products is supported by the basic dissociation steps depicted in equations *(4)* and *(5)*. Furthermore, the presence of heavy aromatics, which are indicators of soot and smoke production, is consistent with the observed increase in smoke density for PFR samples when compared to EGFR samples according to cone calorimeter test data shown in Table 4.2.

The absence of aromatics and polycylic aromatic hydrocarbons (PAHs) in favour of lower molecular weight hydrocarbon species the gases generated from the EGFR sample is consistent with the lower smoke production and lower average SEA values than seen for the NFR or other FR samples and suggests that with the addition of 20%EGFR agent, decomposition follows differing pathways than for the other samples. Again, more quantitative analysis would be required to distinguish further details of the process.

Tables 4.6 and 4.7 show a summary of the compounds identified during Stage **I** testing in the smoke density chamber to simulate poorly ventilated compartment fire environments. During heating in the early stage of these tests, the oxygen level in the test chamber is relatively high and temperature is near ambient temperature leading to emission of a complex mixture of many different gaseous species as the materials thermally decompose. However, oxygen levels decrease as the tests proceed. From

Table 4.6, it can be seen that the gases in this situation contain straight chain hydrocarbons, aldehydes, ketones, ethers, alcohols, nitrogen-containing compounds (nitriles and amines), aromatics and polycyclic aromatic hydrocarbons (PAHs) products. A number of these products are similar to those seen in the cone calorimeter results above as well as products obtained from thermo-oxidative decomposition of rigid polyurethane foams under well ventilated conditions as reported in literature [64, 69]. This suggests that gas samples taken during this stage of smoke density testing may include a mix of species characteristic of foam decomposition under well and poorly ventilated situations.

Table 4.6: Oxidative pyrolysis products in poorly ventilated smoke chamber testing for NFR and 10% FR samples [Stage I]

Compounds	Group Name	NFR	10%BFR	10%EGFR	10%PFR
Propene	Alkenes	x	x	x	x
2-Butene,	Alkenes		x	x	x
Propane	Alkanes			x	
Hexane	Alkanes				x
Acetaldehyde	Aldehydes	x	x		x
Acetone	Ketones	x	x	x	x
Ethane, bromo-	Brominated		x		
Methane, bromo-	Brominated		x		
Ethane, 1,2-dibromo-	Brominated		x		
Ethane, 1-bromo-2-ethoxy-	Brominated		x		
1,3-Dioxolane, 2-methyl-	Ethers	x	x	x	x
1,3-Dioxane, 2-methyl-	Ethers		x		
1,3-Dioxane	Ethers		x		
1,4-Dioxane	Ethers	x	x	x	x
1,3-Dioxolane, 2,2,4-trimethyl-	Ethers	x	x	x	
Hexanoic acid, 2-ethyl-	Aliphatic Acids			x	
Acetonitrile	Nitriles	x	x	x	
2-Propenenitrile	Nitriles		x		
Benzonitrile	Aromatic Nitriles				x
Urea, trimethyl-	Amines		x	x	
Aniline	Aromatic Amines	x	x		x
Toluidine	Aromatic Amines				

Acetamide, N-phenyl-	Aromatic Amines		x		
3,3'-Diaminodiphenylmethane	Aromatic Amines	x			
Benzenamine, 4,4'-methylenebis-	Aromatic Amines	x			
2-Propen-1-ol	Alcohols		x		
1-Propanol	Alcohols		x		
Ethyl alcohol	Alcohols	x	x	x	x
Isopropyl Alcohol	Alcohols	x	x	x	x
1-Hexanol, 2-ethyl-	Alcohols		x		
Phenol	Aromatic Alcohols	x	x	x	
Toluene	Aromatics	x	x	x	x
Benzene	Aromatics	x	x	x	x
Ethylbenzene	Aromatics		x	x	x
p-Xylene	Aromatics	x	x	x	x
Styrene	Aromatics		x	x	x
Limonene	Aromatics			x	
Benzofuran	Fused Ring Aromatics		x		x
Naphthalene	Fused Ring Aromatics		x	x	x
1,2-Benzenedicarboxylic acid	Aromatic Acids		x		x

The presence of aromatic compounds (benzene, toluene, xylene, and styrene) shown in NFR and FR samples is typical in thermal decomposition product gases from polyurethane foams, while the aliphatic oxygenated compounds such as ethers and alcohols identified in the gases sampled during testing of both NFR and BFR samples are linked to the simultaneous decomposition and oxidation of the base foam. It is significant to note the presence of 3,3'-Diaminodiphenylmethane and Benzenamine, 4,4'-methylenebis in the NFR sample gases generated during smoke density chamber testing. These were not seen in the sample gases analyzed from the well ventilated cone calorimeter tests. The generation of such higher molecular weight compounds in the smoke density chamber supports the idea that, due to different test conditions in the smoke density chamber, a less complete pyrolysis of the sample has taken place so gaseous products also include compounds representative of those expected to be formed during initial random scission of the base foam. This suggests that the first two basic decomposition steps shown in equations *(4)* and *(5)* dominate this phase. The absence of these same species in the gases collected during testing of the FR foams points to either differences in the initial

decomposition processes or that the concentrations of these high molecular weight compounds fell below the limit of resolution of the gas analysis method, which is also consistent with FR interaction with the decomposition process.

As would be expected, various aliphatic brominated species are generated during decomposition of the BFR sample in the smoke density chamber. These may be detected again because of less complete interaction of the FR agent in poorly ventilated decomposition processes and because they are present in much higher concentrations in the smoke density chamber gas samples compared to cone calorimeter samples where significant dilution of gases in the exhaust hood takes place before a sample is withdrawn for analysis. The low molecular weight hydrocarbons identified in the decomposition gases generated from smoke density testing of 10%EGFR and PFR samples are typical of gases expected in the early stage of thermal decomposition of rigid polyurethane foam under high oxygen concentration and near ambient temperature conditions. As would be expected, the FR samples generally produce more fused aromatic compounds reminiscent of those formed during initial random scission of the base foam as well as more partial thermal decomposition products and soot precursors than does the reference sample in the smoke density chamber. This point highlights the importance of defining the compartment environment in any assessment of toxic gas production from materials in a real fire scenario.

In Table 4.7, the effect of an increase in FR concentration on the decomposition of samples in the smoke density chamber is clearly seen. Different distributions of pyrolyzed products are identified during decomposition of the 20%FR samples compared to samples with 10%FR concentration under the same fire conditions. Some low molecular weight

hydrocarbon species (propene, acetaldehyde, acetone and ethers) and aromatic species (aniline, benzene, toluene, xylene) generated from NFR

Table 4.7: Oxidative pyrolysis products in poorly ventilated Smoke Density Chamber Testing for NFR and 20%-FR samples [Stage I]

Compounds	Group Names	NFR	20%BFR	20%EGFR	20%PFR
Propene	Alkenes	x	x	x	x
2-Butene,	Alkenes				x
Butane	Alkanes				x
Acetaldehyde	Aldehydes	x	x	x	
Acetone	Ketones	x	x	x	x
Methane, bromo-	Brominated		x		
1,3-Dioxolane, 2-methyl-	Ethers	x	x	x	x
1,4-Dioxane	Ethers	x	x	x	x
1,3-Dioxolane, 2,2,4-trimethyl-	Ethers	x		x	
Acetonitrile	Nitriles	x		x	
2-Propenenitrile	Nitriles			x	
Benzonitrile	Nitriles		x		x
Benzonitrile, 2-methyl-	Aromatic Nitriles				x
Urea, trimethyl-	Aromatic Amines		x		x
Aniline, N-methyl-	Aromatic Amines			x	
o-Toluidine	Aromatic Amines			x	
Aniline	Aromatic Amines	x	x	x	x
3,3'-Diaminodiphenylmethane	Aromatic Amines	x	x		
Benzenamine, 4,4'-methylenebis-	Aromatic Amines	x	x		
Ethyl alcohol	Alcohols	x		x	
Isopropyl Alcohol	Alcohols	x		x	
Phenol	Alcohols	x			
1-Hexanol, 2-ethyl-	Alcohols				x
Benzene	Aromatics	x	x	x	x
Toluene	Aromatics	x	x	x	x
Ethylbenzene	Aromatics			x	
p-Xylene	Aromatics	x	x	x	
Styrene	Aromatics			x	
Benzofuran	Fused Rings Aromatics			x	
Naphthalene	Fused Rings Aromatics		x		
Acridine	Fused Rings Aromatics				x
Carbazole	Fused Rings Aromatics				
1, 2-Benzene, dicarboxylic acid	Aromatic Acids		x		

samples are similar to those collected from the FR samples such as would be expected if they all underwent similar decomposition pathways in the early stages of thermal decomposition in the environment encountered in the smoke density chamber. Bromo-methane is identified, as expected, in the gases collected during testing of the BFR sample. This serves as an indication that, should brominated compounds be present in the sample gases in sufficiently high concentrations, the present TD-GC/MS analysis should be able to identify and track their presence.

Of all the FR samples, 3,3-diaminodiphenylmethane and Benzenamine, 4,4-methylenebis, are seen only in the decomposition gases of the BFR sample; suggesting that BFR may decompose in a fashion similar to the NFR sample in early stages while the action of the other FR additives leads to different overall decomposition processes and thus variations in the product gas composition. For example, the absence of these and other fused aromatic compounds in the gases collected during testing of the EGFR and PFR samples may be a result of the formation of the char layer which insulates the sample surface and may inhibit both the formation and release of heavy aromatic components, at least in concentrations that are detectable by the present GC-MS technique.

Relatively fewer chemical species were identified in the gases generated during testing of the 20%EGFR and PFR samples compared to 10%EGFR and PFR samples. With increasing FR concentration, a thicker surface char layer forms and creates a physical barrier between the heat source and sample so that heat flow and oxygen diffusion to the sample is reduced. This inhibits thermal degradation of the polymer matrix and the decomposition rate and generation of volatiles from the samples are reduced.

Based on the above discussion it can be seen that gases which are generated in the vitiated environment of smoke density chamber exhibit similarities and differences from those generated during well ventilated environment of cone calorimeter tests. This is due to different modes of reaction and thermal decomposition characterized by different samples under various fire conditions. For example, there are a large number of higher molecular weight hydrocarbons (i.e fused aromatic components) seen in the decomposition of 10%FR samples in the oxygen limited environment of smoke density chamber testing (Table 4.6) compared to those same materials under well ventilated cone calorimeter testing (Table 4.4). In contrast, and surprisingly too, the 20%PFR sample produces more fused ring aromatics and furans under cone calorimeter testing (Table 4.5) compared to smoke density chamber testing (Table 4.7). There is no clear explanation for this. In general, it can be stated that the effluents collected during smoke density tests consist of many higher molecular weight aromatic compounds reminiscent of incomplete pyrolysis (in the absence of as much oxidation), while those collected during cone calorimeter tests are relatively less complex, consisting of more thermally stable compounds [58]. As noted above, however, additional more quantitative analysis would be necessary to more fully interpret the foam, FR, oxygen concentration and temperature interactions taking place across the present tests.

4.3.7.2 Stage II: Combustion Products

The combustion environment in the cone calorimeter favours total oxidation as a result of well-ventilated conditions; while incomplete oxidation reactions prevail in the smoke density chamber due to the oxygen limited environment. In both conditions, the flaming tests represent **Stage II** fire where combustion products are collected around the peak heat release rate to simulate a more fully developed fire in the cone calorimeter. Similarly,

combustion gases are collected at a time when the specific optical smoke density approaches its peak value in the smoke density chamber. The results of TD-GC-MS analysis of flaming combustion products evolved from NFR versus FR samples under cone calorimeter and smoke density chamber tests are discussed in this section.

4.3.7.2.1 Combustion products from cone calorimeter test

Table 4.8 shows a list of different gaseous effluents produced across NFR and 10%FR samples in a well-ventilated, fully developed fire. Certain primary gases are produced across all samples such as propene, acetone, benzene, toluene and styrene which are representative of the common gases seen during combustion and soot formation in polyurethane foams and hydrocarbon fuels [165].

Table 4.8: Combustion products in well-ventilated Cone Calorimeter Testing for NFR and 10% FR samples (Stage II)

Compounds	Group Name	NFR	10%BFR	10%EGFR	10%PFR
Propene	Alkenes	X	X	X	X
Propane	Alkanes				
Acetaldehyde	Aldehydes	X			
Acetone	Ketones	X	X	X	X
1,3-Dioxolane, 2-methyl-	Ethers	X	X		
1,4-Dioxane	Ethers	X	X		
Hexanoic acid, 2-ethyl-	Aliphatic Acids		X		
Acetonitrile	Nitriles				
2-Propenenitrile	Nitriles			X	
Benzonitrile	Aromatic Nitriles			X	
Aniline	Aromatic Amines		X	X	X
3,3'-Diaminodiphenylmethane	Aromatic Amines			X	
Benzenamine, 4,4'-methylenebis-	Aromatic Amines		X	X	
o-Toluidine	Aromatic Amines		X		
1-Hexanol, 2-ethyl-	Alcohols	X	X		
Phenol, 2-methyl-	Aromatic Alcohols	X	X		
Phenol	Aromatic Alcohols	X	X		X
Benzene	Aromatics	X	X	X	X

Toluene	Aromatics	x	x	x	x
Xylene	Aromatics	x			
Styrene	Aromatics	x	x	x	x
Limonene	Aromatics		x		
Phenylethyne	Aromatics		x	x	x
1,2-Benzenedicarboxylic acid	Aromatic Acids		x	x	

The formation of aliphatic oxygenated compounds such as aldehydes, ketones, ethers and alcohols during cone calorimeter tests on NFR and BFR samples indicate that oxidation reactions are taking place, consistent with the lower values of percent mass remaining (%PMR) of these samples compared to EGFR and PFR samples (see Table 4.1). The gases collected from the 10%BFR foam sample consist of low molecular weight hydrocarbons such as propene, propane and oxygenated compounds such as, acetaldehyde, acetone and alcohols as well as higher molecular weight aromatic compounds such as limonene, phenylethyne, and benzenedicarboxylic acid. This combination of products suggests combined thermal decomposition, oxidation and soot formation processes consistent with the flame retardant action, relatively high mass loss (Table 4.2) and production of smoke observed during testing of the BFR samples. The absence of brominated species again suggests that if they exist, they are there in concentrations lower than the detection limit of the method.

The presence of 3,3-Diaminodiphenylmethane, Benzenamine, 4,4-methylenebis and benzenedicarboxylic acid, which are long chains of higher molecular weight hydrocarbons in EGFR is an indication of early stages of decomposition of the base foam material. This may be due to the formation of the carbonaceous char layer on the sample that prevents heat penetration, oxygen diffusion and fuel vapourization from the burning sample. The absence of these and other fused aromatic compounds in the gases collected during testing of the PFR sample is consistent with theory that initially a porous char layer forms over the burning sample, which does

not fully inhibit heat penetration and oxygen diffusion to the polymer matrix. Therefore decomposition and oxidation reactions proceed further than for the EGFR sample at the same stage in the test. This is consistent with the various discussions about the porous nature of the surface char layer observed to form around the time of peak HRR as described in Section 4.2.4.

Table 4.9 shows a list of combustion products from NFR and 20%FR samples in well-ventilated cone calorimeter tests. Only few compounds such as propene (olefins), benzene and toluene are common across all the samples. This implies that addition of 20%FR agents significantly alters the chemical structure and burning characteristics of the base foam.

Table 4.9: Combustion products in well-ventilated Cone Calorimeter Testing for NFR and 20% FR samples (Stage II)

Compounds	Group Names	NFR	20%BFR	20%EGFR	20%PFR
Propene	Alkenes	x	x	x	x
1-Buten-3-yne	Alkynes		x		
Acetaldehyde	Aldehydes	x		x	
Acetone	Ketones	x	x		
Methane, bromo-	Brominated		x		
1,3-Dioxolane, 2-methyl-	Ethers	x			
1,4-Dioxane	Ethers	x			
2-Propenenitrile	Nitriles		x		x
Acetonitrile	Nitriles				x
Benzonitrile	Aromatic Nitriles			x	x
Benzyl nitrile	Aromatic Nitriles				x
Benzonitrile, 2-methyl-	Aromatic Nitriles				x
1-Hexanol, 2-ethyl-	Alcohols	x			
Phenol	Aromatic Alcohols	x			
Phenol, 2-methyl-	Aromatic Alcohols	x			
Benzene	Aromatics	x	x	x	x
Toluene	Aromatics	x	x	x	x
p-Xylene	Aromatics	x			
Styrene	Aromatics	x			x
Indene	Aromatics				x
Phenylethyne	Aromatics				x

Benzofuran	Aromatic Fused Rings				x
Naphthalene	Aromatic Fused Rings			x	x
Acridine	Aromatic Fused Rings		x		
Carbazole	Aromatic Fused Rings		x		

From the standpoint of the NFR sample, the presence of oxygenated hydrocarbons and alcohols in the combustion exhaust gases, coupled with the absence of heavy aromatic compounds, can be attributed to more complete oxidation reactions since there are no FR additives to interfere with the combustion process. It is anticipated that the BFR additives will slow down the combustion process as the concentration level of BFR agent increases to 20%. The presence of multiple fused ring aromatics (acridine and carbazole) in the exhaust samples taken from 20%BFR foam may be linked to high smoke development (Table 4.2) or may also be due to primary thermal decomposition of the polymeric chains involving scission of the weakest bonds leading to heavier decomposition products. The identification of bromo-methane confirms interaction of the FR agent with the combustion process; the absence of other brominated species may be because they are present in concentrations that are below the detection limits of the GC/MS system.

It can be seen that fewer combustion products are identified in the gases evolved during heating of the BFR and EGFR samples as the additive concentration increases from 10-20%. By increasing the concentration of EGFR, the thickness of the surface char layer also increases, creating a shield over the burning polymer matrix. This reduces the incident heat flux reaching the surface of the sample during heating and, in turn leads to higher values of PMR at the end test. Similarly, the absence of oxygenated hydrocarbons in the gases generated during testing of the 20%BFR samples suggests differing paths of oxidation compared with even the 10%BFR

sample. On the contrary, as the weight percent PFR in the foam increases from 10-20%, the surface char layer limits oxygen access to the reaction zone of the burning sample leading to the generation of more partially oxidized, higher molecular weight aromatics and multiple fused rings aromatic compounds such as benzofuran and naphthalene which are key indicators of soot formation. This is consistent with the other observations that the 20%PFR sample exhibits higher levels of smoke production [107] and is also in agreement with the cone calorimeter data shown in Table 4.2, where the smoke density for the 20% PFR samples is higher than any other samples tested under well ventilated conditions. The results also indicate that increasing level of PFR concentration does not necessarily reduce measured values of peak HRR and smoke density which therefore suggests there may be an optimum FR loading for improved fire performance of PFR foams.

4.3.7.2.2 Combustion products from smoke density chamber tests

During smoke density chamber testing, it was observed that only NFR, 10%BFR and 10% and 20%PFR samples ignited and flamed. Table 4.10 shows the list of combustion products collected from those three samples at a time when the specific optical smoke density in the chamber approaches its peak value. The other samples were not considered here because they underwent thermal decomposition with no combustion and as such, cannot be considered comparable to the other samples.

As would be expected, there are large numbers of both aliphatic and aromatic hydrocarbons ranging from alkenes, aldehydes, ketones, ethers, aromatic amines and other fragments of aromatic compounds which are formed during this phase of the smoke density tests since the quantity and type of gaseous products of combustion and rate at which they are produced largely depend on the ventilation conditions [167].

Table 4.10: Combustion products from NFR and FR samples in flaming mode in poorly ventilated Smoke Density Chamber Test (Stage II)

Compounds	Group Name	NFR	10% BFR	10%PFR	20%PFR
Propene	Alkenes	x	x	x	x
2-Butene,	Alkenes		x		x
Butane	Alkanes				x
Acetaldehyde	Aldehydes	x	x		x
Acetone	Ketones	x	x	x	x
Ethane, bromo-	Brominated		x		
Methane, bromo-	Brominated		x		
Heptane, 2-bromo-	Brominated		x		
Propane, 1-bromo-	Brominated		x		
Ethane, 1-bromo-2-ethoxy-	Brominated		x		
1,3-Dioxolane, 2-methyl-	Ethers	x	x	x	
1,3-Dioxane, 2-methyl-	Ethers				x
1,4-Dioxane	Ethers	x	x	x	x
1,3-Dioxolane, 2,2,4-trimethyl-	Ethers	x	x		
Hexanoic acid, 2-ethyl-	Aliphatic Acids				
Acetonitrile	Nitriles	x	x		x
2-Propenenitrile	Nitriles		x		
Benzonitrile	Aromatic Nitriles				x
Benzonitrile, 4-methyl-	Aromatic Nitriles				
O-Toluidine	Aromatic Amines	x			
Urea, trimethyl	Aromatic Amines		x		
Aniline	Aromatic Amines	x	x		
Aniline, N-methyl					x
Formamide, N-phenyl-	Aromatic Amines				
3,3'-Diaminodiphenylmethane	Aromatic Amines	x			
Benzenamine, 4,4'-methylenebis-	Aromatic Amines	x			
2-Propen-1-ol	Alcohols		x		
Ethyl alcohol	Alcohols	x	x		
Isopropyl Alcohol	Alcohols	x	x		
1-Hexanol, 2-ethyl-	Alcohols				
Phenol	Aromatic Alcohols	x	x	x	
Phenol, 2-methyl	Aromatic Alcohols				x
Toluene	Aromatics	x	x	x	x

Benzene	Aromatics	x	x	x	x
Ethylbenzene	Aromatics	x	x		
p-Xylene	Aromatics	x	x	x	x
Styrene	Aromatics				x
Limonene	Aromatics			x	x
Benzene, 1-isocyanate-2-methyl	Aromatics				x
Benzofuran	Aromatic Fused Rings	x			x
Indene	Aromatic Fused Rings				x
Naphthalene	Aromatic Fused Rings		x		
Acridine	Aromatic Fused Rings				x
Carbazole	Aromatic Fused Rings				x
1,2-Benzenedicarboxylic acid	Aromatic Acids		x	x	

These include acetaldehyde, acetone, a group of ethers, alcohols, and aromatic amines, but measurable levels of polycylic aromatic hydrocarbons (PAHs) are absent. This is consistent with development of relatively lower smoke density compared to that observed for samples with PFR agents as discussed in Section 4.2.4 and Figure 4.13. A plethora of brominated species are observed in these tests, probably due to the higher concentrations of these species produced under the vitiated atmosphere of smoke chamber (and contrary to results obtained from cone calorimeter tests for the same amount of FR addition). Further, the many brominated species identified in these poorly ventilated conditions may be indicative of the overall lower rates of oxidation in these tests, limiting the interaction of the BFR with the key chemical reactions driving the behavior.

Apart from the primary fire effluents which are typical of thermal decomposition and combustion of rigid polyurethane foams, fewer species of gases were collected from 10%PFR samples than from any other samples. On the other hand, the gases from the 20%PFR are characterized by multiple fused ring aromatic species contrary to what is observed in gases

generated from the NFR and other FR samples under flaming combustion. These gaseous products, particularly the higher molecular weight aromatics such as benzofuran, indene, acridine and carbazole shown in Table 4.10 can be linked to the considerable increase in smoke production seen when testing the 20%PFR sample as discussed under Section 4.2.4, Table 4.3. In general, a plethora of higher molecular weight aromatic compounds were identified in the gases collected during testing of all samples. Many are reminiscent of those expected during incomplete combustion of the foam, which is expected to occur in the vitiated environment of the smoke density chamber.

4.3.7.2.3 Gaseous products from non-flaming combustion under smoke density chamber test

Table 4.11 is a summary of volatile organic compounds collected from 20%BFR, 10%EGFR and 20%EGFR samples during non-flaming decomposition when the specific optical density of each sample approaches its maximum value in the smoke density chamber. In contrast to the behavior of these samples under well-ventilated cone calorimeter testing, where they all ignited within 6 seconds of exposure to the same incident heat flux these samples did not ignite in the low levels of oxygen characteristic of smoke density testing. Instead, they pyrolyzed and smouldered, leading to generation of a large number of different fire effluents compared to those identified under well ventilated conditions. This observation is also in agreement with our discussions in Section 4.2.4 and Table 4.3.

From the Table, it can be seen certain groups of organic compounds generated (alkenes, aldehydes, ketones, ethers, alcohols nitriles, aromatic amines and simple aromatic compounds) are common across all the samples and are characteristic in hydrocarbon decomposition under limited oxygen

environments. Further the presence of propene (olefins), alcohols and amines across all the samples is expected from the basic decomposition steps in equations (4) and (5).

Table 4.11: Chemical products of samples in non flaming mode in poorly ventilated smoked density chamber test

Compounds	Group Name	20%BFR	10%EGFR	20%EGFR
Propene	Alkenes	x	x	x
2-Butene,	Alkenes		x	x
1-Propene, 2-methyl-	Alkenes			x
Butane	Alkanes			x
Acetaldehyde	Aldehydes	x	x	
Acetone	Ketones	x	x	x
Ethane, bromo-	Brominated	x		
Methane, bromo-	Brominated	x		
1,3-Dioxolane, 2-methyl-	Ethers	x	x	x
1,3-Dioxane, 2-methyl-	Ethers		x	x
1,4-Dioxane	Ethers	x	x	
1,3-Dioxolane, 2,2,4-trimethyl-	Ethers	x	x	
Hexanoic acid, 2-ethyl-	Aliphatic Acids		x	
Acetonitrile	Nitriles	x	x	x
2-Propenenitrile	Nitriles	x		
Benzonitrile	Aromatic Nitriles	x	x	x
Benzonitrile, 4-methyl-	Aromatic Nitriles		x	
Urea, trimethyl	Aromatic Amines	x		x
Aniline	Aromatic Amines	x	x	x
Formamide, N-phenyl-	Aromatic Amines		x	
3,3'-Diaminodiphenylmethane	Aromatic Amines		x	
Benzenamine, 4,4'-methylenebis-	Aromatic Amines		x	
2-Propen-1-ol	Alcohols	x		
Ethyl alcohol	Alcohols	x	x	x
Isopropyl Alcohol	Alcohols	x	x	x
1-Hexanol, 2-ethyl-	Alcohols		x	
Toluene	Aromatics	x	x	x
Benzene	Aromatics	x	x	x
Ethylbenzene	Aromatics	x	x	

p-Xylene	Aromatics	x	x	x
Limonene	Aromatics		x	
Benzofuran	Aromatic Fused Rings		x	
Naphthalene	Aromatic Fused Rings		x	
Acridine	Aromatic Fused Rings			x
1,2-Benzenedicarboxylic acid	Aromatic Acids		x	

The detection of brominated compounds is consistent with our earlier discussion on the identification of brominated species from gas samples taken from poorly ventilated smoke density chamber tests. With less oxygen available for the reaction process in vitiated atmospheres, there will be correspondingly fewer H* and OH* radicals to be intercepted by the brominated species; and with the addition of 20%BFR, more dissociated brominated species were collected in the fire environment for analysis. Therefore, BFR agents lead to a generally slower oxidation reaction compared to well-ventilated conditions as evidenced in the release of some partially oxidized products such as ethers, ketones, aldehydes and emission of aromatic compounds such as benzene, toluene, ethylbenzene, xylene.

 The formation of polycylic aromatic hydrocarbons (PAHs) in 10%EGFR is indicative of higher smoke production compared to that observed during heating of the 20%EGFR sample. This is in agreement with the specific optical smoke density data shown in Figure 4.14 and suggests that an increase in EGFR addition from 10-20% results in an improvement on smoke production of EGFR systems in an oxygen limited environment. Overall, the differences observed point to the importance of understanding the action of different fire retardant additives and concentrations in the reference materials involved in a given real fire scenario, as well as carefully defining the compartment environment in any assessment of toxic gas production from materials in a real fire.

4.3.7.3 Stage III: Post Fire Effluents

During the final stage of fire, either the available fuel is consumed or the available oxygen concentration is too low to sustain flaming combustion within the fire environment. Since fire fighters and other personnel are invariably exposed to gases that linger in post-suppression environments, it is important to learn more about the nature and types of those gases. Therefore, post fire gases were collected in **Stage III** during well-ventilated cone calorimeter and poorly ventilated smoke density chamber tests when the HRR dropped to about 40% of its peak value and optical density decayed to 40% of the maximum optical density respectively. Results are further discussed in the following sections.

4.3.7.3.1 Post fire effluents of NFR and 10%FR from well-ventilated cone calorimeter test

Table 4.12 is a summary of major chemical species identified in the final decay phase of the fire. Appendix 4.4 shows the different points on the time scale where gases are collected from all the samples. The different points are influenced by the different modes of action of each FR agent. Therefore, results across FR additives may not be entirely comparable. Gases collected from NFR base foam sample during post fire conditions reveal relatively few compounds compared to gases identified under **stage II** flaming combustion. These gases are mainly aromatic compounds. Gas effluents from the BFR samples during this latter stage of burning include a wide range of components: alkenes, alcohols, aliphatic and aromatic species. The presence of alkenes and partially oxidized products such as alcohols suggests that the BFR sample is still undergoing oxidation reactions during this stage of sampling; consistent with chemical species listed in Table 4.8 and also supported by the data in Table 4.1 which indicates that over 90% of sample mass is consumed over the extended burning period.

167

Table 4.12: Chemical products in well-ventilated Cone Calorimeter Testing for NFR and 10% FR samples (Stage III)

Compounds	Group Name	NFR	10% BFR	10%EGFR	10%PFR
Propene	Alkenes		X		X
Propane	Alkanes				X
Acetone	Ketones				X
Hexanoic acid, 2-ethyl-	Alipahtic Acids		X		
Acetonitrile	Nitriles				X
2-Propenenitrile	Nitriles				X
Aniline	Aromatic Amines		X		X
1-Hexanol, 2-ethyl-	Alcohols		X		
Phenol	Aromatic Alcohols		X		X
Benzene	Aromatics	X	X	X	X
Toluene	Aromatics	X	X	X	X
Styrene	Aromatics	X	X		X
Limonene	Aromatics		X		
Phenylethyne	Aromatics	X	X		X
1,2-Benzenedicarboxylic acid	Aromatic Acids		X		

The high smoke production is traceable to the array of aromatic compounds (i.e soot precursors) prevalent in the hot sample gases as well as with smoke data in Table 4.2 which shows BFR having the highest smoke density after the PFR samples tested.

The observations on the EGFR and PFR samples are quite interesting. Very few gases are detected with the current TD-GC-MS method in effluent samples collected from EGFR and PFR foams during Stage III sampling when compared to Stage II products. This is consistent with the idea that a surface char layer forms over each sample and protects the burning material from the air, thereby suffocating the flames. Emission of quite different gaseous products is observed in the post-fire environment of 10%PFR sample in comparison with the 20% PFR sample.

This appears consistent with the nature of char layer formed on the surface of the samples which is characterized by differing distributions of pores and cracks, for the two sets of test samples. Figure 4.30 shows the differences in

the surface characteristics of the char formed during testing of 10% and 20%PFR samples.

a (10%PFR)   b (20%PFR)

Figure 4.30 Different surface characteristics of char layers between10%PFR and 20%PFR after tests

It is possible that the char layer on the 10%PFR is porous enough to allow some transmission of gases evolved during heating of the samples while that on the sample with 20% is less porous and more insulating in nature. Evidently, the nature and characteristics of phosphorous char layer clearly merits further study in a post flashover fire environment to better understand the preliminary results presented here.

The list of chemical species produced from NFR and 20%FR samples is shown in Table 4.13. The production of various low molecular weight hydrocarbon gases, including alkenes and alkynes, aldehydes, ketones, nitrogen-containing compounds, and aromatics can be seen in results taken from BFR test samples. Identification of these gases strongly suggests that the sample is still undergoing active oxidation reactions over the extended burning period. This is consistent with the fact that a significant amount of

mass of the sample was consumed in the latter stages of the test, leaving only 16% PMR at the end of test (see Table 4.1). The presence of bromo-methane is again indicative of active participation of the bromine agent in the fire behaviour.

Table 4:13: Chemical products in well ventilated Cone Calorimeter Testing for NFR and 20% FR samples (Stage III)

Compounds	Group Names	NFR	20%BFR	20%EGFR	20%PFR
Propene	Alkenes		X		
1,3-Butadiene	Alkenes		X		
Propyne	Alkynes		X		
Propyne	Alkynes				
1-Buten-3-yne	Alkynes		X		
Acetaldehyde	Aldehydes				
Acetone	Ketones		X		
Methane, bromo-	Brominated		X		
2-Propenenitrile	Nitriles		X		
Acetonitrile	Nitriles		X		
Benzonitrile	Aromatic Nitriles				
Benzene	Aromatics	X	X		X
Toluene	Aromatics	X	X		X
Styrene	Aromatics	X	X		
Phenylethyne	Aromatics	X	X		
Acridine	Fused ring Aromatics		X		

Contrary to results obtained from testing of 10%PFR samples, there are only a very few aromatic species that were identified from gas samples collected during cone calorimeter testing of the 20%PFR foams under the conditions characteristic of the post fire environment. This may be a result of the small amounts of samples involved in the reactions resulting in low concentrations of the gases of interest. It may also be due to the presence of a fibrous highly cross-linked carbonaceous char layer that forms on the surface of the sample (Figure 4.30b)).

By increasing the level of concentration of PFR from 10 to 20%, the thickness of this surface char layer also increases preventing further release of gaseous products.   For the same reasons, by increasing the EGFR concentration to 20%, it is not surprising that no gases are measured. This is consistent with the results shown in Table 4.12 where only very few gases are measured from testing of the 10%EGFR sample due to the formation of an effective carbonaceous surface char layer.   Figure 4.31 shows surface characteristics of the EGFR samples.   In both cases the layers are such that they greatly inhibit or prevent the release of gaseous products into the fire.

a (10%EGFR)   b (20%EGFR)

Figure 4.31: Residual char layer of 10% and 20%EGFR after tests

4.3.7.3.2 Post fire effluents from vitiated smoke density chamber test

For those samples that are characterized with flaming combustion under smoke density chamber tests, post fire effluents are collected from stage III environments. Table 4.14 shows the list of measured gases from NFR and other FR samples. Due to different fire environments, it is expected that there would be differences in the number and nature of gases measured

from NFR, 10%BFR and PFR samples when compared to gases collected from the same materials under well ventilated cone calorimeter testing.

Table 4.14: Chemical products of 10% BFR, and PFR samples in flaming mode in poorly ventilated Smoke Density Chamber Testing (Stage III)

Compounds	Group Name	NFR	10%BFR	10%PFR	20%PFR
Propene	Alkenes	x	x	x	x
2-Butene,	Alkenes		x		
Butane	Alkanes				x
Acetaldehyde	Aldehydes		x	x	
Hexanal	Aldehydes		x		
Acetone	Ketones	x	x		x
1,3-Dioxolane, 2-methyl-	Ethers	x	x	x	x
1,4-Dioxane	Ethers	x			x
Hexanoic acid, 2-ethyl-	Aliphatic Acids			x	
Benzonitrile	Aromatic Nitriles				x
Benzenamine, 4,4'-methylenebis-	Aromatic Amines	x			
Ethyl alcohol	Alcohols		x		
Phenol	Aromatic Alcohols		x	x	
Toluene	Aromatics	x	x	x	x
Benzene	Aromatics	x	x	x	x
Limonene	Aromatics		x	x	
1,2-Benzenedicarboxylic acid	Aromatic Acids	x	x	x	

In the closed compartment of the smoke density chamber, a number of low molecular weight and aromatic compounds typical of those expected from thermal decomposition and combustion of PUR foams were detected in the post fire gas samples across all the samples. Gases were not collected from 20%BFR and EGFR materials which did not ignite in the low levels of oxygen characteristic of smoke density tests, but continued smouldering; which is a slow, low temperature, flameless form of combustion of the condensed fuel throughout test period [166]. Figure 4.32 shows the char residue of 20%EGFR sample after smouldering in the smoke density chamber. It is

therefore assumed that the gaseous products will not be any different from those collected during **Stage II**.

Figure 4.32: Char residue of 20%EGFR sample after smouldering in the smoke density chamber

3.4 Health Effects and Toxicity of Fire Gases

Information on the gaseous products of thermal decomposition and flaming combustion of polyurethane foams as determined in the present research can be important in fire hazard assessment. From analysis of the fire gases, the gaseous products can be classified under two main headings: asphyxiants and irritants. The main asphyxiants seen in previous measurements of fire gases generated from rigid polyurethane foam are CO, CO_2, low O_2 and HCN [62]. These asphyxiants can interact producing additive effects, resulting in higher toxicity. Irritants that have been identified in this study under various burning conditions and compositions include all the halogenated compounds and nitrogen oxides (NO_x) [168], with the exception of HCN and SO_2. The positive identification of HCN using Miran 205B FTIR was hampered due to CO_2 interference as both gases occur

within the same range of wave numbers as shown in Figure 3.7. However, the identification of such compounds as benzyl cyanide by the TD-GC/MS may be indicative of the presence of HCN. Table 4.15 shows the data for measured concentration values of some of the toxic fire gases compared with the Immediately Dangerous to Life and Health (IDLH) values which are defined by the US National Institute for Occupational Safety and Health (NIOSH) for exposure to airborne contaminants at levels likely to cause death or immediate or delayed permanent adverse health effects or prevent escape from such an environment [170].

Table 4.15: Measured concentration values versus Immediately Dangerous to Life and Health IDLH

Toxic Gas	NFR	10%BFR	10%EGFR	10%PFR	20%BFR	20%EGFR	20%PFR	IDLH
O2 (%)	20.53	20.54	20.60	20.55	20.66	20.68	20.51	6
CO (ppm)	80	180	60	410	130	50	680	1200
CO2 (%)	0.368	0.365	0.335	0.359	0.27	0.267	0.368	4
NO (ppm)	18	25	15	70	20	8	50	100
NO_2 (ppm)	9	12	4	30	20	5	24	20
THC (ppm)	100	200	900	600	250	200	450	-

Although, CO has been identified as a prominent toxic gas leading to fire death, the amount of CO produced in the current study from each of the samples suggests that the amount of CO produced under laboratory conditions may not pose serious danger to life in real fire situations, since it has been established that cone calorimeter test results correlate well with data from full scale fire testing. For instance, Table 4.15 indicates that the

gases generated during heating of the 20%PFR sample are characterized by the highest peak value of CO of about 700ppm, but this value is low when compared to 1200ppm IDLH value. For all samples, oxygen and CO_2 concentrations do not appear to constitute any problem to human survivability in the fire environment under well ventilated conditions. However, the production of peak NO concentrations of about 70ppm from 10%PFR may pose a threat when compared to the 100ppm IDLH. Also, the NO_2 peak values of 30, 20 and 24ppm from 20%BFR, 10%PFR and 20%PFR samples respectively, when compared to 20ppm IDLH value, indicate that an exposure to NO_2 from the burning of these samples at these concentrations could be lethal.

Important additional information on the fire gases can be obtained through examination of the volatile organic compounds released during cone calorimeter and smoke density tests. Many of the fire gases measured during thermal decomposition and combustion of NFR and FR rigid polyurethane foam samples are known to be, or reasonably suspected to be, carcinogenic [169]. These gases range from low molecular weight hydrocarbons such as acetaldehyde and acrylonitrile (2-propenitriles) through aromatics such as benzene, styrene and aniline to higher molecular weight compounds which are used in the preparation of isocyanates and polyisocyanates in production of rigid polyurethane foams [29]. Other compounds such as acetonitrile and benzyl cyanide are major precursors to the formation of hydrogen cyanide and therefore suggest the presence of HCN and other important toxic gases that were previously reported in the literature [103] but were not themselves detected in the present study. Another compound of interest produced in principally poorly ventilated conditions is 3,3-diaminodiphenylmethane which is a high molecular weight carcinogenic compound listed as a substance of very high concern to the European Chemical Agency. Of course many of the hydrocarbon species

identified in the test gases are incompletely oxidized and may be carcinogenic. The measured concentrations are characterized by the availability of oxygen, temperature and chemical compositions, and time of exposure will define the lethality of such compounds.

3.5 General Remarks

Characterization of fire gases, fire performance and smoke development measurements have been made during thermal decomposition and combustion of fire and non-fire retarded rigid polyurethane foams using a number of experimental techniques. It was intended to investigate the effects of varying levels of fire retardants on commercial base foam formulations in terms of their impacts on fire behavior, smoke and gas generation under different fire conditions. It has been established that although addition of fire retardants to the base foam improves fire performance of sample materials tested in terms of reduced HRR and other fire hazard indices, it increases smoke density and generates numerous additional gaseous products. By utilizing different gas analysis methods with appropriate instrumentation, a unique combination of these analytical techniques has been developed. This has led to detailed characterizations of many gaseous products resulting from thermal decomposition and combustion in well-ventilated and poorly ventilated fire conditions. Such gases include carbon monoxide, carbon dioxide, benzyl cyanide (a major precursor for hydrogen cyanide), halogenated hydrocarbons, and a large number of organic irritants, such as propene, acetaldehyde, acetones, alcohols, aromatic and polycylic aromatic hydrocarbons (PAHs).

Overall, it is established that the examination of thermal decomposition and combustion products generated during smoke density chamber tests provides more information about the molecular mechanisms of degradation.

This information is important in understanding the thermal effects on fire retarded rigid polyurethane foams which are decomposed in real fires under vitiated conditions. Quantification of the identified species would provide much additional input to more detailed decomposition and combustion models for rigid PUR, and perhaps other forms of polyurethanes as well.

Chapter Five: Conclusions and Future Work

Rigid polyurethane foam is an important material used for thermal insulation in building construction, transportation and industrial applications, but brings attendant safety concerns due to its inherent flammability in fires. The introduction of flame retardants into the base foam reduces ignitability and flammability of the material, but there are potential detrimental increases in smoke generation and variations in fire gas evolution when this is done. In this experimental work, the effects of three different fire retardant additives (brominated, phosphorus-based and expandable graphite) on the fire performance of rigid polyurethane foams under varying ventilation conditions have been studied, cross-examining the impacts of two different concentrations of fire retardant on fire behavior, smoke development and fire gas evolution when applied in consistent base foam formulations. This chapter contains a summary of the major contributions of the present work and highlights the key findings associated with fire performance, smoke characterization and gas production from the fire retarded and non-fire retarded rigid foam samples while making reference to potential areas for future work.

5.1 Research Contributions

Previous studies into the fire performance of fire retarded polyurethanes have focused primarily on the identification of thermal decomposition and combustion products as averaged across the entire fire performance test period. In contrast, this study identifies the key fire gases produced from rigid polyurethane foams with varying levels of fire retardants via measurements taken at three characteristic stages of fire development (i.e pyrolysis, steady burning and post-fire) under different ventilation conditions. Furthermore, the study advances the development of suitable

gas sampling and analysis methods which are necessary to obtain consistent data across tests for the identification of VOCs evolved during pyrolysis and burning of polyurethane foams. This work has also significantly improved our understanding of the chemistry of interactions between fires, fire retardants and prolysis/combustion gases evolved from fire retarded rigid polyurethane foam. However, extreme caution should be exercised in using the fire performance characteristics of the fire retarded samples tested; particularly in the PFR samples where significant variations were observed in the test results.

5.2   Findings

5.2.1 Flame Retardation and fire performance characteristics under different fire conditions

(i) From this study, it is established that cone calorimeter and smoke density chamber tests of materials enable simulation of well-ventilated and poorly ventilated fire conditions. As a consequence, use of both methods for complementary testing leads to better understanding of the thermo-oxidative degradation and combustion products that may be generated by flame retarded rigid polyurethane foams in real fire situations.

(i)   The fire environment, whether as well-ventilated or less-ventilated conditions, significantly alters the burning characteristics of rigid polyurethane foams with and without FR additives; leading to production of numerous gaseous species of both aliphatic and aromatic compositions.

(ii) The addition of EGFR and PFR into the base foam increases the residual char when compared to NFR foams which is evidence of improvement on the flame retardant action of those samples. The addition of 20%EGFR to the present foam provided the best overall

results compared to other samples tested in terms of HRR, THR, CO yield and smoke toxicity index. It is thought that the expanded carbon layer formed at the burning surface of 20%EGFR significantly impacts the production of combustible products.

(iii)   The increase in smoke toxicity index (CO/CO_2 weight ratio) of 20%PFR is a direct reflection of less completeness of combustion and is due to a physical barrier effect of the char layer which restricts oxygen diffusion to the burning material. The reduction in CO_2 yields and increase in CO production due to incomplete combustion products increases the smoke toxicity index.

5.2.2 Flame retardation and smoke development under varying fire conditions

(i) The addition of BFR and PFR increases the overall smoke density of rigid polyurethane foams over the NFR and EGFR samples, especially under vitiated atmospheres. Amongst all the FR products considered under flaming combustion in both well ventilated and vitiated conditions, PFR samples develop more smoke and show enhanced soot formation than any other FR samples at all levels of fire retardant additive. For materials under non flaming combustion, 20%EGFR samples generate the least amount of smoke while the 10%EGFR and 20%BFR samples develop comparable amounts of smoke.

(ii) Under smoke density chamber testing, there are indications that samples of the same foam formulation subjected to different burning conditions (i.e flaming and non-flaming modes), generate different amounts of smoke. In this study, more smoke is produced under non-flaming conditions than flaming conditions as would be expected.

5.2.3 Flame retardation and fire gases generated under varying fire conditions

(i) The addition of FR agents to rigid polyurethane foams affects the nature of gases generated in well-ventilated and vitiated environments of cone calorimeter and smoke density chamber tests, highlighting the impact of different fire retardant mechanisms and reaction modes during thermal decomposition and combustion processes. Tests conducted in well ventilated environments are characterized by gases consistent with high oxygen levels and relatively low temperature decomposition (pre-ignition); and also low oxygen concentration with high temperature hydrocarbon combustion (flaming) products; the exact nature of the products is modified by the FR additives used.

(ii) Tests in the vitiated environment of the smoke density chamber lead to a plethora of higher molecular weight aromatic compounds reminiscent of those expected from incomplete combustion and soot formation. The combustion of NFR and FR rigid polyurethane foams can produce numerous gaseous products under varying fire environments; the examination of thermal decomposition and combustion products generated under smoke density chamber provides more information about the molecular mechanisms of degradation. This information is important in understanding the thermal effects on materials which are decomposed in real fires under vitiated conditions.

(iii)   Apart from production of CO as an indicator for incomplete combustion, the higher concentrations of total unburned hydrocarbons (THC) which are detected in both EGFR and PFR formulations, coupled with the nature of the organic compounds identified by using TD-

GC/MS strongly suggest that combustion is incomplete in such samples.

(iv)　　Predicting fire gases characteristics of different samples by submitting them to a series of tests in different conditions enables the author to state that the base foam formulations show improved fire performance with enhanced fire properties when treated with EGFR agents. The study highlights differences in the composition of thermal decomposition and combustion products due to additions of different concentrations of FR agents to the base foam formulations under different fire conditions (i.e temperature, oxygen availability and ventilation). Depending on the fire scenario and flame retardant mechanism, FR agents can result in the production of vastly different amounts of CO, CO_2 and other major combustion products from the same base material.

5.2.4 Gas Measurements and Techniques

(i) For purposes of gas analysis, new information on possible material behavior under different real fire scenarios is feasible using cone calorimeter (well ventilated) and smoke density (vitiated) fire test systems. The sampling approach using sorbent tubes in this study has proven to be complementary and does serve to maximize our ability to detect a wide range of volatile organic products. No single approach could satisfy all requirements, so a variety of techniques is evolved. The unique combination of these analytical techniques has proved to be a valuable method for beginning to understand the thermal decomposition and combustion processes of rigid polyurethane foams.

(ii) Thermal desorption gas chromatography mass spectrometry (TD-GC-MS) technique was fully developed for the analysis and validation and standardization of volatile organic compounds evolved from the thermal decomposition and combustion of flame retarded rigid polyurethane foam samples. The combination of TD-GC-MS as applied to the thermo-oxidative degradation and combustion is a good example of the possibilities of the combination of complementary analytical techniques for the unambiguous identification of the gaseous products in fire testing which serves as alternative to the use of FTIR and solvent extraction for the collection of the evolved gases.

5.3 Recommendations for Future Work

(i) In depth analysis of the present results, coupled with further testing using the approach adopted in this study with additional chemical analysis and quantification should contribute improved understanding of the degradation mechanisms and combustion processes occurring in both non-fire retarded and fire retarded foams in various fire situations.

(ii) Based upon the results from this study, and the fact that the results seen for EGFR and PFR samples may be concentration dependent, it is recommended that a 15%FR loading be studied It is envisaged that such study will give a better picture and general outlook of fire behaviour and effectiveness of the various FR additives.

(iii) It is also recommended that Novatech 695 gas analyzing units which measures O_2, CO, CO_2, NOx and unburned total hydrocarbon concentrations in real time be also interfaced with the smoke density chamber to further assess other gaseous products in an oxygen limited environment. This will be a step

further from the present study to measure these products in vitiated fire conditions; and it will enhance our understanding of time history of thermo-oxidative and combustion products.

References

[1] Centre for Polyurethane Industry, "*Flexible Polyurethane Foams (FPFs) used in Upholstered Furniture and Bedding*", Technical Bulletin Doc. No. AX 239. Arlington, VA: American Chemistry Council (2008)

[2] Mustafa Keskin et al.; "*Case Report on Polyurethane Spray Foam Burn*", *Journal of Science Direct* 34 (7), pp 1041-1043 (2007)

[3] "*Canadian Housing Statistics (CHS)-Residential Building Activity*", Housing and Market Information, Canada Mortgage and Housing Corporation, Ottawa, ON Canada (2012) < www.cmhc-schl.gc.ca/odpub/esub/64681/64681_2012_A01.pdf>

[4] John U. Ezinwa,; "*Modelling Full-Scale Fire Test Behaviour of Polyurethane Foams Using Cone Calorimeter Data*", M.Sc Thesis, Department of Mechanical Engineering, University of Saskatchewan, Saskatoon. (2009)

[5] Usman Sorathia, Richard Lyon, Richard G Gann Louis Gritzo; "*Materials and Fire Threat*", Sample Journal Vol. 32(3), pp 8-15 (1996)

[6] Hartzell, G. E., "*The Combustion Toxicology of Polyurethane Foams*", Journal of Cellular Plastics, Vol. 28, No. 4 pp 330-358, (1992)

[7] Harwood, B., and Hall, J.R. Jr., "*What Kills in Fires: Smoke Inhalation or Burns?*" Fire Journal, pp. 29-34. (1989)

[8] Gann, R. G., "*Sublethal Effects of Fire Smoke: Finding How to include them in Fire Safety Decisions*", Fire Safety Development Emerging Needs, Products Developments, Non-Halogen FR's, Standards and Regulations Proceedings, Fire Retardants Chemical Association, Washington DC, pp 171-177 (2000)

[9]   Welling L. et al. "*Medical Management after indoor fires: A Review*", Burns 31, pp 673-678 (2005)

[10]   Robinson, A., and Bourgoyne, J. H., *"The Scandinavian Star Incident - A Case Study*", Fire Engineers Journal 59, 198, 36-38(1999)

[11]   Per Blomqvist, **"*Emissions from Fires- Consequences for Human Safety and the Environment*"**, PhD Thesis, Department of Fire Safety Engineering, *Lund Institute of Technology,* Lund University, Lund, Sweden (2005)

[12]   Council of Canadian Fire Marshals and Fire Commissioners (CCFMFC), "*Fire losses in Canada: Annual Report 2002*", Ottawa, ON. (2002)

[13]   Arthur E., Cote, P.E., "*Fundamentals of Fire Protection*", SFPE Handbook Fire Protection Engineering, National Fire Protection Association, Quincy, Massachusetts, pp. 91, (2004)

[14]   John R. Hall Jr., "*Fire in the U.S and Canada*", Fire Analysis and Research Division, *National Fire Protection Association*, Quincy, MA. (2005) same as above

[15]   Orzel, R.A. "*Toxicological aspects of fire smoke: polymer pyrolysis and combustion",* Journal of Occupational Medicine, State of the Art Review Vol. 8 (3), pp 414-429 (1993)

[16]   Sumi, K., Tsuchiya, Y., "*Toxic Gases and Vapours Produced at Fires",* CBD 144, Canadian Building Digest, National Research Council Canada, (1971)

[17]   Thomas L. Junod, *"Gaseous Emissions and Toxic Hazards Associated with Plastics in Fire Situations- A Literature Review*", National Aeronautics and Space Administration, Lewis Research Center, Cleveland, Ohio 44135, Washington, D. C. (1976)

[18] Krasny, J.F., Parker, W.J., and Babrauskas, V., "*Fire Behavior of Upholstered Furniture and Mattresses"*, William Andrew Publishing, Norwich NY (2001)

[19] Mehaffey J.R., "*Polyurethane Insulation and its Effects on the Intensity of Fire",* Proceedings of the Society of the Plastics Industry of Canada, Sixth Annual Rigid Polyurethane Foam Committee, Fall General Meeting and Conference, No. 9, pp 14, Quebec (1985)

[20] *"Making the Nation Safe from Fire: A Path Forward in Research"*, Committee to Identify Innovative Research Needs to Foster Improved Fire Safety in the United States, National Research Council (2003)

[21] Woolley W.D, Raftery, M.M., "*Smoke and Toxicity Hazards of Plastics in Fires",* Journal of Hazardous Materials Vol.1, pp 215-222. (1975/76)

[22] Guillaume, E; Chivas, C; Sainrat, A; *"Regulatory Issues and Flame Retardant Usage in Upholstered Furniture in Europe".* LNE-CEMATE-Fire Behaviour Division Research, Studies Fire Safety Engineering Activities*, Trappes Cedex, France (2008), < http://www.see.ed.ac.uk/FIRESEAT/files08/04-Guillaume.pdf>

[23] Stockholm Convention on Persistent Organic Pollutants, *"Guidance on flame retardant alternatives to Pentabromodiphenyl ether (PentaBDE)"*, Persistent Organic Pollutants Review Committee Fourth Meeting, UNEP/POPS/PORPC.4/INF/13, Geneva (2008)

[24] Babrauskas V., *"Effects of FR Agents on Polymer Performance",* Heat Release in Fires, Chapter 12, pp 423-446, Elsevier Applied Science, NY, (1992)

[25] Sophie Duquesne; Michel Le Bras; Serge Bourbigot; Rene Delobel; Franck Poutch; Giovanni Camino; Berend Eling; Chris Lindsay; Toon

Roels; *"Analysis of Fire Gases Released from polyurethane and Fire-Retarded Polyurethane Coatings"*, Journal of Fire Sciences, vol. 18, no. 6, pp 456-482 (2000)

[26] Schartel B; Hull T. R; *"Development of fire-retarded materials—Interpretation of cone calorimeter data"*, Fire and Materials, Fire Mater 31 pp 327–354. (2007)

[27] Mouritz, A. P., Gibson, A. G., *"Fire Properties of Polymer Composite Materials, Solid Mechanics and Its Applications"*, Fire Properties of Polymers Composite Materials, Chapter 12, Vol.143, pp 394 Publisher: Springer (2006)

[28] Maureen Rouhi A., *"Chemophobia and Fire Safety"*, *Chem. Eng. News*, *90* (44), pp 3 (2012)

[29] Harpal Singh, A. K. Jain, *"Ignition, Combustion, Toxicity, and Fire Retardancy of Polyurethane Foams: A Comprehensive Review"*, Journal of Applied Polymer Science, Vol. 111, 1115-1143 (2009)

[30] Fisk, P.R., Girling, A. E., Wildey, R.J., *"Prioritisation of Flame Retardants foe Environmental Risk Assessment"*, Environmental Agency, Chemicals assessment Section, U.K (2003)

[31] Yang W, Macosko C, Wellinghoff S*; "Thermal degradation of urethanes based on 4,4-diphenylmethane diisocyanate and 1,4-butanediol(MDI/BDO)"*, Polymer 27(8), pp 1235-1240 (1986)

[32] Ohtani H, Kimura T, Okamoto K, Tsuge S*, "Characterization of Polyurethanes by high-resolution pyrolysis capillary gas chromatography",* Journal of Analytical & Applied Pyrolysis" 12 (2), pp 115-133 (1987)

[33] Alaee M., Wenning R.J., "*The Significance of Brominated Flame Retardants in the Environment: Current Understanding, Issues and Challenges", Chemosphere* 46, pp 579-582 (2002)

[34] Sarah Janssen; "*Brominated Flame Retardants: Rising Levels of Concerns", Health Care without Harm*, Arlington, VA. (2005)

[35] Zhong Tang, et al.,"*Thermal degradation behaviour of rigid polyurethane foams prepared with different fire retardant concentrations and blowing agents*", Polymer**,** Vol. 43(24), pp 6471–6479 (2002)

[36] Beyler C. L, Hirschler M. M; "*Thermal Decomposition of Polymers*", Section One, Chapter 7 in SFPE Handbook of Fire Protection Engineering (3rd Ed), pp 1-123, NFPA, Quincy, MA (2001)]

[37] George Woods; "*Flexible Polyurethane Foams-Chemistry and Technology", Applied Science Publishers LTD*, London and New Jersey, pp 86. (1982)

[38] André Leisewitz, Hermann Kruse, Engelbert Schramm; "*Substituting Environmentally Relevant Flame Retardants: Assessment Fundamentals",* Published by the Western Germany Federal Environmental Agency, Berlin (2001)

[39] Horrocks, A.R., Price D., "*Flame retardants Materials", Wood Head Publishing Limited*, pp 73 (2001)

[40] Harry Salem, Sidney A. Katz; "*Inhalation toxicology*", 2nd Edition, Published by CRC Press, pp 207. (2006)

[41] Kimmerle, G., Eben, A., Groning, P., Thyssen, J., "*Acute Toxicity of Bicyclic Phosphorous Esters", Archives of Toxicology* Vol.35(2), pp149-152 (1976)

[42] Marine Accident Investigator's International Forum, "*Chemistry and Physics of Fire*"

[43] Sterling Larson, "*Fire retardants*", Proceedings of 1976 International Symposium on Flammability and Fire Retardants, Toronto, Ontario, Canada (1976)

[44] Kurt, C. E; Reegen, S.L, "*In Flame Retardant Polymeric Materials*", Lewin, M., Ed.; Plenum: New York, pp 291(1975)

[45] Sophie Duquesne et al.,"*Expandable graphite: a fire retardant additive for polyurethane coatings*", Fire and Materials, 27(3), pp 103–117 (2003)

[46] Lewin, M.; Weil, E.D. "*Mechanism and Modes of Action in Flame Retardancy of Polymers*". In *Fire Retardant Materials;* Horrocks, A.R., Price, D., Eds.; Woodhead Publishing: Cambridge, UK, pp. 31-57 (2001)

[47] F. Laoutid et al., "*New Prospects in Flame Retardant Polymer Materials: From Fundamentals to Nanocomposites*", Materials Science and Engineering R Vol. 63, pp 100-125(2009)

[48] Isao Watanabea, Shin-ichi Sakai; "Environmental release and behavior of brominated flame retardants", *Environment International* 29, pp 665– 682. (2003)

[49] Linda S. Birnbaum, Daniele F. Staskal*, "Brominated Flame Retardants: Cause for Concern?*" Environmental Health Perspectives, Vol. 112 (1), 2004

[50] Ling Ye et al., "*Flame Retardant and Mechanical Properties of high density rigid polyurethane foam filled with decabrominated Diphenyl*

ethane and expandable graphite", Journal of Applied Polymer Science, Vol. 111, pp 2372-2380 (2009)

[51] Sergei V. Levchik and Edward D. Weil, "*A Review of Recent Progress in Phosphorus-based Flame Retardants*", Journal of Fire Sciences 24; pp 345 (2006)

[52] Vytenis Babrauskas et al., "*Fire Hazard Comparison of Fire-Retarded and Non-Fire-Retarded Products*", NBS Special Publication 749, Fire Measurement and Research Division, Centre for Fire Research, National Bureau of Standards, Gaithersburg MD 20899 (1988)

[53] Checchin M, Cecchini C, Cellarosi B, Sam F.O; "Use of Cone Calorimeter for evaluating the fire performances of polyurethane foams", Polymer Degradation and Stability Vol.64, pp 573-576 (1999)

[54] Yeng-Fong Shih et al., "*Expandable graphite systems for phosphorous-containing unsaturated polyesters-Enhanced thermal properties and flame retardancy*", Polymer Degradation and Stability, 86, pp 339-348 (2004)

[55] Qingliang He et al., "*Flammability and Thermal Properties of a Novel Intumescent Flame Retardant Polypropylene*", Journal of Fire Sciences 27, pp 303 (2009)

[56] Modesti M., Lorenzetti A., Simioni F Gilbert M., "*Influence of Expandable Graphite on physical-mechanical properties and fire behaviour of flame retarded PIR-PUR foams*", A paper presented at Polyurethane Expo 2001, Columbus, OH, USA (2001)

[57] Modesti M., Lorenzetti A., Simioni F., Camino G., "*Expandable graphite as an intumescent flame retardant in polyisocyanurate-polyurethane*

foams", Polymer Degradation and Stability, Vol. 77 (2), pp 197-202 (2002)

[58] Modesti M., Lorenzetti A., *"Flame retardancy of polyisocyanurate polyurethane foams: use of different charring agents"*, Polymer Degradation and Stability, Vol. 78 (2), pp 341-347 (2002)

[59] Modesti M., Lorenzetti A., Simioni F., Checchin M., "*Influence of different flame retardants on fire behaviour of modified PIR/PUR polymers*", Polymer Degradation and Stability Vol.74, pp 475–479 (2001)

[60] Michele Modesti, Alessandra Lorenzetti; *"Improvement on fire behaviour of water-blown PIR-PUR foams: use of an halogen-free flame retardant"*, European Polymer Journal, (2003)

[61] Xiang-Cheng et al., "*Dependence of flame retardant properties on density of expandable graphite filled rigid polyurethane foam*", Journal of Polymer Science Vol. 104 (5), pp 3347-3355 (2007)

[62] Maya Paabo, Barbara C. Levin*, "A review of the literature on the gaseous products and toxicity of generated from the pyrolysis and combustion of rigid polyurethane foams"* Fire and Materials Vol. 11, (1987)

[63] Claire Austin, "*Wildland firefighter health risks and respiratory protection*", IRSST – Communications Division, 505, De Maisonneuve Blvd West, Montréal (Québec) 2008

[64] Andja Alajbeg,"*Products of Non-flaming Combustion of Rigid Polyurethane Foam*", Journal of Analytical and Applied Pyrolysis Vol. 10, pp 215-224 (1987)

[65] Dyer E, Newborn G.E, Wright G. C Jr., "*Thermal Degradation of Carbamates*", Delaware Chemical Symposium (1958)

[66] Backus J.k, Darr W.C, Gemeinhardt P.G, Saunders J.H; *"Thermal Decomposition of Rigid Urethane Foams"*, Journal of Cellular Plastics (1965)

[67] Voorhees K.J, Hileman F.D, Einhorn I. N, Futrell J.H., "*An Investigation of the Thermolysis Mechanism of Model Urethanes*", Journal of Polymer Science: Polymer Chemistry Edition, Vol. 16,213-228 (1978)

[68] Napier D. H, Wong T. W., *"Toxic Products from the Combustion and Pyrolysis of Polyurethane Foams",* British Polymer Journal, Vol. 4(1), 45-52 (1972)

[69] Woolley W. D, Fardell P.J, Buckland I.G; "*The Thermal Decomposition Products of Rigid Polyurethane Foam under laboratory Conditions*", Fire Research Note No 1039, Fire Research Station, UK (1975)

[70] Le Bras, M., Bourbigot, S,Revel, B. *"Comprehensive study of the degradation of intumescent EVA-based material during combustion"*, Journal of Materials Science Vol.34, pp 5777-5782 (1999)

[71] Davidson, R. G., "*Pyrolysis-Evolved Gases-FTIR Analysis of Polyurethanes*", Microchimica Acta, Vol. 94, No. 1-6, pp 301-304 (1988)

[72] Blomqvist P, Hertzberg T, Tuovinen H, Arrhenius K, Rosell L, "*Detailed Examination of Smoke Gas Contents suing a small-scale controlled*

equivalence ratio tube furnace method", Fire and Materials 31, pp 495-521 (2007)

[73] Drysdale D. "An introduction to fire dynamics" West Sussex, England: John Wiley & Sons; (1998)

[74] Ball G.W, Ball L. S, Walker M.G, Wilson W. J; "Fire test data for urethane-based and isocyanurate-based rigid cellular plastics", Plastics and Polymers Vol.40, pp 290-293(1972)

[75] Claire Austin, "*Municipal firefighter exposures to toxic gases and vapours*", PhD Thesis, Department of Occupational Health, Faculty of Medicine, McGill University Montréal, Québec, Canada (1997)

[76] ASTM E 1354: Standard Test Method for Heat and Visible Smoke Release Rates for Materials and Products Using an Oxygen Consumption Calorimeter

[77] Parker W.J.; "*Calculations of the Heat Release Rate by Oxygen Consumption for Various Applications*", *Journal of Fire Sciences Vol 2(5),* pp 380-395 (1984)

[78] Babrauskas, V., Peacock, R. D., "*Heat Release Rates: The Single Most Important Variables in fire Hazard*", *Fire Safety Journal* 18, pp. 255-272 (1992)

[79] Redfern J.P., "*Rate of heat release measurement using the cone calorimeter*", Journal of Thermal Analysis, Vol. 35, pp 1861-1877 (1989)

[80] Babrauskas V. "*Why was the fire so big? HHR: The role of heat release rate in described fires",* Fire Arson Investigation 47, pp 54–57 (1997)

[81] E.J Weckman, D.O Adeosun, J. Rigg, B. Epling, D. Torvi; "*Preliminary Cone- and Furniture-Scale Calorimeter Tests of Non-FR and FR Laminated Polyurethane Foams*", Fire and Materials, 11th International Conference and Exhibition, San Francisco, USA. Interscience Communications (2009)

[82] Sumi, K., Tsuchiya, Y., "*Toxic Gases and Vapours Produced at Fires*", CBD 144, Canadian Building Digest, National Research Council Canada, (1971)

[83] ASTM E176-04; "*Standard Terminology of Fire Standards*", ASTM International, W. Conshohocken, PA. (2004)

[84] George W Mulholland, "*Smoke Production and Properties*", SFPE Handbook of Fire Protection Engineering, 2nd Edition, Chapter 15, Section 2, pp 2/217 -2/227(1995)

[85] Hartitz J. E, Yount R. A., "*A Rigid Poly(Vinyl Chloride) Compound With Improved Combustion Characteristics*", Polymer Engineering and Science, Vol. 18(7), pp 549-555 (1978)

[86] Mansurov Z. A., "*Soot Formation in Combustion Processes (Review)*", Combustion, Explosion, and Shock Waves, Vol. 41(6), pp 727–744, (2005)

[87] Rasbash D. J, Drysdale D.D., "*Fundamentals of Smoke Production*", Fire Safety Journal Vol.5, pp 77-86 (1982)

[88] Thomas G. Cleary, James G. Quintiere; "*Flammability Characterization of Foam Plastics*", Fire Measurement and Research Division, Centre for Fire Research, NISTIR 4664, National Bureau of Standards, Gaithersburg MD 20899 (1991)

[89]   Mouritz A.P, Mathys Z. Gibson A.G., *"Heat release of polymer composites in fire"*, Composites Part A: Applied Science and Manufacturing**,** Vol. 37 (7), pp 1040-1054 (2006)

[90]   Kanabus-Kaminska M., et.al   *"Determination of Major and Minor Components of Smoke from Full –Scale Fire Tests of Furnishings by FTIR Spectroscopy"*, National Research Council Ottawa, Ontario, *Fire and Materials* 2001, San Francisco, CA, pp 407-417 (2001)

[91]   Michal J., *"Determination of carbon monoxide in thermal degradation products of polymeric materials"*, *Fire and Materials Vol. 5(4), pp* 149-52 (1981)

[92]   Bott B, Firth J.G, Jones T.A, *Evolution of toxic gases from heated plastics'*, British. Polymer Journal Vol. 1 (5), pp 203-204 (1969)

[93]   Tasic T et al. *"Gasoline and LPG Exhaust Emission Comparison"*, Advances in Production Engineering and Management, Vol.6 (2), pp 87-94 (2001)

[94]   Hilado, C.J., *"Flammability Handbook for Plastics,"* Technomic Publishing, Lancaster, PA, USA, pp. 265 (1998)

[95]   Hull, T.R., Stec, A.A., and Purser, D.A., *"Fire Toxicity"*, Boca Raton: CRC Press ; Oxford Wood head Pub., Boca Raton, FL, USA, Chap. 17, pp. 583 (2010)

[96]   Kannan G. K, Kumar N. S, *"Studies on fire and toxicity potential of bromo-butyl rubber of respiratory mask in a simulated closed*

environment", Indian Journal of Chemical Technology Vol. 18, pp. 152-160 (2011)

[97] Daniel T. Gottuk; "*Generation of Carbon monoxide in compartment fires*", Fire Measurement and Research Division, Centre for Fire Research, NIST GCR-92-619, National Bureau of Standards, Gaithersburg MD 20899

[98] Paul K.T., "*Use of FTIR to Analyse Fire Gases from Burning Polyurethane Foams*", *Proceedings of the Cellular Polymers II Conference*, Coventry, Paper 2, 6124, Rapra Technology Ltd. (1995)

[99] SAFIR, "*An International Programme to Investigate the Use of FTIR to Analyse Fire Effluents*", VTT Building Technology, Espoo, Finland (1999)

[100] Barbara C. Levin, Maya Paabo, Mary Lou Fultz and Cheryl S. Bailey, "*Generation of hydrogen cyanide from flexible polyurethane foam decomposed under different combustion conditions*", Fire and Materials Vol. 9(3), pp125-134 (1985)

[101] Mullens J. et al. "*The Determination of the gases released during heating of a flame retardant for polymers coupling of TG with FTIR, MS and GC-MS*", Journal of Thermal Analysis, Vol. 49, pp 1061-1067 (1997)

[102] Mumford N.A, Chatfield D.A, Einhorn I.N; "*Component Analysis of Rigid Polyurethane Foams*", Fire Research Vol.1, pp 107-117 (1977/78)

[103] Einhorn I.N, "*Physiological and Toxicological Aspects of Smoke Produced during the Combustion of Polymeric Materials*", Environmental Health Perspectives Vol. 11, pp. 168-189(1975)

[104] Omar Abdulaziz O. Aljumaiah, "*Combustion Products from Ventilation Controlled Fires: Toxicity Assessment and Modelling*", Energy and Resources Research Institute, School of Process, Environmental, and Materials Engineering, University of Leeds, UK (2012)

[105] Stauffer R. C et al. "*Dibromoneopentyl Glycol-Its Effect on Smoke Evolution in Unsaturated Polyester*", Journal of Fire Retardants Chemistry Vol.3, pp 34-43 (1976)

[106] Miller D.P, Petrella R. V, Manca A; "*An evaluation of some factors affecting the smoke and toxic gas emission from burning unsaturated polyester resins*", Proceeding of Annual Conference, Reinforced Plastic/Composite Institute. Society of Plastics Industry Vol.31, pp 20-c, 1-8(1976)

[107] Emil Braun and Barbara C. Levin "*Polyesters: A Review of the Literature on Products of Combustion and Toxicity*", Fire and Materials Vol. 10 pp 107-123 (1986).

[108] Brenda Ann Prine, "*Fire Testing Standards for Transportation Applications- A Global Comparison*", Mechanical and Mechatronics Engineering, University of Waterloo, Waterloo Canada (2013)

[109] Gann, R. G., Babrauskas, V., Grayson, S. J., "*Hazards of Combustion Products: Toxicity, Opacity, Corrosivity, and Heat Release: The Experts' Views on Capability and Issues*," Fire and Materials, 35(2) pp. 115-127 (2011)

[110] Iolanda Rotaru et al., "*Synthesis of new aromatic mannich polyols for rigid polyurethane foams*", U.P.B Scientific Bulletin series B, Vol. 69 (2) (2007)

[111] Edward D. Weil, Sergei V. Levchik, "*Commercial Flame Retardancy of Polyurethanes*", Journal of Fire Sciences, Vol. 22 (3), pp 183-210 (2004)

[112] Moore S.E, Williams S.J, "*Significantly Reduced Catalyst Consumption in Rigid Foams*", Journal of Cellular Plastics, Vol. 36(1), (2000)

[113] Babrauskas V, "*Smoke and Gas Evolution rate measurements on Fire Retarded Plastics with the cone calorimeter*", Fire and Materials Vol.14, pp 135-142 (1989)

[114] Babrauskas V, Grayson S. J., "Heat release in fires", Interscience Communications Ltd London (2009)

[115] Vytenis Babrauskas, *"Effective Measurement Techniques for Heat, Smoke, and Toxic Fire Gases"*, Fire Safety Journal Vol.17, pp 13-26 (1991)

[116] Atle William Heskestad, Per Jostein Hovde, *"Assessment of Smoke Production from Building Products"*, Fire Safety Science-Proceedings of the Fourth International Symposium, pp 527-538 (1994)]

[117] Hull T.R, Stec A. A, "*Fire effluent toxicity: bench-scale generation of toxic products*", in: Proceedings of the 6th International Seminar on Fire and Explosion Hazards, Leeds, UK (2010)

[118] ASTM Standard E662-09 "*Standard Test Method for Specific Optical Density of Smoke Generated by Solid Materials*". ASTM International, West Conshohocken, PA (2009)

[119] Prager F.H et al. "*Risk-Oriented Testing and Assessment of Smoke Density*", Journal of Fire Sciences, Vol. 10 (2), pp 118-132 (1992)

[120] Bernhard Schartel, "Phosphorous-based Flame Retardancy Mechanisms-Old Hat or a Starting Point for Future Development?", Materials Vol 3, pp 4710-4745 (2010)

[121] Airbus Industries "Smoke Emission Requirements." Technical Specification ATS 10000.001

[122] ASTM E1995 - 12 "*Standard Test Method for Measurement of Smoke Obscuration Using a Conical Radiant Source in a Single Closed Chamber, With the Test Specimen Oriented Horizontally*"

[123] Fire Testing Technology Limited "User's Guide for the Smoke Density Chamber", Issue 3.0, Distributed by Fire Testing Technology Limited, East Grinstead, West Sussex, United Kingdom (2008), <http://www.fire-testing.com>

[124] ISO 5659-2: "*Plastic-Smoke-Generation-Part 2: Determination of Optical Density by a Single Chamber Test*"

[125] Umberto Flisi, "*Testing the Smoke and Fire Hazard*", Polymer Degradation and Stability Vol.30, pp 153-168(1990)

[126] Cornelissen A.A.,"*Smoke Release Rates: Modified Smoke Chamber versus Cone Calorimeter-Comparison of Results*", Journal of Fire Sciences 10 (1), pp3-19 (1992)

[127] Instructional Manual for Model 8800A Heated Total Hydrocarbon Analyzer, Baseline-Mocon Company, P.O. Box 649, Lyons, CO 80540 <www.baseline-mocon.com>

[128] Koen Desmet, Marc Schelfaut, Tadeusz Górecki, Pat Sandra, "*Evaluation of the suitability of sampling on Tenax TA and polydimethylsiloxane for the analysis of combustion gases*", Talanta, Vol.79, pp 967–970 (2009)

[129] Markes International Limited, "*Thermal Desorption Technical Support, Note 5: Advice on Sorbent Selection and Conditioning Sample Tubes*", Unit D3, Llantrisant Business Park, Pontyclun, RCT, CF72 8YW, United Kingdom. <http://www.markes.com>

[130] ASTM D 6196-97, "*Standard Practice for Selection of Sorbents and Pumped Sampling/Thermal Desorption Analysis Procedures for Volatile Organic Compounds in Air*" (1997)

[131] Adeosun, D., Jones, B., Weckman, E. & Epling, W. "FTIR Analysis of Fire Gases in Flame Retarded Polyurethane Foams". Proceedings of Combustion Institute Canadian Section Spring Technical Meeting, pp 261-266 (2010)

[132] Su, J.Z, Kanabus-Kaminska, M., "*FTIR Gas Measurement in Home Smoke Alarm Tests*", Institute for Research in Construction, National Research Council of Canada, IRC-RR-107. (2002)

[133] Milhail Lonescu; "*Chemistry and Technology of Polyols for Polyurethanes*",Published by Smithers Rapra Technology, pp 420 (2005),[ISBN 978-1-84735-035-0]

[134] Tuula Hakkarainen et al. "*Smoke Gas Analysis by Fourier Transform Infrared Spectroscopy- Summary of the SAFIR Project Results,*" *Journal of Fire and Materials Vol.*24, pp 101-112. (2000)

[135] Louise C Speitel; "*Fourier Transform Infrared Analysis of Combustion Gases*", U.S Department of Transportation, Federal Aviation Administration, Research and Development Division, *National Technical Information Service* (NTIS), Springfield, Virginia 22161. (2001)

[136] Bhagat, V,J., "*Behaviour of Expandable Graphite as a Flame Retardant in flexible polyurethane Foam*", Research & Development Center,

Presented at the Polyurethane Foam Association (PFA), Arlington, Virginia, USA (2001)

[137] Instructional Manual for *"MIRAN 205B Series SapphIRe Portable Ambient Air Analyzers"* Thermo Electron Corporation Environmental Instruments, 27 Forge Parkway Franklin Massachusetts 02038, (2004), <www.thermo.com/eid>

[138] Bruce Quimby, *"Detection of Toxic Industrial Compounds: A Guide to Analytical Techniques"*, Agilent Technologies Inc; 2850 Centreville Road, Wilmington, DE 19808-1610, USA (2003) <www.agilent.com/chem>

[139] De Vos, B.J, *"Organic Vapors emitted from the plumes of pool fire on carpet materials",* Journal of Fire Sciences, 17(5), pp 383-420 (1999)

[140] Elizabeth Woolfenden, *"Sorbent-based sampling methods for volatile and semi-volatile organic compounds in air Part 1: Sorbent-based air monitoring options"*, Journal of Chromatography A, Vol.1217 (16), pp 2674–2684 (2010)

[141] CDS Analytical, *"Instruction Manual for ACEM 9300 Series"*, 465 Limestone Road, P.O Box 277, Oxford, PA 19363-0277, USA, <www.cdsanalytical.com>

[142] Agilent Technologies Inc, *"Agilent G1701EA MSD Productivity Chemstation Software version E.02.00.493"*, 5301 Stevens Creek Boulevard, Santa Clara, CA 95052 (2010)

[143] *National Institute of Standards and Technology,* "NIST 11 EPA/NIH Mass Spectral Database and Search Program (NIST11/NIST08), version 2.0"

[144] Fatemi, M.H, "Simultaneous modeling of the Kovats retention indices *on OV-1 and SE-54 stationary phases using artificial neural networks*", Journal of Chromatography *A Vol.* 955(2), pp 273-280 (2002)

[145] Gil-Moltó J, Varea M, Galindo N, Crespo J; "*Application of an automatic thermal desorption–gas chromatography–mass spectrometry system for the analysis of polycyclic aromatic hydrocarbons in airborne particulate matter*" Journal of Chromatography A**,** Vol. 1216 (9), pp 1285–1289 (2009)

[146] Alexander B. Morgan, Matthew Bundy, *"Cone Calorimeter Analysis of UL-94 rated Plastics"*, Fire and Materials Vol.31, pp 257-283 (2007)

[147] Enright P. A, Fleischmann C. M, "*Uncertainty of heat release rate calculation of the ISO 5660 cone calorimeter standard test method"*, Fire Technology Vol. 35 (2), pp 153-169 (1999)

[148] Arnaud Marchal, et al., "*Effect of intumescent on polymer degradation*", Polymer Degradation and stability Vol.44, pp 263-272(1994)

[149] Bashirzadeh R., Gharehbaghi A., "*An investigation of on reactivity, mechanical and fire properties of PU flexible foam*", Journal of Cellular Plastics Vol.00-2009

[150] Alexander B. Morgan, Matthew Bundy, "Cone Calorimeter Analysis of UL-94 rated plastics, Fire and Materials, Vol. 31, pp 257-283 (2007)

[151] Serge Bourbigot et al. "*Recent Advances for Intumescent Polymers*", Macromolecular Materials and Engineering Vol.289, pp 499-511 (2004)

[152] Maries K; "*Measurements of Smoke in Fires - A Review*", Fire and Materials, Vol. 2(1), pp 2-6 (1978)

[153] Ostman B, "Smoke and Soot", Heat Release in Fires, Elsevier Applied Science, NY, Chapter 12, pp 423-426 (1992)

[154] Hirschler M. M; *"Soot from Fires: II. Mechanisms of Soot Formation"*, Journal of Fire Sciences, Vol. 3 (6), pp 380-414 (1985)

[155] Anna Andersson et al., *"Intumescent Foams—A Novel Flame Retardant System for Flexible Polyurethane Foams"*, Journal of Applied Polymer Science, Vol. 109, pp 2269–2274 (2008)

[156] Stec, A.A, Hull, T.R. *"Assessment of the fire toxicity of building insulation materials"*, *Energy and Buildings* Vol.43, pp 498-506 (2011)

[157] Arthur F. Grand, *"The Use of the cone calorimeter to assess the effectiveness of fire retardant polymers under simulated real fire test conditions"*, presented at the Seventh International Fire Science and engineering Conference Interflam 96 Cambridge England (1996)

[158] Rasbash D.J, Pratt B.T; "Estimation of the Smoke Produced in Fires", Fire Safety Journal, Vol. 2(1), pp 23–37 (1980)

[159] Hermann Sand "Assessment of Smoke Production of Building Materials Using the ISO-Dual Smoke Chamber (ISO/TR 5924)", Journal of Fire Sciences Vol. 9(2), pp 162-170 (1991)]

[160] Atkinson, G., Drysdale D., *"A Note on the Measurement of Smoke Yields"*, Fire Safety Journal, Vol. 15(4), pp 331-335 (1989)

[161] Papazoglou, E. *"Flame Retardants for Plastics"* In: Harper C.A. (ed), Chapter 4 p4.1 -4.88, Handbook of Building Materials for Fire Protection, McGraw-Hill (2004)

[162] Paul K.T, Hull T. R, Lebek K, Stec A. A *"Fire smoke toxicity: The effect of nitrogen oxides"*, Fire Safety Journal, Vol. 43, pp 243–251(2008)

[163] Herrington, R.M, "*The rate of heat, smoke and toxic gases release from polyurethane foams*," Journal of Fire and Flammability, Vol.10, pp308–325 (1979)

[164] Instruction Manual for TML 41M/H Nitrogen Oxides Analyzer, Teledyne Monitor Labs, 35 Inverness Drive East, Englewood, CO 80112 USA <http://www.teledyne-ml.com/pdf/TML41MHmanual.pdf>

[165] Barnard, J.A.,Bradley, J.N, "Flame and Combustion" Chapter 20, pp 308, 2nd Ed., Chapman and Hall, London (1985)

[166] Guillermo Rein,"Smouldering Combustion Phenomena in Science and Technology", International Review of Chemical Engineering, Vol 1, pp 3-18 (2009)

[167] Alex Bwalya*, "An Overview of Design Fi*res for Building Compartments", Fire Technology Vol. 44, pp 167-184 (2008)

[168] Wakefield J.C, "*Toxicological Review of the Products of Combustion*", HPA Chemical Hazards and Poisons Division, Chilton Didcot, Oxfordshire, OX11 0RQ, ISBN 978-0-85951-663-1(2010)

[169] Report on Carcinogens 12th edition, U.S. Department of Health and Human Services, Public Health Service National Toxicology Program (2012)

[170] "*Chemical Listing and Documentation of Revised IDLH Values",* NIOSH Publications and Products, Centers for Disease Control and Prevention (2012).

Appendices

Appendix 3.1: Repeatability of FR samples Test Results
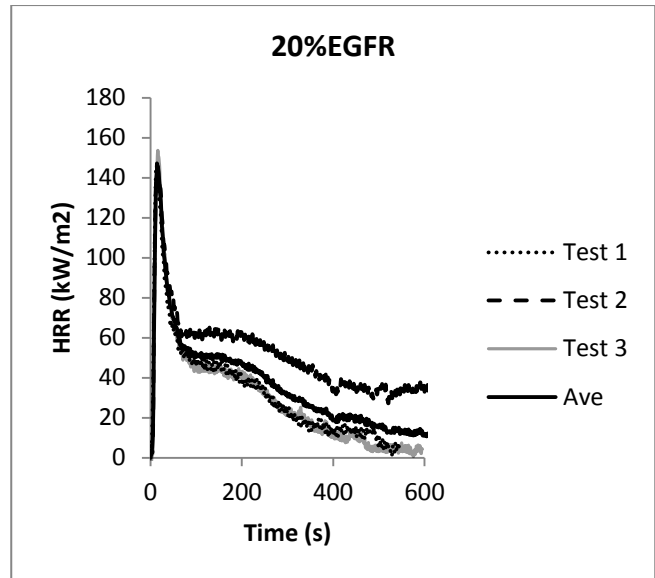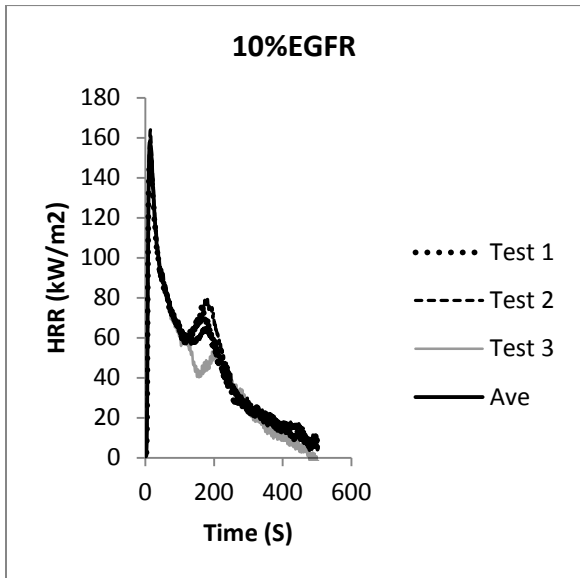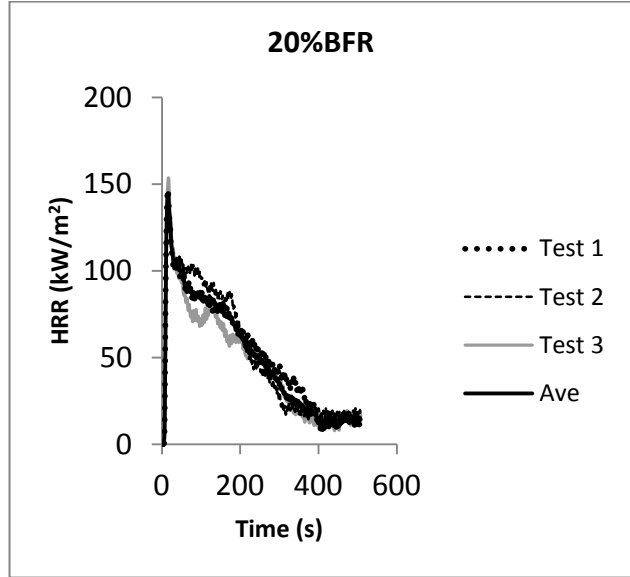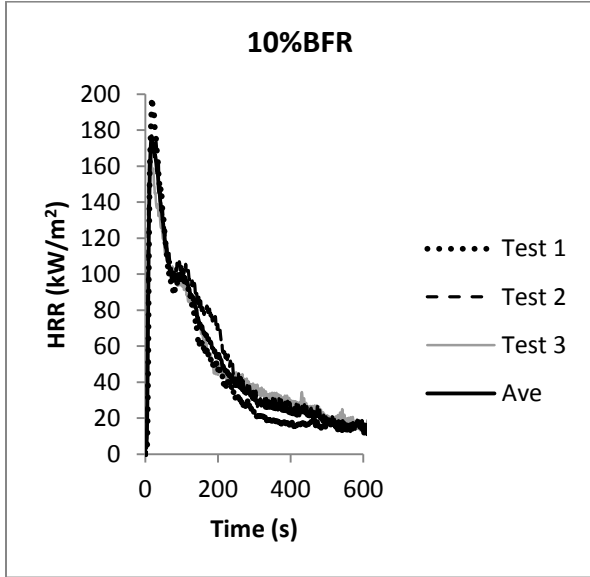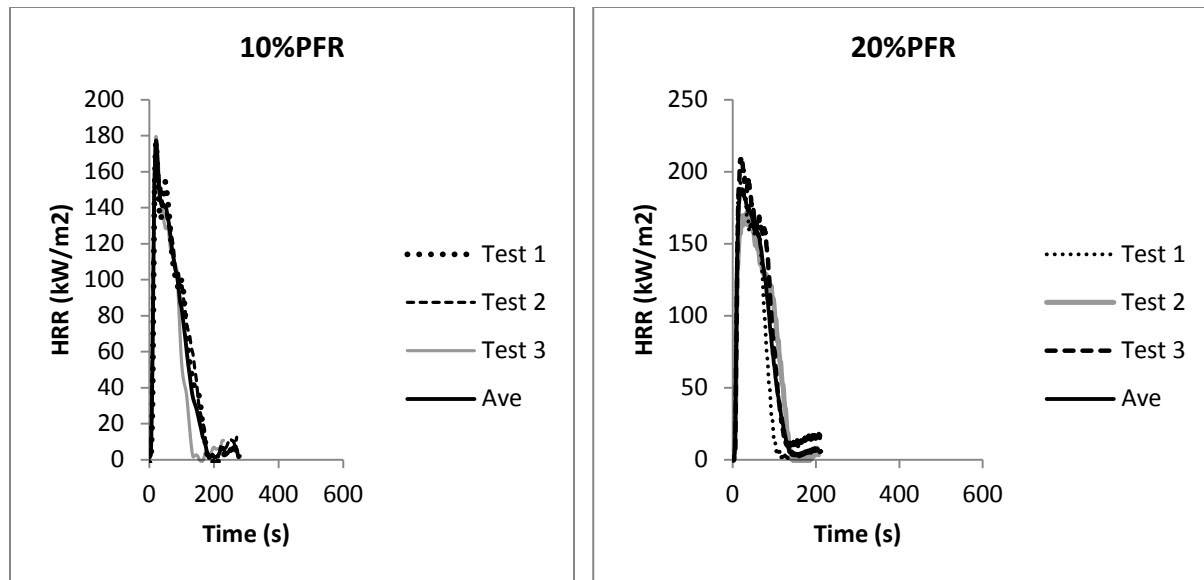
Appendix3. 2: Variability of **Average CO** of the NFR and FR samples

Sample Material		Sample Size n	Mean of Ave CO $\bar{x}$ [kg/kg]	Standard Deviation, s [kg/kg]	Margin of Error	95% Confidence Interval for $\bar{x}$	Coefficient of Variation
NFR		3	0.1317	0.0067	0.0076	0.1317±0.0076	0.0509
BFR	10%	3	0.1706	0.0213	0.0241	0.1706±0.0241	0.1249
	20%	3	0.1327	0.0548	0.0620	0.1327±0.0620	0.4130
EGFR	10%	3	0.0626	0.0125	0.0072	0.0626±0.0072	0.1997
	20%	3	0.0678	0.0233	0.0264	0.0678±0.0264	0.3437
PFR	10%	3	0.1021	0.0089	0.0101	0.1021±0.0101	0.0872
	20%	3	0.1439	0.0050	0.0057	0.1439±0.0057	0.0347

Appendix 3.3: Variability of **Average CO_2** of the NFR and FR samples

Sample Material		Sample Size n	Mean of Ave CO_2 $\bar{x}$ [kg/kg]	Standard Deviation, s [kg/kg]	Margin of Error	95% Confidence Interval for $\bar{x}$	Coefficient of Variation
NFR		3	1.9067	0.0309	0.0350	1.9067±0.0350	0.0162
BFR	10%	3	1.9033	0.0569	0.0644	1.9033±0.0644	0.0299
	20%	3	1.8267	0.0513	0.0581	1.8267±0.0581	0.0281
EGFR	10%	3	1.9400	0.2443	0.2765	1.94±0.2765	0.1259
	20%	3	2.0500	0.2773	0.3138	2.05±0.3138	0.1353
PFR	10%	3	1.4100	0.0255	0.0289	1.41±0.0289	0.0181
	20%	3	1.1500	0.1000	0.1132	1.15±0.1132	0.0870

Appendix 3.4: Variability of **Average SEA** of the NFR and FR samples

Sample Material		Sample Size n	Mean of Ave SEA $\bar{x}$ [m²/kg]	Standard Deviation, s [m²/kg]	Margin of Error	95% Confidence Interval for $\bar{x}$	Coefficient of Variation
NFR		3	99	37.07	41.95	99±41.95	0.3744
BFR	10%	3	326	42.62	48.23	326±48.23	0.1307
	20%	3	494	121.71	137.73	494±137.73	0.2464
EGFR	10%	3	102	4.53	2.62	102±2.62	0.0444
	20%	3	156	105.96	119.91	156±119.91	0.6792
PFR	10%	3	867	37.00	41.87	867±41.87	0.0427
	20%	3	1132	57.17	64.69	1132±64.69	0.0505

Appendix 3.5: Variability of **Max specific optical density** of the NFR and FR samples

Sample Material		Sample Size n	Mean of Max. SOD $\bar{x}$	Standard Deviation, s	Margin of Error	95% Confidence Interval for $\bar{x}$	Coefficient of Variation
NFR		3	166	14.02	15.87	166±15.87	0.0845
BFR	10%	3	230	50.11	56.70	230±56.70	0.2179
	20%	3	451	15.51	17.55	451±17.55	0.0344
EGFR	10%	3	437	18.01	20.38	437±20.38	0.0412
	20%	3	319	1.58	1.79	319±1.79	0.0050
PFR	10%	3	489	11.51	13.02	489±13.02	0.0235
	20%	3	437	37.00	41.87	437±41.87	0.0847

Appendix 4.1: Cone Calorimeter Test Results

Table 4.1a: Showing comprehensive data from the cone calorimeter tests for NFR and FR samples

Fire Performance Data	NFR	10% - BFR	20%- BFR	10%- EGFR	20%- EGFR	10%- PFR	20%- PFR
Time to Ignition, t_{ig} (s)	3	3	6	2	3	6	4
Heat Release Rate, **Peak HRR** (kW/m^2)	196	168	148	163	145	186	190
Time to Peak HRR, t_{pHRR} (s)	16	22	16	14	13	20	19
Fire Growth Rate, **FIGRA** (kW/m^2.s)	12	8	9	12	11	9	10
Heat Release Rate, **Average** HRR (kW/m^2)	37	42	41	44	42	86	102
Total Heat Release, **THR** (MJ/m^2)	33	32	29	22	23	16	15
Effective Heat of Combustion **Average EHC** (MJ/kg)	19	18	18	17	21	13	14
Ave. Mass Loss Rate, **MLR** (g/s)	0.016	0.02	0.02	0.022	0.018	0.065	0.052
Specific Extinction Area, **Peak SEA** (m^2/kg)	2903	3431	4734	2722	3925	4600	4968
Ave. Specific Extinction Area, **SEA$_{ave}$** (m^2/kg)	98	286	469	134	164	1014	1131
Total Smoke Production **TSP** (m^2)	1.37	4.43	6.7	1.5	1.5	10.6	10.6
Total Smoke Release, **TSR** (m^2/m^2)	154	502	760	170	166	1165	1198
Average CO Yield (kg/kg)	0.1344	0.1704	0.1475	0.0704	0.0735	0.1043	0.1439
Average CO$_2$ Yield (kg/kg)	1.96	1.84	1.77	1.9	2.14	1.2	1.15
CO/CO$_2$ Weight Ratio (smoke toxicity index)	0.0685	0.093	0.0834	0.0367	0.0343	0.0869	0.1251
Total Oxygen Consumed, **O$_2$** (g)	21.03	22.67	20.33	17.37	15.43	10.8	10.07
Specimen Initial Mass, **M** (g)	15.65	17.23	16.94	16.35	16.05	15.2	14.12
Specimen Mass Lost **M$_L$** (g)	14.03	15.47	14.3	11.23	9.17	10.45	9.37

Percent Mass Remaining, PMR (%)	10	10	16	31	43	31	34
Average Density (kg/m^3)	61	63	67	65	68	63	62

Appendix 4.2: Superposition of HRR & CO$_2$ and CO$_2$ & CO Concentration-time curves of NFR sample
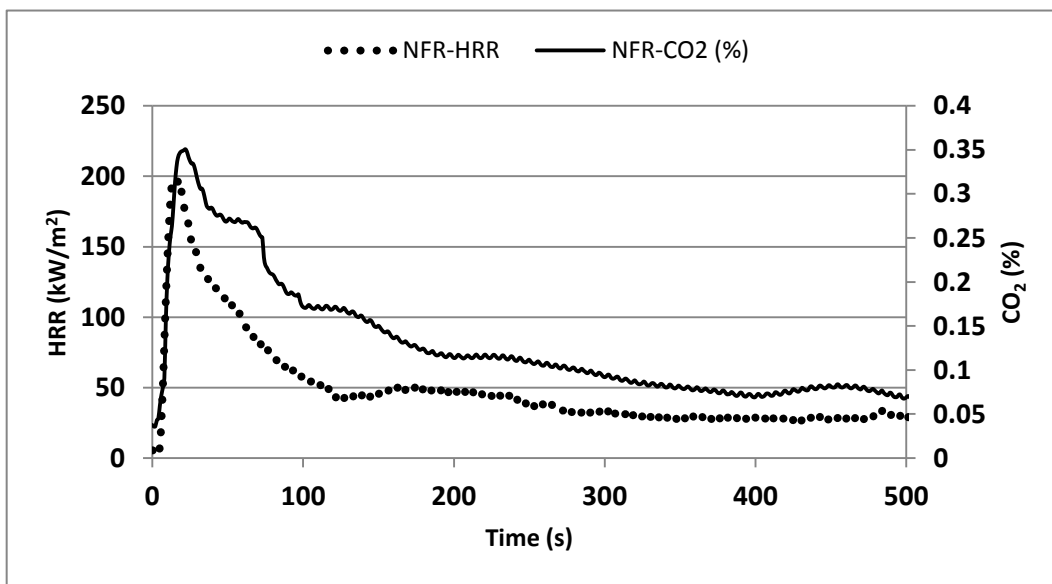

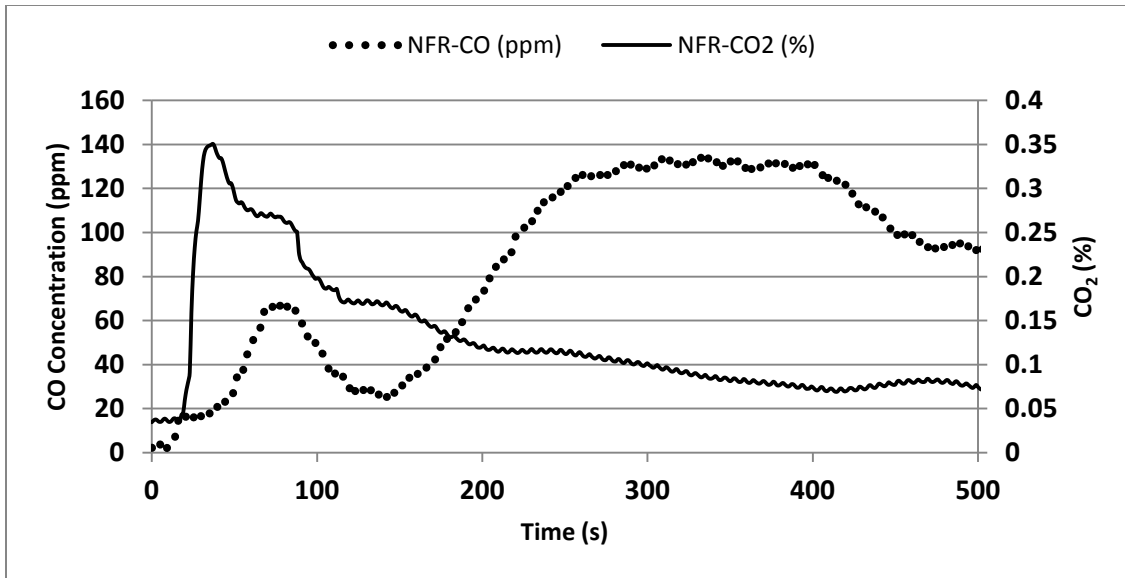**Figure 4.2a**: Overlay of HRR and CO$_2$ production of NFR sample peaking at the same time

Figure 4.2b: Overlay of CO_2 and CO production of NFR sample showing peak values at different times

Appendix 4.3: Mass Loss versus time for NFR and FR samples in Cone Calorimeter Testing
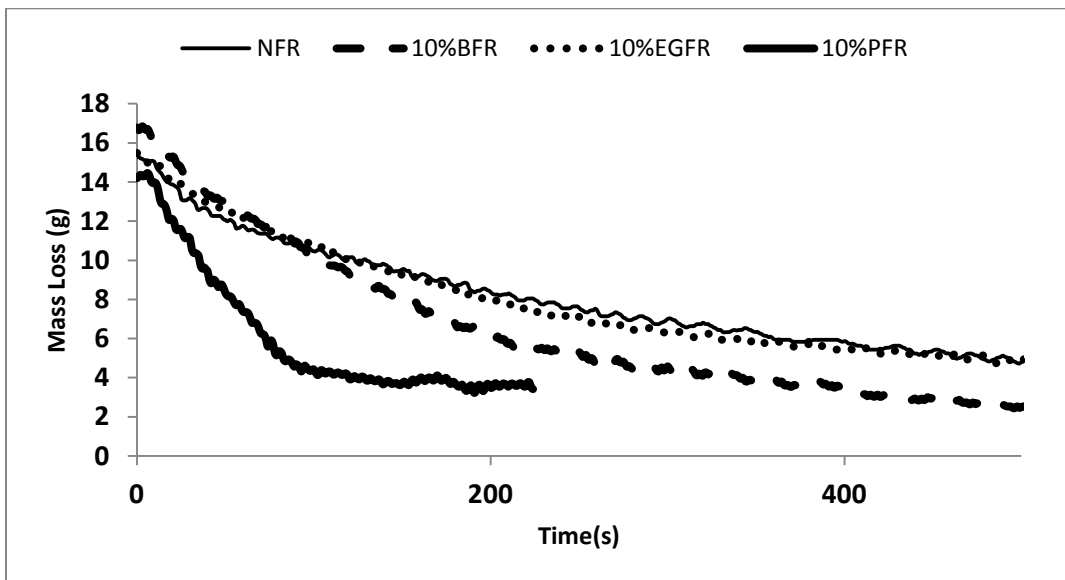
Figure 4.3a: Mass Loss versus time for NFR and 10% FR samples under cone calorimeter testing
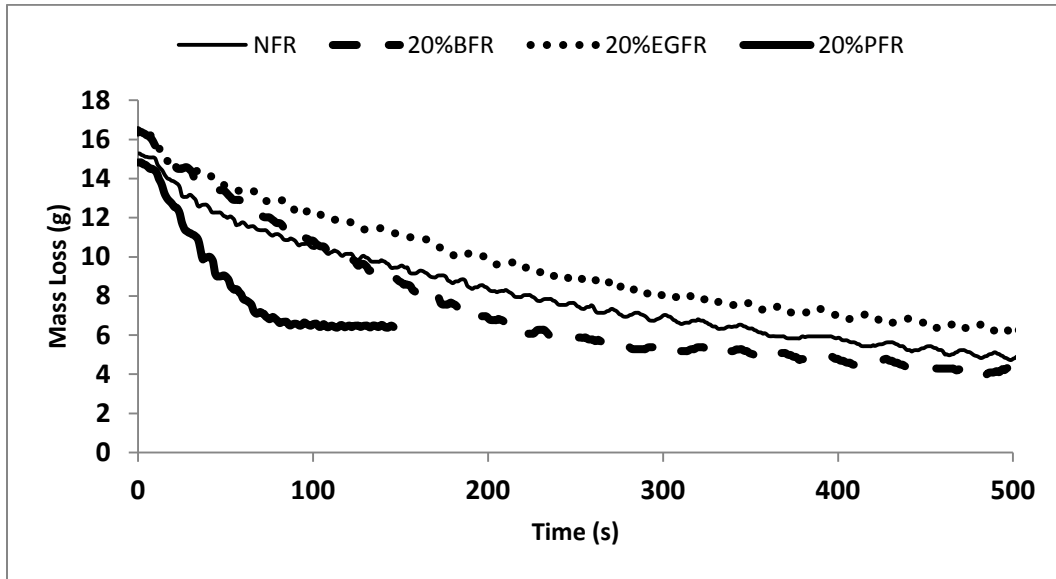
Figure 4.3b: Mass Loss versus time for NFR and 20% FR samples under cone calorimeter testing

Appendix 4.4: Sampling points on the HRR-time curves for NFR and FR samples
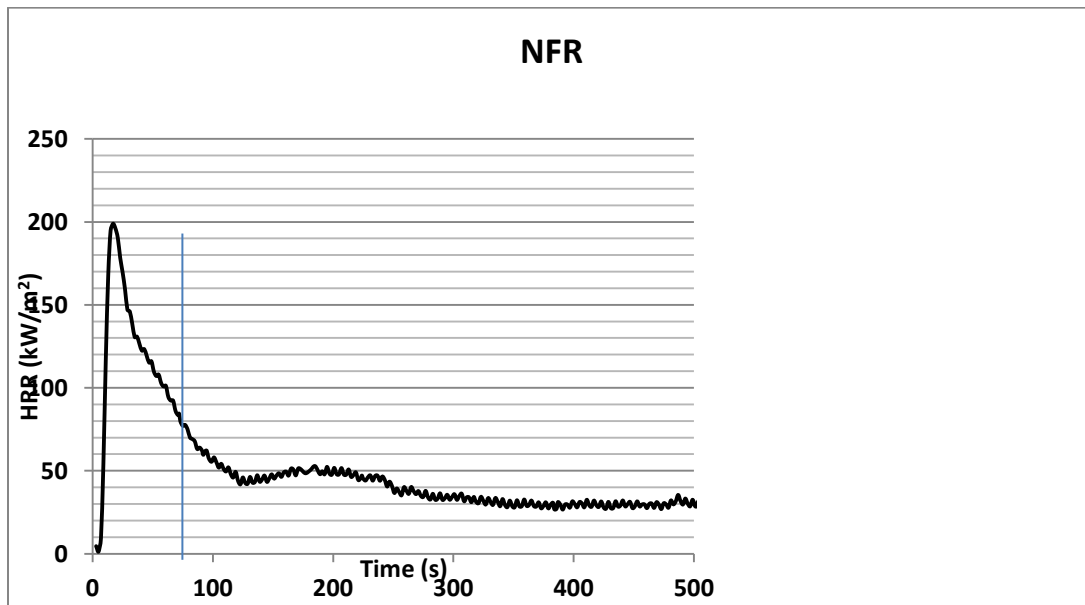
Figure 4.4a: Shows sampling point (80kW/m^2 @75s) on the HRR-time curve of NFR sample
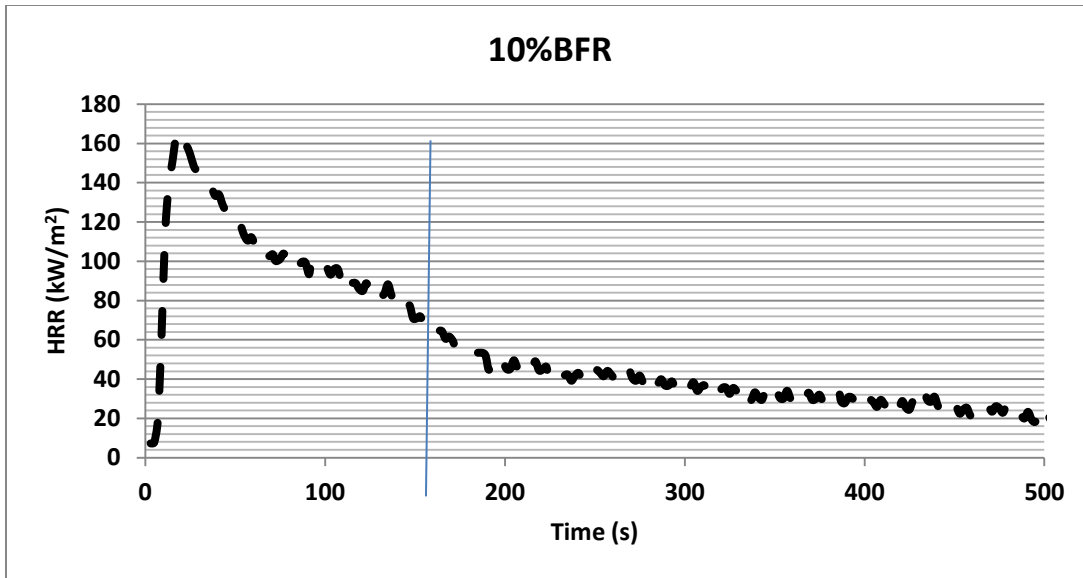
Figure 4.4b: Shows sampling point (65kW/m^2 @165s) on the HRR-time curve of 10%BFR sample
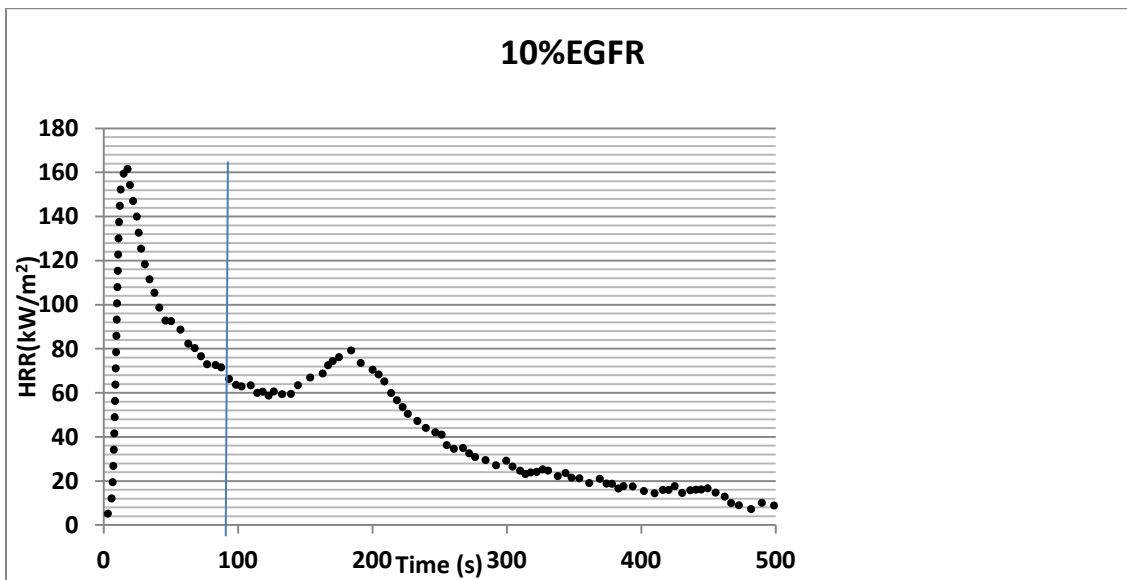
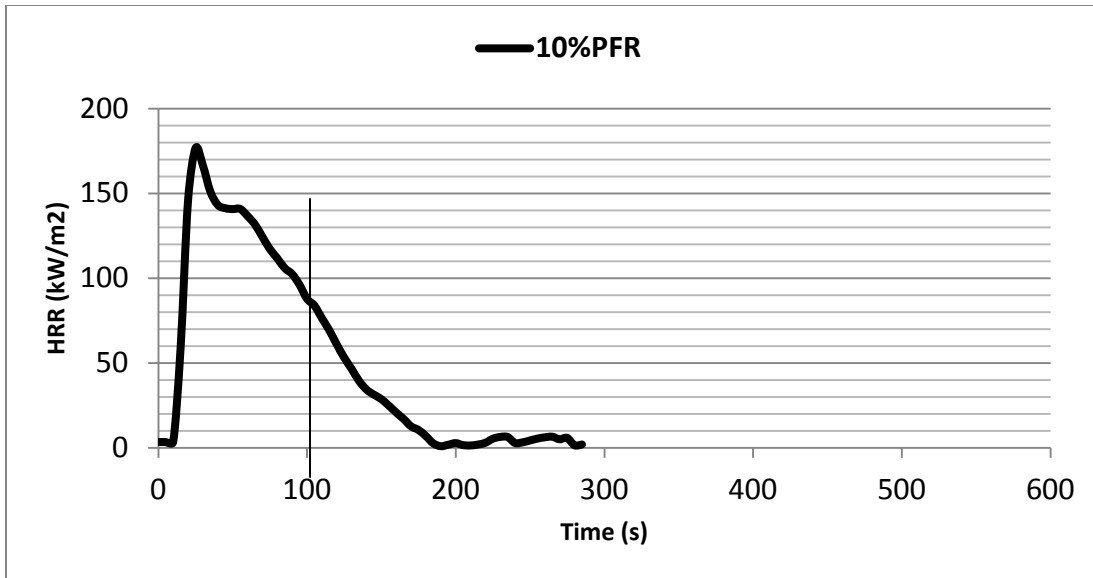**Figure 4.4c:** Shows sampling point (70kW/m^2 @87s) on the HRR-time curve of 10%EGFR sample

213

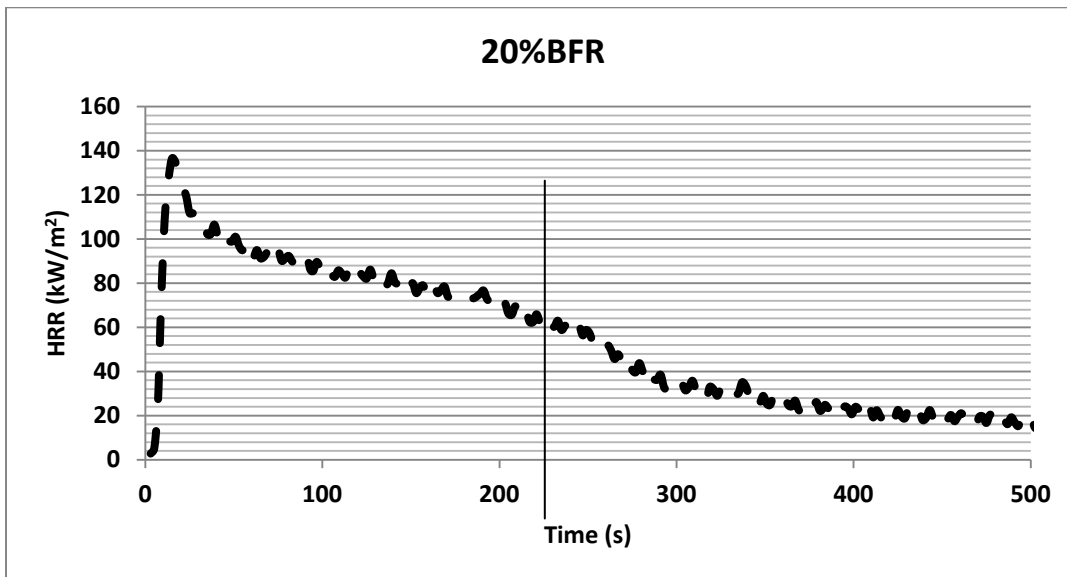**Figure 4.4d:** Shows sampling point (75kW/m^2 @100s) on the HRR-time curve of 10%PFR sample

Figure 4.4e: Shows sampling point (65kW/m^2 @227s) on the HRR-time curve of 20%BFR sample
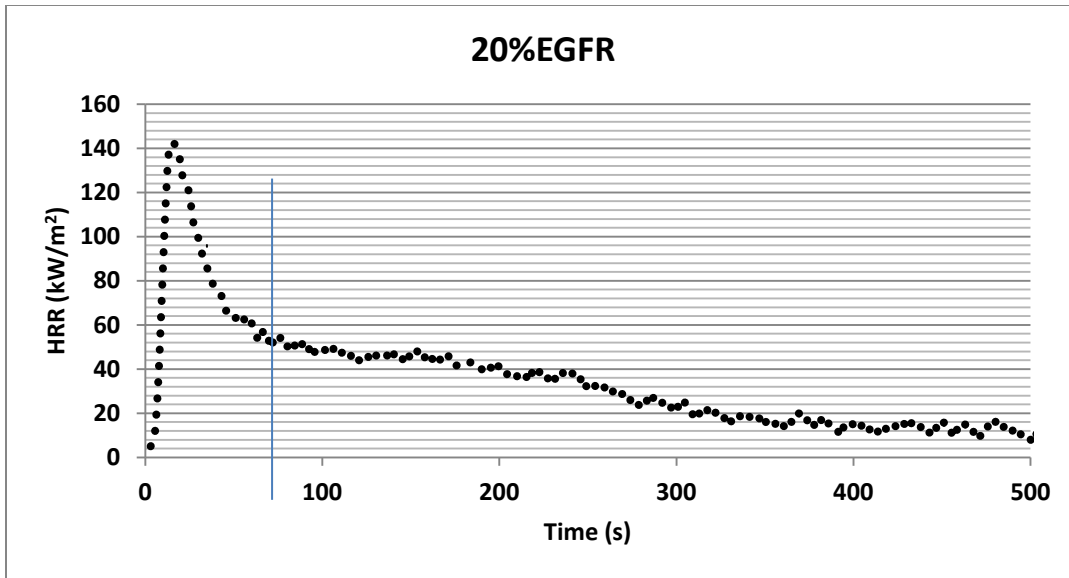
214

Figure 4.4f: Shows sampling point (55kW/m^2 @60s) on the HRR-time curve of 20%EGFR sample
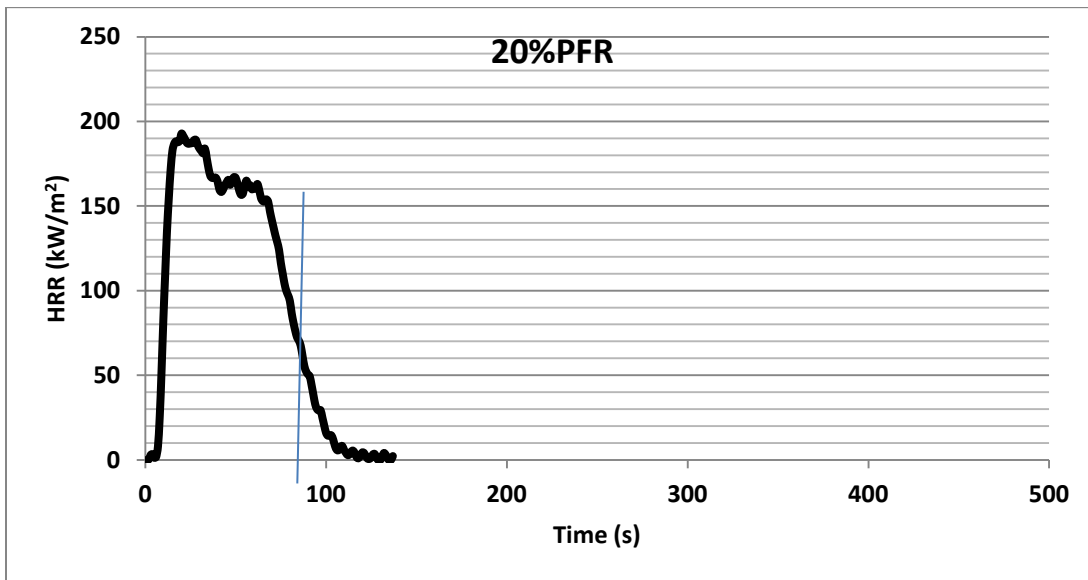

Figure 4.4g: Shows sampling point (75kW/m^2 @80s) on the HRR-time curve of 20%PFR sample